Technical Report Documentation Page

1. Report No.	2. Government Accession No.	3. Recipient's Catalog No.
4. Title and Subtitle **MBTC 2014** **Development of Simplified Asphalt Concrete Stiffness/Fatigue Testing Device** **Final Report**		5. Report Date **March 2004** 6. Performing Organization Code
7. Author(s) **Nam H.Tran** **Kevin D. Hall**		8. Performing Organization Report No.
9. Performing Organization Name and Address **University of Arkansas, Department of Civil Engineering** **4190 Bell Engineering Center** **Fayetteville, AR 72701**		10. Work Unit No. (TRAIS) 11. Contract or Grant No. **MBTC-2014**
12. Sponsoring Agency Name and Address **Mack-Blackwell National Rural Transportation Study Center** **4190 Bell Engineering Center, Fayetteville, AR 72701** **Arkansas State Highway and Transportation Department** **P.O. Box 2261, Little Rock, AR 72203-2261**		13. Type of Report and Period covered **Final Report** **1 Feb 01 thru 30 Jun 03** 14. Sponsoring Agency Code
15. Supplementary Notes **Conducted in cooperation with U.S. Department of Transportation, Federal Highway Administration**		

16. Abstract

Mechanistic-empirical flexible pavement design procedures proposed for use within the 2002 Design Guide require the input of the dynamic modulus (E*) of hot-mix asphalt concrete. In addition, the E* test has been proposed as a "simple performance test" for use in mixture design and construction quality control. The objective of this study included conducting the dynamic modulus test, evaluating the accuracy/variability of test results, and constructing master curves for the mixtures tested. The hot-mix asphalt mixes tested in this research are typically used for pavement construction in Arkansas, and binder content and air voids were varied to simulate typical construction variability. The analysis showed that the variability of the average dynamic modulus for each set of four replicates was acceptable. Since the dynamic modulus tests were run at intermediate temperatures in this study, a modified procedure, using Arrhenius and power functions, was employed to construct the master curves. Based on the master curves, the effects of aggregate size, binder content, and air voids on the tested asphalt mixtures were evaluated and determined to be consistent and reasonable. The testing procedure and results of this study were recommended for use in a new project to characterize the stiffness of Arkansas mixtures to prepare input data for the proposed 2002 Design Guide.

17. Key Words **Asphalt, Asphalt Mix Design, Superpave, Stiffness, Simple Performance Test, Fatigue, Dynamic Modulus**	18. Distribution Statement **No Restrictions**

19. Security Classif. (Of this report) **(none)**	20. Security Classif. (Of this page) **(none)**	21. No. of Pages **377**	22. Price

Form DOT F 1700.7 (8-72) Reproduction of completed page authorized

FINAL REPORT

MBTC 2014

Development of Simplified Asphalt Concrete Stiffness/Fatigue Testing Device

by

Nam Tran and Kevin D. Hall

Conducted by

Department of Civil Engineering
University of Arkansas

In cooperation with

Mack-Blackwell National Rural Transportation Study Center

Arkansas State Highway and Transportation Department

US Department of Transportation
Federal Highway Administration

University of Arkansas
Fayetteville, Arkansas 72701

March 2004

EXECUTIVE SUMMARY

Mechanistic-empirical flexible pavement design procedures proposed for use within the 2002 Design Guide require the input of the dynamic modulus (E*) of hot-mix asphalt concrete. In addition, the E* test has been proposed as a "simple performance test" for use in mixture design and construction quality control. The objective of this study included conducting the dynamic modulus test, evaluating the accuracy/variability of test results, and constructing master curves for the mixtures tested. The hot-mix asphalt mixes tested in this research are typically used for pavement construction in Arkansas, and binder content and air voids were varied to simulate typical construction variability. The analysis showed that the variability of the average dynamic modulus for each set of four replicates was acceptable. Since the dynamic modulus tests were run at intermediate temperatures in this study, a modified procedure, using Arrhenius and power functions, was employed to construct the master curves. Based on the master curves, the effects of aggregate size, binder content, and air voids on the tested asphalt mixtures were evaluated and determined to be consistent and reasonable. The testing procedure and results of this study were recommended for use in a new project to characterize the stiffness of Arkansas mixtures to prepare input data for the proposed 2002 Design Guide.

TABLE OF CONTENTS

LIST OF FIGURES

LIST OF TABLES

CHAPTER 1

INTRODUCTION

1.1 BACKGROUND

Most state agencies used the Marshall and Hveem mix design methods before the Strategic Highway Research Program (SHRP) developed a new system for specifying asphalt materials. Even though the Marshall mix design method addresses the proper volumetric proportions of mixture materials for achieving a durable hot mix asphalt (HMA), it does not address the rutting resistance of the designed mixture. The Marshall impact method of compaction does not simulate mixture densification as it occurs in a real pavement, and the Marshall stability test does not adequately estimate the shear strength of HMA. For the Hveem method, the advantages of the method are that the kneading compaction may better simulate the densification characteristics of HMA in a real pavement and that the method measures the ability of a test specimen to resist lateral displacement from application of a vertical load. The disadvantage is that the Hveem method is too subjective and probably results in non-durable HMA with too little asphalt [1].

In 1987, SHRP began developing a new system for designing asphalt mixtures under the Contract SHRP A-005. One final product of the SHRP asphalt research program is an asphalt mixture design and analysis system called Superpave, short for *Superior Performing Asphalt Pavements* [2]. The Superpave system consists of performance-based specifications, asphalt binder and mix tests, a mixture design and analysis system, performance models, and computer software. Many agencies have adopted different parts of the system, including the Performance-Graded (PG) binder specification and the volumetric mixture design method [3].

In March 1993, the Federal Highway Administration (FHWA) developed a long-term strategy for the implementation of the results from the SHRP asphalt research program. A major task of the implementation plan under the National Cooperative Highway Research Program (NCHRP), the project NCHRP 9-19, is the further refinement and validation of the SHRP pavement performance models. In July 1995, the FHWA awarded a 5-year, two-phase contract entitled *Superpave Support and Performance Models Management* to the University of Maryland and a team of subcontractors. Phase I, completed in September 1996, evaluated the Superpave performance models developed through the SHRP. Based on the findings from the model evaluation, the FHWA and model evaluation team concluded that the distress prediction models developed in the SHRP asphalt research program were not ready for publication at that time because the reliability and accuracy of those predictions were questionable for widespread use over a wide range of environmental conditions and pavement structures. The team also recommended many significant enhancements for the models and that a simple performance test (SPT) be developed [4].

In Phase II, which began in November 1997, the contractor was tasked with development and validation of an advanced material characterization model and the associated calibration and testing procedures for hot mix asphalt used in highway pavements. This development included Task C, the development of a simple performance test to be incorporated in the Superpave volumetric mix design method [5].

A draft report of Task C in Phase II entitled *Simple Performance Test: Test Results and Recommendations* was submitted to FHWA for review to members in the work of the NCHRP in November 2000. During the first part of Task C, a questionnaire was sent to industry representatives across Northern America to determine which distress type was considered most important to the future acceptance of the SPT. As a result, rutting was rated as the most important distress for consideration by the SPT, followed by fatigue cracking and then thermal cracking.

Consequently, there are five draft test protocols for the candidate test methods of the SPT proposed in the report as follows [3]:

- Standard Test Methods for Simple Performance Test for Permanent Deformation
  - Standard Test Method for Dynamic Modulus of Asphalt Concrete Mixtures for Permanent Deformation
  - Standard Test Method for Repeated Load Testing of Asphalt Concrete Mixtures in Uniaxial Compression
  - Standard Test Method for Static Creep/Flow Time of Asphalt Concrete Mixtures in Compression
- Standard Test Methods for Simple Performance Test for Fatigue Cracking
  - Standard Test Method for Dynamic Modulus of Asphalt Concrete Mixtures for Fatigue Cracking
- Standard Test Methods for Simple Performance Test for Thermal Cracking
  - Standard Test Method for Indirect Tensile Creep Testing of Asphalt Mixtures for Thermal Cracking

1.2 OBJECTIVE OF PROJECT

The overall objective of this project is to conduct the *Standard Test Method for Dynamic Modulus of Asphalt Concrete Mixtures for Fatigue Cracking* proposed in the SPT. The results of the test will be analyzed to determine the accuracy of average dynamic modulus and the effects of aggregate size, binder content, air void content, test temperature and test frequency on the dynamic modulus of asphalt concrete. Furthermore, the test results will be presented using isothermal, isochronal, and master curves of dynamic modulus.

The testing protocol, developed in this project, will be used in future research sponsored by the Arkansas State Highway and Transportation Department (AHTD) to determine the expected range of dynamic modulus of Arkansas mixtures and provide pavement designers guidance regarding the input values required for HMA in the proposed *2002 Guide for the Design of New and Rehabilitated Pavement Structure*.

1.3 SCOPE OF PROJECT

This project provides an extensive search of historic and current literature relating to the analysis and performance-based test procedures of HMA fatigue characteristics, and the role of the performance-based tests in the quality control and pavement performance predictions in flexible pavement design.

The laboratory study is conducted using two primary HMA mixes. While the effect of gradation on mixture performance is not determined in the project, the aggregate size, asphalt content and percentage of air voids of HMA are varied from the job mix formulas to determine the effects of aggregate size, asphalt content and air void content of HMA on the dynamic modulus of HMA. The dynamic modulus test is performed on the laboratory samples at different temperatures and frequencies in the civil engineering laboratories of the University of Arkansas using the test devices and procedures in accordance with the testing protocols proposed in Task C of the project 9-19.

CHAPTER 2

LITERATURE REVIEW

2.1 MATERIAL PROPERTIES AND FATIGUE CRACKING RELATIONSHIPS

Material properties must be used to characterize the field behavior of pavement materials because they permit the use of mechanics in predicting the behavior of a pavement under the service conditions of traffic and weather. They are typically presented in the form of mathematical equations. The material properties, such as elastic, viscoelastic, plastic, and fracture and healing properties, are utilized to predict the flexible pavement distresses, which are rutting, thermal cracking, and load-related fatigue cracking. While rutting predictions require elastic, viscoelastic, and plastic properties, thermal cracking is described by viscoelastic, fracture and healing properties. Fatigue cracking predictions require elastic, viscoelastic, fracture and healing properties, and only the fracture and healing properties relating to fatigue cracking are discussed in this thesis.

2.1.1 Load-Related Fracture Properties

Fatigue is a process in which microfractures in a material under repeated loading grow in size and become more densely concentrated until cracks of visible size develop. The visible cracks then propagate until they reach the boundaries of the material. The two phases of the development of the fracture are commonly termed crack initiation and crack propagation. Both of these phases are used to model fatigue in asphalt concrete pavements. In the first phase, crack initiation is modeled as the growth of microcracks that obey the same fracture law, as does the visible crack in the crack propagation phase. The fundamental fracture law is Paris' law, developed by Paris and Endogan, and some modifications thereof.

The Paris' law for linearly elastic materials is as follows [6]:

$$\frac{dc}{dN} = A(\Delta K)^n \tag{2.1}$$

where:

c	= the crack length
N	= the number of load applications
$\frac{dc}{dN}$	= the "crack speed" or rate of crack growth
ΔK	= the change of stress intensity factor during loading and unloading
A, n	= fracture parameters for the asphalt mixture

The stress intensity factor has units of (force × length$^{-3/2}$). It varies with crack length and is situated at the tip of the crack.

The Paris' law for non-linearly elastic materials using the J-integral is written as follows:

$$\frac{dc}{dN} = A'(J)^{n'} \tag{2.2}$$

The J-integral, which can be measured experimentally, is defined as the rate of change of dissipated energy per unit area of crack growth in the following form:

$$J = \frac{\Delta(DE)}{b\Delta c} \tag{2.3}$$

where:

$\Delta(DE)$	= the change of dissipated energy
Δc	= the change of crack length
b	= the width of the sample being tested

The theoretical relation between the J-integral and the stress intensity factor, K, for linearly elastic materials under plane strain conditions is as follows:

$$J = \frac{K^2}{E}(1-\nu^2) \tag{2.4}$$

Equation 2.2 can be used for linearly elastic materials if the following relationships are satisfied:

$$n' = \frac{n}{2} \tag{2.5}$$

and

$$A' = A\left(\frac{E}{1-\nu^2}\right)^{\frac{n}{2}} \tag{2.6}$$

Since the fundamental fracture law of viscoelastic materials is still being developed, the J-integral form of Paris' law still governs the growth of cracks in non-linear viscoelastic materials. The viscoelastic "J-integral" is designated as the J_v-integral, which varies with the time of loading.

Schapery's work in 1973 (qtd. in [6]) and subsequent developments demonstrated that the fracture parameters A and n were described in the following formulation for linearly viscoelastic materials:

$$A = \left[\frac{D_1 \lambda(m) \pi^{1+2m}}{4}\right]^{\frac{1}{m}} \int_0^{\Delta t} \frac{w(t)^n \, dt}{\Gamma^{\frac{1}{m}} \sigma_t^2 \mathrm{I}^2} \tag{2.7}$$

$$n = 2\left(1+\frac{1}{m}\right) \quad \text{or} \quad \frac{2}{m} \tag{2.8}$$

where:

D_1 = the compliance coefficient, D1, in the power-law creep compliance

m = the slope of the log compliance vs. log time graph

σ_t = the tensile strength of the material

Γ = released strain energy storage density of the material, also called fracture energy density

$\lambda(m)$ = a function of m which has a nearly constant value of 1/3

Δt = the time the load is applied

$w(t)$ = the normalized wave-form of the applied load with time. Its values range between 0 and 1

I = value of the integral of the dimensionless stress-strain curve of the material. Its values range between 1 and 2

2.1.2 Healing Properties

There is a rest period between the applications of loading on a material. The rest period in laboratory tests is very short compared to the rest periods observed between load applications in the field. When observing increase in the amount of dissipated energy with each load cycle and longer fatigue life after a longer period of rest, rates of healing are found to vary widely with different asphalt binders, with and without modifiers or additives. The relationship between fatigue life and the rest period between load applications is well described in the form of a power law. The relation between laboratory and field fatigue life is described as follows [6]:

$$N_{f(field)} = N_{f(lab)} \times (SF) \tag{2.9}$$

where:

SF = shift factor which has a value of 1 or more

The shift factor, SF, is related to three separate processes in the material, and it is the product of the shift factors for the processes, healing, residual stresses, and resilient dilation, as follows:

$$SF = SF_h \times SF_r \times SF_d \tag{2.10}$$

where:

SF_h = the shift factor due to healing, commonly ranging between 1 and 10

SF_r = the shift factor due to residual stresses, commonly ranging between 1/3 and 3, depending on whether the residual stresses are tensile or compressive, respectively

SF_d = the shift factor due to resilient dilation, commonly ranging between 1 and 5, depending on how much larger the Poisson's ratio is greater than 0.5

The form of the equation for the healing shift factor is as follows:

$$SF_h = 1 + a(t_r)^b \tag{2.11}$$

where:

t_r = the rest period, commonly recorded in seconds

a, b = the healing coefficient and exponent, respectively

The forms of the equations for residual stress and resilient dilation have not been established. However, the residual stress shift factor was found depending on the size of the Poisson's ratio, which depends on the stress state and temperature level in the asphalt.

2.1.3 Relationship Between Fracture Mechanics and Phenomenological Fracture Rules

A phenomenological equation may be constructed from fundamental fracture mechanics, starting with the basic Paris' law as follows:

$$\frac{dc}{dN} = A(K)^n \tag{2.12}$$

The dimensionless stress intensity factor is described in a function of a dimensionless crack length as follows [6]:

$$\frac{K}{\sigma\sqrt{d}} = r(\frac{c}{d})^q \tag{2.13}$$

where:

d = the length the crack must grow

σ = the stress at the extreme fiber

r, q = coefficients found from the analysis of the stress-intensity factor, K, as it varies with crack length, c

Paris' law may be integrated in the following form:

$$\int_0^{N_f} dN = \int_{C_o}^{d} \frac{dc}{Ar^n \sigma^n d^{\frac{n}{2}-nq} c^{qn}} \tag{2.14}$$

where:

c_o = the initial crack size

N_f = the number of load cycles to reach failure

The phenomenological equation after the integration is as follows:

$$N_f = \frac{d^{1-\frac{n}{2}}}{Ar^n (1-nq)E^n}\left[1-\left(\frac{c_o}{d}\right)^{1-nq}\right]\left(\frac{1}{\varepsilon}\right)^n \quad (2.15)$$

The form of the phenomenological equation is derived as follows:

$$N_f = K_1\left(\frac{1}{\varepsilon}\right)^{K_2} \quad (2.16)$$

The phenomenological equation has been widely used to develop the model predicting the rate of fatigue propagation in the flexible pavement structures.

2.2 PERFORMANCE MODELS AND PERFORMANCE-BASED TEST PROCEDURES FOR FATIFUE CRACKING DEVELOPED UNDER SHRP

The SHRP was a five-year research program initiated within the United States under the 1987 Highway Act. One of the program's targets was to identify and define the physicochemical properties of asphalt binders and the structural properties of asphalt concrete that influence pavement performance. Another was to develop tests and specifications to establish and control the pavement performance standards. Figure 2.1 provides an overview of Superpave performance prediction system. The SHRP A-005 project developed detailed pavement performance models to support performance-based specifications for asphalt binders and mixture designs using three distress modes: rutting, fatigue cracking, and thermal cracking. The SHRP A-003A project developed and evaluated performance-related tests of asphalt aggregate mixtures. The main findings and recommendations on the asphalt fatigue characteristics from the two projects above are briefly discussed in this report.

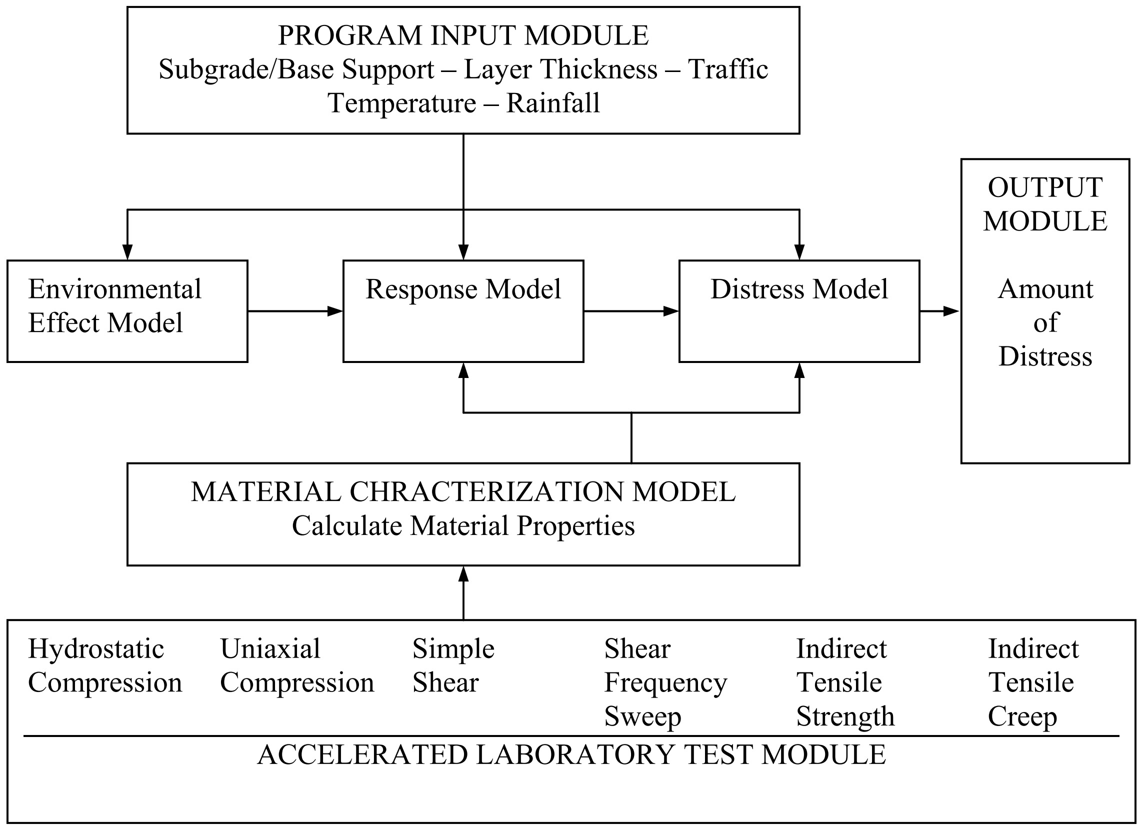

Figure 2.1. Overview of Superpave Performance Prediction System [9]

2.2.1 Performance-Based Tests for Fatigue Cracking Developed Under SHRP A-003A

The objectives of the project SHRP A-003A were to develop a series of accelerated performance-related tests for asphalt mixtures and to identify methods for analyzing asphalt concrete distresses that significantly affect pavement performance. The scope of the project included the development of a test method for fatigue cracking, one of major distress mechanisms that affect asphalt pavement performance. Development of the accelerated performance-related test for fatigue cracking consisted of a number of phases as follows [7]:

- Review of candidate tests and response parameters
- Conduct a pilot test program to evaluate the candidate tests and to select appropriate tests for defining mixture fatigue response

- Conduct an expanded test program using selected tests to validate test specification and to develop surrogate models of fatigue behavior that might substitute for laboratory testing when it is appropriate
- Develop a mix design and analysis system to investigate fatigue cracking

Candidate Test Methods and Variables

Table 2.1 provides an overview of test methods evaluated in the fatigue program, and Table 2.2 lists significant mix and test variables for the fatigue study.

The mode of loading in the test methods is important in mix analysis because, for similar initial conditions, fatigue life is typically greater in controlled-strain loading than in controlled-stress loading and stiffer mixtures tend to perform better in controlled-stress loading but worse in controlled-strain loading [8].

Hypotheses [8]

The investigation is influenced by a number of hypotheses about the fatigue behavior of asphalt mixtures, as summarized below:

Hypothesis 1: Fatigue cracking is caused by tensile stresses and/or strains at the bottom of the asphalt layer under the repetitive application of traffic loads.

Hypothesis 2: The critical stress and/or strain state can be estimated with acceptable accuracy using the theory of linear elasticity.

Hypothesis 3: Testing to destruction under cyclic loading is necessary to measure accurately the fatigue response.

Table 2.1. Test Methods Evaluated in SHRP A-003A [8]

Test Method and Conditions	**Mode of Loading**
Flexural beam fatigue test	Pulsed loading (1.67 Hz)
	Controlled-stress or controlled-strain
Direct tension – correlation with fatigue	
Notched beam – C*-line integral	
Trapezoidal cantilever fatigue tests	Sinusoidal loading (20 Hz)
	Controlled stress
Uniaxial tension compression	Sinusoidal loading (20 Hz)
	Controlled stress
Diametral fatigue tests	Pulsed loading (1.67 Hz)
	Controlled-stress or controlled-strain

Hypothesis 4: Pulsed loading is preferred over sinusoidal loading in laboratory fatigue test because stress relaxation in the rest period is similar to that in traffic conditions.

Hypothesis 5: Test specimens can be evaluated equally under either tensile or flexural loading.

Hypothesis 6: Mode of loading is a critical concern in mix design systems because mix effects are quite different between controlled-stress and controlled-strain loading systems.

Hypothesis 7: Mixes are ranked in essentially the same way regardless of stress and/or strain levels.

Table 2.2. Significant Mix and Test Variables for Fatigue Study [8]

Variable	Level of Treatment		
	1	2	3
Aggregate			
Stripping potential	Low		High
Gradation		Medium	
Asphalt			
Temperature susceptibility	Low		High
Content		Optimum	High
Compaction			
Air voids (percent)	4 ± 1		8 ± 1
Test conditions			
Temperature	0^{o}C		20^{o}C
Stress and/or strain level	Low		High

Hypothesis 8: Under simple loading, crack initiation in a given mix is related to strain or stress level as follows:

$$N_f = a\ (1/\varepsilon)^b \quad \text{or} \quad N_f = c\ (1/\sigma)^d \tag{2.17}$$

where:

N_f = number of load applications to crack initiation

ε, σ = tensile strain and stress

a,b,c,d = experimentally-determined coefficients dependent on test temperature

Hypothesis 9: Under mixed loading, cracking in a given mix is initiated when the linear summation of cycle ratios equals one as follows:

$$\Sigma (n_i/N_i) = 1 \tag{2.18}$$

where:

n_i = number of applications of stress σ_i or strain ε_i

N_i = number of applications to failure at stress σ_i or strain ε_i

Hypothesis 10: The principles of fracture mechanics represent the most feasible mechanistic approach for estimating rates of crack propagation in pavement structures.

Significant Findings and Products of the Fatigue Program

The results of both flexural beam and trapezoidal cantilever tests were judged to be reasonable and considered as equivalent means for assessing the fatigue behavior of asphalt-aggregate mixtures. However, the authors prefer the flexural beam fatigue test because they are familiar with it and the design of the test equipment and its software interface is sophisticated. The test is also advantageous because the stress distribution is uniform and gluing is unnecessary. Other tests were eliminated because of complication of testing or limitation to mode of loading and unacceptable fracture patterns [7].

Considerable effort was made to investigate a unique relationship existing between the number of cycles to failure and the cumulative energy dissipated to failure in the flowing form:

$$W_N = A\,(N_f)^z \tag{2.19}$$

where:

N_f = number of cycles to failure

W_N = cumulative dissipated energy to failure

A, z = experimentally determined coefficients

However, the uniqueness of this relationship could not be substantiated, and the relationships were different for different mixes, being affected by both test temperature and mode of loading. Nevertheless, the initial energy dissipated during each loading cycle is a good predictor of cycles to failure. Moreover, dissipated energy is significantly correlated with stiffness decreases during testing and helps to explain the effects of mode of loading on mix behavior [7].

The final product of the fatigue program is an abridged analysis system [8], including the test equipment and procedure, for fatigue cracking of asphalt concrete. The analysis system is used to judge whether a trial mix identified in a specific set of traffic, environmental condition, and designed cross section would perform satisfactorily. If not, a modification in the mix design or pavement cross section would be necessary. As defined in the analysis system, a mix is satisfied in terms of fatigue cracking if the mix resistance (N_{supply}) equals or exceeds the traffic demand (N_{demand}) as follows:

$$N_{supply} \geq M \times N_{demand} \tag{2.20}$$

where:

M = a multiplier whose value depends on the design reliability and on the variability of the estimates of N_{supply} and N_{demend}

The traffic demand is determined using the following equation:

$$N_{demand} = \frac{ESAL_{20^o C}}{SF} \tag{2.21}$$

where:

N_{demand} = design traffic demand (laboratory-equivalent repetitions of standard load)

$ESAL_{20^oC}$ = design ESALs adjusted to a constant temperature of 20°C

SF = empirically-determined shift factor

For routine mix design (Level 1), fatigue resistance of a mix is estimated from the following model:

$$N_{supply} = 2.738\ (10^5)\ (e^{0.077 \bullet VFB})\ (\varepsilon_o^{-3.624})\ (S_o''^{-2.720}) \qquad (2.22)$$

where:

N_{supply} = number of load repetitions to 50-percent reduction in stiffness (crack initiation)

e_0 = base of the natural logarithms

ε = flexural strain, in/in

S_o'' = initial flexural loss stiffness at 50th loading cycle, psi

VFB = voids filled with bitumen, percent, as measured using frequency-sweep specimens or as determined from volumetric proportioning process

The flexural loss stiffness, S_o'', is determined using the following regression equation, and the shear loss stiffness, G_o'', in the equation is estimated from shear frequency sweep tests on a single briquette specimen, conducted in accordance with SHRP Test Method M-003:

$$S_o'' = 81.125\ (G_o'')^{0.725} \qquad (2.23)$$

where:

S_o'' = initial flexural loss stiffness at 50th loading cycle, psi

G_o'' = shear loss stiffness at 10 Hz, psi

For reliable decision making (Level 2), fatigue resistance of a mix is measured in the laboratory by flexural beam fatigue test at 20°C (68°F) at 10 Hz in accordance with SHRP Test Method M-009. At the completion of testing, a model of the following form is fit to the data:

$$N_f = K_1 \varepsilon^{K_2} \tag{2.24}$$

The fatigue life (N_{supply}) corresponding to the design strain at the bottom of the asphalt layer determined using multilayer elastic analysis is then computed using the equation above.

The general analysis system (Level 3), used for evaluation of mixes having binders of atypical temperature sensitivity, is quite complex because of necessity to simulate the broad range of in-situ temperature conditions. A detailed description of the analysis system can be found elsewhere [8].

The selected fatigue test in the fatigue program was the flexural beam (third-point loading) fatigue test conducted in the controlled-strain mode of loading, which was considered to be compatible with the crack propagation concept and pavement fatigue cracking models that were being developed as a part of the contract SHRP A-005. The test equipment is illustrated in Figure 2.2.

The test specimen size is 63.5mm × 50.0mm ×381mm (2.5in. × 2.0in. × 15.0in.), and sinusoidal loads up to 25Hz and up to 30°C can be applied with or without rest periods. The test equipment can characterize the fatigue response of an asphalt mix in 24 hours with the variation coefficient for fatigue life of nearly 40 percent. The detailed flexural beam fatigue test procedure can be found in SHRP Test Method M-009.

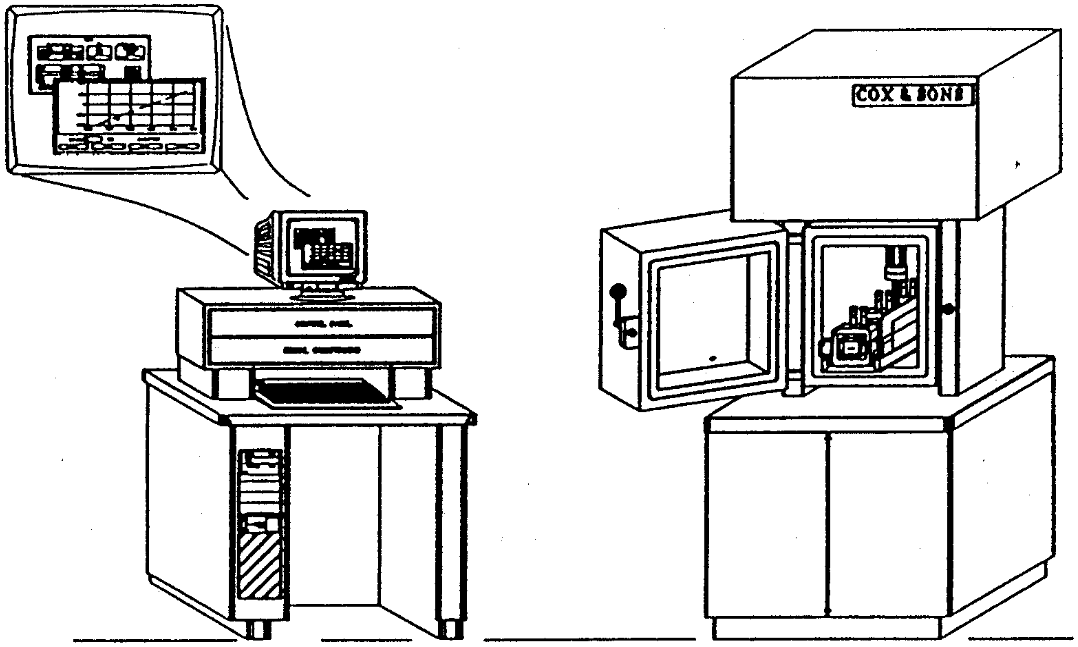

a. **Overall View with Computer Control Unit and Controlled Temperature Chamber**

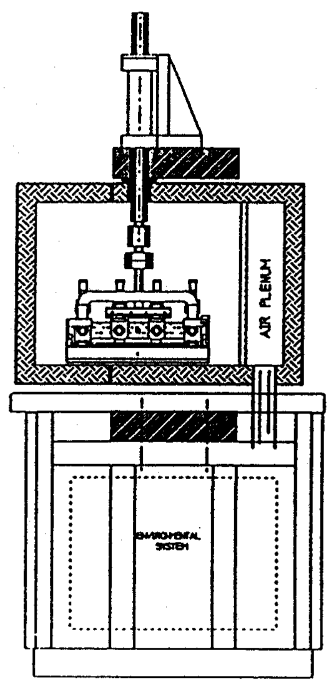

b. **Side View**

Figure 2.2. Schematics of Flexural Beam Fatigue Test Apparatus [8]

2.2.2 Performance-Related Models for Fatigue Cracking Developed under SHRP A-005 [6]

The objectives of the contract SHRP A-005 were to develop detailed pavement performance models to support pavement performance-based specifications for asphalt binders and mixture designs emphasizing three distress modes: rutting, fatigue cracking, and thermal cracking. However, only findings of this extensive research effort on fatigue cracking are discussed in this section.

Fatigue cracking is considered to be a tensile phenomenon under the repetitive application of tensile forces, and the fatigue cracking model is based on the damage accumulated during the pavement's service life. The development of a fatigue crack at the pavement surface is a two-step phenomenon: crack initiation and crack propagation. First, the microfracture damage initiates in the tensile zone under the repetitive application of traffic loads, and the crack propagates only when the microfracture damage has resulted in a crack of visible size. For pavements in service, tensile strains and stresses induced in the structure vary widely as a result of variations in the traffic loading magnitude and configuration, and failure in the pavement under mixed loading is expected when the following relative damage obtained by using linear Miner's law reaches one:

$$D_j = \sum_{i=1}^{j} \frac{n_i}{N_{fi}} \tag{2.25}$$

where:

n_i = actual number of load repetitions during period of time i

N_{fi} = number of load repetitions that will cause failure for the conditions prevailing during period of time i

The number of load cycles to reach failure above will be the summation of the number of load repetitions that will cause both crack initiation and propagation as follows:

$$N_{fi} = N_{ii} + N_{pi} \qquad (2.26)$$

where:

N_{ii} = number of load repetitions that will cause crack initiation for the conditions prevailing during period i

N_{pi} = number of load repetitions that will cause crack propagation to the surface for the conditions prevailing during period i

Figure 2.3 illustrates the logic flow chart of the Superpave performance models for fatigue cracking, and figure 2.4 indicates the constitutive parameters used in the models discussed later.

Crack Initiation Model

The model for determining the number of load cycles to reach crack initiation is an empirical equation developed from the results of stress-controlled beam fatigue tests conducted under the SHRP A-003A project as follows:

$$\begin{aligned}\log N_i = b_0 &+ \left\{b_1 + b_2\sigma_m + b_3\left[(\sigma_m)^2 + 2(1+\mu)(\tau_{oct})^2\right]\right\}E \\ &+ \left(b_4 \log\sigma_m + b_5 \log E\right)(\%AC) \\ &+ \left\{b_6\left[(\sigma_m)^2 + 2(1+\mu)(\tau_{oct})^2\right]/E + b_7 \log\sigma_m\right\}(\%Air) \\ &+ \left[b_8(\sigma_m/E) + b_9 \log\sigma_m\right](\sigma_m/E)\end{aligned} \qquad (2.27)$$

where:

N_i = number of load cycles to crack initiation

σ_m = mean principal stress, psi

τ_{oct} = octahedral shear stress, psi

E = asphalt concrete modulus, psi

$\%AC$ = asphalt content by weight percent

$\%Air$ = air voids content, percent

μ = Poisson's ratio

b_0 to b_9 = regression coefficients that can be found elsewhere [6]

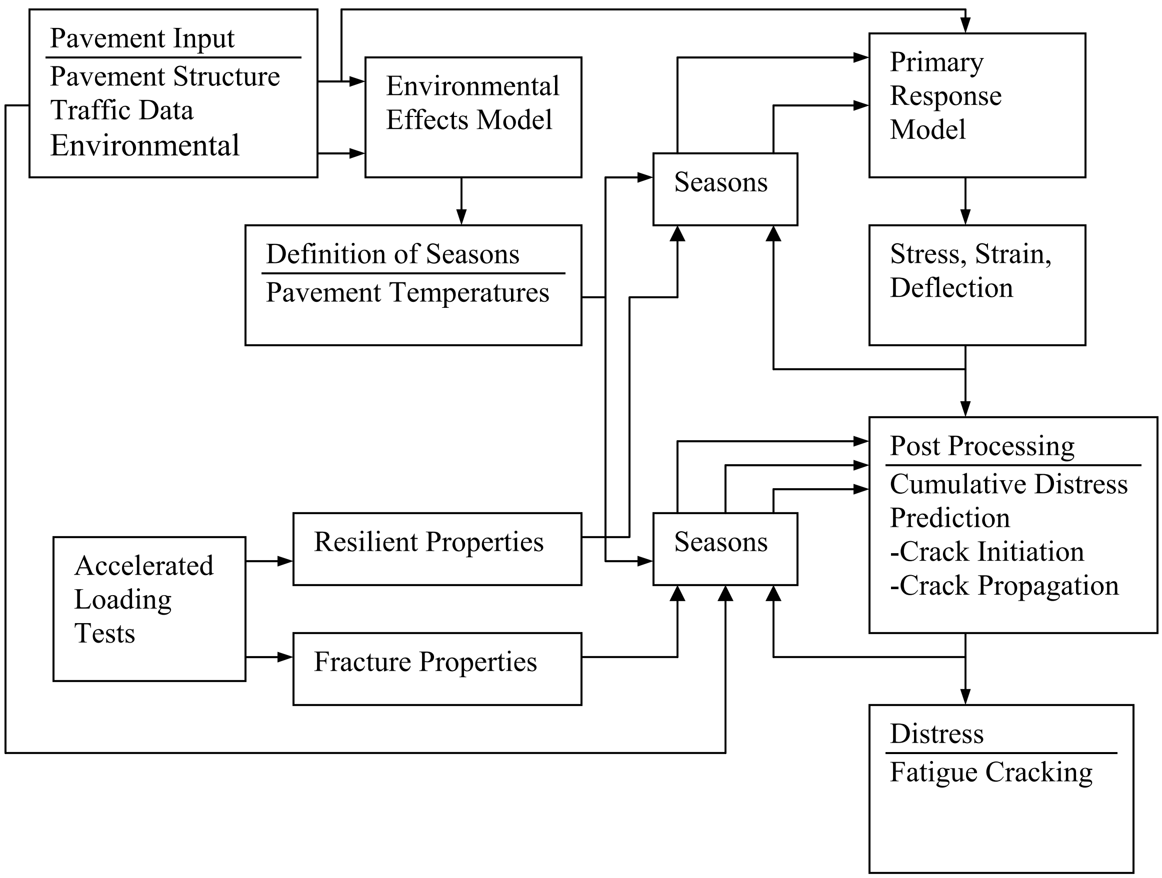

Figure 2.3. Flow Chart of Superpave Model for Fatigue Cracking [9]

The number of load cycles to reach crack initiation is shifted due to healing in rest periods as follows:

$$N_{if} = SF_n \times N_i \tag{2.28}$$

$$SF_n = 1 + g_5 t_r^{g6} \tag{2.29}$$

where:

N_i = the number of load cycles to reach crack initiation in the laboratory

N_{if} = the number of load cycles to reach crack initiation in the field

SF_n = the shift factor due to the healing of microcracks

t_r = the rest period between the application of traffic loads, in seconds

g_5, g_6 = healing properties of the asphalt mix determined by field calibration

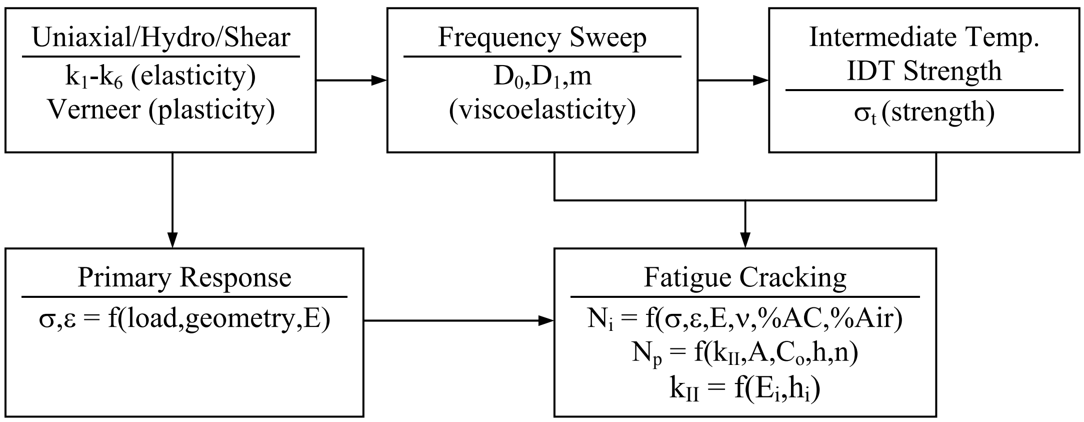

Figure 2.4. Usage of Material Parameters in Superpave Model for Fatigue Cracking [9]

Crack Propagation Model

The crack propagation is defined using the Paris' law relation as follows:

$$N_p = \frac{1}{A}\int_{c_0}^{h}\frac{dc}{k^n} = \frac{1}{A}\int_{c_0}^{h}\frac{dc}{k_{II}^n} = \frac{1}{A}I_{k_{II}} \tag{2.30}$$

where:

N_p = number of load repetitions to propagate a crack of initial length c_o to the surface (c_o assumed to be equal to 0.3 in.)

h = layer thickness, in.

c_o = initial crack length

k = stress intensity factor

A, n = material fracture properties

k_{II} = Mode II (shear) stress intensity factor

I_{kII} = crack propagation integral

The crack propagation integral, I_{kII}, is related to various pavement parameters using plane strain linearly elastic finite element parametric studies of a three-layer pavement system. The crack propagation integral can be adequately predicted by the pavement characteristics, layer thicknesses, and moduli ratios in the following regression equation form:

$$I_{k_{II}} = f(h_{AC}, h_B, \frac{E_{AC}}{E_{SG}}, \frac{E_B}{E_{SG}}) \tag{2.31}$$

where:

h_{AC}, h_B = asphalt concrete and base layer thickness, in.

E_{AC}, E_B, E_{SG} = moduli of asphalt concrete, base and subgrade layers

Since the material fracture properties, A and n, are not measured directly in Superpave's test procedures, they are estimated using the following equations, which were calibrated in the project, based on Schapery's theory:

$$\log A = g_2 + \left(\frac{g_3}{n}\right) \log D_1 + g_4 \log \sigma_t \tag{2.32}$$

$$n = g_0 + \frac{g_1}{m} \tag{2.33}$$

with

$$D(t) = D_0 + D_1 t^m \tag{2.34}$$

where:

$D(t)$ = creep compliance

D_0, D_1, m = creep compliance material parameters in the power law expression

σ_t = tensile strength of the mix

a_0 to a_4 = field calibration coefficients

The creep compliance material parameters, D_0, D_1, m, are not measured directly but are computed from the shear frequency sweep test results based on viscoelastic LaPlace transform technique.

2.3 SUPERPAVE PERFORMANCE MODEL EVALUATION AND SIMPLE PERFORMANCE TEST PROCEDURE FOR FATIFUE CRACKING DEVELOPED UNDER NCHRP 9-19

The objectives of the project NCHRP 9-19 are (1) to provide a detailed, comprehensive, and unbiased evaluation of the theory, application, implementation, research results, and conclusions of the original SHRP Superpave performance models; (2) to develop simple performance tests for permanent deformation and fatigue cracking for incorporation in the Superpave volumetric mix design method; and (3) to develop and validate an advanced material characterization model and the associated calibration and testing procedures for HMA for incorporation in the AASHTO 2002 Design Guide developed in the project NCHRP 1-37A. Since the project has not been completed, only the project reports available for loan on request from NCHRP are reviewed in this report [5]. Moreover, only the parts of reports that are relating to fatigue characteristics of HMA are discussed below.

2.3.1 Evaluation of Superpave Models for Fatigue Cracking under task D of NCHRP 9-19 [9]

In general, the conclusions from the model evaluation are that the Superpave performance models provide significant advances compared to any technology now in use in the world for mix design and analysis and that the existing modular model framework developed by the SHRP A-005 team provides an excellent basis for any short or long term future revisions and enhancements to the Superpave system. However, the Superpave system contains several problems found in software code, technical documents, and distress performance models, and the corrections, modifications, and enhancements to the present Superpave performance models are necessary for acceptance and use by industry.

The model framework developed by the SHRP A-005 team, having a two-phase process, is a good way of approaching load-related fatigue cracking. The fatigue cracking model is based on the damage accumulated during the pavement service, and the number of load applications to fatigue failure is defined in a two-phase process: crack initiation and crack propagation. However, there are some “areas of concern” found in the model framework.

General

- The current Superpave fatigue model is highly empirical and is not applicable for modified binders because only conventional asphalt binders were considered during the development of many of these regression models.

- The evaluation team in NCHRP 9-19 did not agree with the SHRP A-005 team’s assumption that fractures always initiate at the bottom of the asphalt and propagate upward. They proposed to conduct some coring programs on existing cracked pavement sections to address the argument.

- In some instances, the predictions resulted from the fatigue cracking models are questionable when the Superpave fatigue subsystem predicts that colder temperature, higher mixture modulus, stiff binders, and/or aging will improve the fracture resistance of the asphalt mixture.

Crack Initiation

- The crack initiation model is not based on fundamental material properties but on empirical regression relation. The range of applicability of this approach is unclear.

- The use of mean principal stress instead of tensile strain as a primary response in Equation 2.27 contradicts the results in the previous research on asphalt mixture fatigue.

- The asphalt modulus in Equation 2.27 is increased by 7.5 to adjust for loading rate as applied in the SST in comparison to the loading rate assumed in the models (Interstate highway traffic speeds), but the adjustment is not made in the pavement response models used to calculate stresses and strains applied in the fatigue model. Thus, the inconsistency causes significant errors in the fatigue model.

Crack Propagation

- The use of Mode II (shear) fracture propagation instead of Mode I (tensile) fracture propagation in Equation 2.30 contradicts to the wide acceptance in fracture mechanics that the physical processes causing fracture are predominately Mode I (tensile).

- The key fracture propagation material parameters A and n are not measured directly but are indirectly estimated via a combination of theory and empirical relations. The accuracy and validity of this approach are uncertain.

There are some other “areas of concern” in the calibration and validation of the model, and they are described elsewhere [9].

2.3.2 Simple Performance Test Procedure for Fatigue Cracking Developed under Task C of NCHRP 9-19

The objectives of the Task C of NCHRP 9-19 are to select, evaluate and calibrate protocols for simple performance tests that can be adopted by AASHTO to incorporate in the Superpave volumetric mix design method to evaluate an HMA mixture’s resistance to three typical distresses: permanent deformation, fatigue cracking, thermal cracking [5].

Results from the initial evaluation of different test methods, documented in an Interim Task C Report entitled “Preliminary Recommendations for the Simple Performance test”, showed that no “perfect” test method for all types of HMA mixtures placed under varying traffic and climatic conditions is available, so the different test methods were evaluated to select “a test method(s) that accurately and reliably measures a mixture response parameter(s) that is highly correlated to the occurrence of pavement distress” under varying traffic and climatic conditions. Three test methods measuring three parameters: (1) the dynamic modulus term, ($E^*/\sin\phi$) determined from the triaxial dynamic modulus test, (2) the flow time (F_T) from the triaxial static creep, and (3) the flow number (F_N) from the triaxial repeated load test, were selected as the SPT candidates for evaluating an HMA mixture’s resistance to rutting. One test method, the triaxial compression test at low test temperatures measuring dynamic modulus, and the other test method, the indirect tensile creep test measuring compliance at 1,000 seconds, were selected for evaluating an HMA mixture’s resistance to fatigue cracking and thermal cracking, respectively. These test methods and mixture response parameters are under the follow-up field validation work. However, only the process of selecting the "best" test for fatigue cracking is briefly described in this section; the others can be found elsewhere [3].

Table 2.3 shows the different test methods and material parameters that were considered in the initial evaluation for fatigue cracking, and Table 2.4 lists the test methods and response parameters that were evaluated under the test program of Task C of NCHRP 9-19 for fracture distresses.

The experimental plan was designed to investigate the manifestation of fatigue cracking, and the goal of the experimental plan was to use field projects with a diverse range of distress magnitudes to select the test methods and mixture response parameters that are most highly correlated to fatigue cracking. The following test sites were employed to evaluate the test methods for fatigue cracking: (1) lanes 1-4 of Accelerated Loading Facility (ALF) at Turner Fairbanks and (2) Sections 2, 5, 6, and 24 of WesTrack. Table 2.5 lists the target binder content, air void content, and number of passes at 100m of cracking for each lane at ALF. Table 2.6 lists the same information for the sections at Westrack and the percent fatigue cracking reported at 2.8 MEASLs. All mixtures were designed with the Superpave volumetric mixture design method.

All test specimens were prepared according to the current AASHTO Test Methods. The air void content and other volumetric properties of the specimens were matched with the in-place properties measured after placement and compaction of the HMA mixtures for each test section. The specimens were compacted using a gyratory compactor to a height of 160 mm and a diameter of 150mm. Then, test specimens, 100mm in diameter, were cored from the center of the gyratory compacted specimens, and approximately 5mm were sawed from each end. The air void tolerance used to accept or reject the test specimens for testing was ± 0.5 percent.

Table 2.3. Test Methods and Material Properties Relating to Fatigue Cracking [3]

Test Methods	Material Properties
Superpave Shear Tests	Dynamic/Resilient Modulus, Creep Compliance
Quasi/Direct Shear Tests	Dynamic/Resilient Modulus, Creep Compliance
Torsional or Rotational Shear Tests	Dynamic/Resilient Modulus, Creep Compliance
Triaxial Tests (with Constant Confining Pressures)	Dynamic/Resilient Modulus, Bulk Modulus, Creep Compliance, Poisson's Ratio
Uniaxial Unconfined Compression Tests	Dynamic/Resilient Modulus, Creep Compliance, Poisson's Ratio
Indirect Tensile Tests	Dynamic/Resilient Modulus, Secant or Tangent Modulus, Strength, Energy, Creep Compliance, Flow Time, Poisson's Ratio, Fatigue Parameters
Direct Tension Tests	Dynamic/Resilient Modulus, Secant or Tangent Modulus, Energy, Creep Compliance, Flow Time, Poisson's Ratio, Fatigue Parameters
Hydrostatic Pressure Tests	Bulk Modulus, Creep Compliance, Poisson's Ratio
Lateral Pressure Tests	Dynamic/Resilient Modulus, Bulk Modulus, Creep Compliance, Poisson's Ratio
Flexural Beam Tests	Dynamic/Resilient Modulus, Secant or Tangent Modulus, Strength, Energy, Creep Compliance, Fatigue Parameters

Table 2.4. Candidate Test Methods for Simple Performance Test for Fatigue Cracking [3]

Test Methods	Mixture Response Parameters
Dynamic Modulus Test	Dynamic Modulus
	Phase Angle
Indirect Tensile Creep Test	Creep-Compliance/Modulus
	Slope and Intercept of Creep-Compliance versus Load Time
Indirect Tensile Fatigue/Repeated Load Test	Number of Cycles to Failure
	Resilient Modulus, Total and Instantaneous
	Plastic Strain
	Slope and Intercept of Accumulated Permanent and Total Strains
Indirect Tensile Strength Test	Tensile Strength
	Tensile Strain at Failure
	Fracture Energy

Table 2.5. Target Asphalt Mixture Properties for the ALF Lanes [3]

ALF Lane	Binder Type	AC Layer Thickness, mm	Nominal Size, mm	Asphalt Content, %	Air Void Content, %	ALF Passes @ 100m of Line Cracking	
						19°C(66°F)	28°C(82°F)
1	AC-5	100	19.0	4.8	6.1	7,500	221,000
2	AC-20	100	19.0	4.9	6.5	75,000	177,000
3	AC-5	200	19.0	4.7	7.7	164,000	354,000
4	AC-20	200	19.0	4.9	9.7	544,000	528,000

Table 2.6. Target Asphalt Mixture Properties for the WesTrack Sections [3]

WesTrack Section	Binder Type	Nominal Size, mm	Asphalt Content, %	Air Void Content, %	% Cracking (2.8 MEASL)
2	PG 64-22	12.5 Fine	4.76	9.3	7
5	PG 64-22	12.5 Coarse	5.61	7.0	51
6	PG 64-22	12.5 Coarse	5.89	11.3	100
24	PG 64-22	12.5 Coarse	5.78	7.5	0

For the experimental analysis plan, statistical analyses were conducted to assess all measured laboratory responses on how they compared with observed distress measurements. The plots of the distresses for each test section versus the laboratory measured test parameters were developed. The statistical parameters of coefficient of determination (R^2), standard error of estimate (Se), and relative accuracy (Se/Sy) were used to assess trends and regression models, which were linear and nonlinear models, and the nonlinear models were based on the power law.

Finally, the research team recommended the dynamic modulus measured at low test temperatures for the follow-up field validation work because: (1) it resulted in an overall fair correlation to the measured amount of cracking, (2) it is compatible with the fatigue cracking prediction model from NCHRP Project 1-37A, and (3) it provides some consistency in the tests between rutting and cracking [3].

The criteria for interpretation and acceptance of test results for volumetric mix design are being developed in the project NCHRP 1-37A, *the 2002 Guide for Design of New and*

Rehabilitated Pavement Structures, so they are not included in this report. The detailed test specimen preparation and testing procedure for the triaxial compression test at low temperatures measuring dynamic modulus for evaluating fatigue cracking will be described in the next chapter of this report.

Dynamic Modulus of Asphalt Concrete [3]

When a continuous uniaxial sinusoidal (haversine) compressive stress is applied to an unconfined or confined viscoelastic cylindrical test specimen, as shown in figure 2.5, the stress-to-strain relationship for linear viscoelastic is defined by a complex number called the complex modulus (E*). The absolute value of the complex modulus, |E*|, is defined as the dynamic modulus, and the dynamic modulus is a ratio between the maximum (peak) dynamic stress (σ_o) and the peak recoverable axial strain (ε_o) as follows:

$$\left|E^*\right| = \frac{\sigma_o}{\varepsilon_o} \tag{2.35}$$

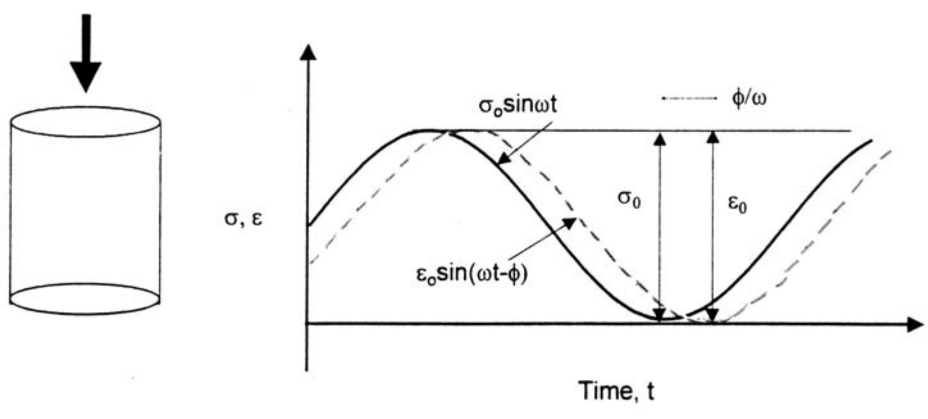

Figure 2.5. Haversine Loading Pattern for the Dynamic Modulus Test [3]

The complex modulus (E*) consists of two components: (1) the storage or elastic component (E'), which is referred to the real portion, and (2) the loss or viscous modulus (E"), which is referred to as the imaginary portion. The complex modulus can be described in the following form:

$$E^* = E' + i\,E'' \quad (2.36)$$

Using the phase angle, ϕ, the angle at which the ε_o lags behind σ_o, as an indicator of the viscous properties of the material being evaluated, Equation 2.36 can be written as follows:

$$E^* = |E^*|\,\cos\phi + i\,|E^*|\,\sin\phi \quad (2.37)$$

$$\phi = \frac{t_i}{t_p} \times (360) \quad (2.38)$$

where:

t_i = time lag between a cycle of stress and strain (sec)

t_p = time for a stress cycle (sec)

i = imaginary unit

For purely elastic materials, $\phi = 0$, and Equation 2.37 is written as follows:

$$E^* = |E^*| \quad (2.39)$$

For purely viscous materials, $\phi = 90^o$, and equation is described as follows:

$$E^* = i\,|E^*| \quad (2.40)$$

The response parameters used in the fatigue cracking analysis of HMA mixtures are $|E^*|$ and ϕ, and the stiffness factor in the analysis is $|E^*|\ \sin\phi$.

2.4 SUMMARY

This chapter provides literature review relating to the analysis and performance-based test procedures of HMA fatigue characteristics. The constitutive fracture properties were briefly discussed to characterize the fatigue behavior of HMA materials and to use mechanics in predicting the fatigue behavior of a pavement in service. The fatigue cracking in a pavement was described as a two-phase process: crack initiation and crack propagation, and the fundamental Paris' law was used to model the growth of cracking in the pavement.

The SHRP effort was the first national program trying to develop standardized performance-based test procedures for HMA mixture and a set of performance-related models for predicting pavement performance. Even though the products of the program were not ready for acceptance and use in industry, they provided a good basis for future development. The main product of the fatigue program of SHRP A-003A was an abridged analysis system, including the test equipment and procedure, for identifying performance of a trial mix in a specific condition. Nevertheless, the principal product of SHRP A-005 was a set of detailed pavement performance models, including permanent deformation, fatigue cracking, and thermal cracking models to support the specifications for asphalt binders and mixture designs.

The project NCHRP 9-19 was designed to evaluate the performance models developed in the contract SHRP A-005 and to develop a simple performance test for incorporating in the AASHTO 2002 Design Guide developed in the project NCHRP 1-37A. The conclusions of the model evaluation team on the performance models for predicting fatigue cracking in the pavement was that the Superpave performance models for fatigue cracking provided a good framework for future enhancements and that the models contained several problems and were not ready for use in industry. The candidate test for fatigue cracking proposed for use in the simple performance test was the triaxial compression test at low temperatures measuring dynamic modulus.

CHAPTER 3

TESTING PLAN

3.1 MATERIALS AND MIXTURES

This section described the materials and mixtures used in the proposed laboratory test program. One aggregate type with two nominal maximum sizes and one binder type were used in this study. The binder and air void contents were varied to determine the effects of binder and air void contents on the dynamic modulus of HMA mixture.

Aggregates

Aggregate types and sources used in this study were shown in Table 3.1, and the aggregate gradations were shown in Table 3.2 and Table 3.3.

Table 3.1. Aggregate Types and Sources

Aggregate Types	Nominal Maximum Sizes, mm	Aggregate Sources
Limestone (MCA)	12.5	McClinton-Anchor
	25.0	(Sharps)

Mixtures

One type of asphalt binder and two primary HMA mixtures typical in the State of Arkansas were used in the research, as shown in Table 3.4. The binder contents for 12.5mm mix were the optimum binder content and plus and minus 0.5 percent from the optimum binder content. The binder content for 25.0mm mix was the optimum binder content. Volumetric properties of the mixes were retested in the Asphalt Laboratory of the University of Arkansas in accordance with the AASHTO Test Method T209, "Maximum Specific Gravity of Compacted

Bituminous Mixtures," and ASTM PS131, "Standard Test Method for Bulk Specific Gravity and Density of Compacted Bituminous Mixtures Using Automatic Vacuum Sealing Method."

Table 3.2. Aggregate Gradations for the Maximum Nominal Size of 12.5mm

Sieve Size, mm	Percent Passing, % MCA
19	100
12.5	91
9.5	76
4.75	42
2.36	29
1.18	19
0.6	12
0.3	8
0.15	5
0.075	3.4

3.2 TEST SPECIMEN PREPARATION AND CONDITIONING

The mixing and compaction temperatures were selected according to the mix designs that were used in the Arkansas projects. The mixing and compaction temperatures used to prepare the specimens were shown in Table 3.5.

All mixtures were conditioned before compaction in the oven for 4 hours at 135^{o}C for short-term mixture conditioning for mechanical property testing, according to the AASHTO Designation PP2-00, "Standard Practice for Short and Long Term Aging of Hot Mix Asphalt."

Table 3.3. Aggregate Gradations for the Maximum Nominal Size of 25.0mm

Sieve Size, mm	**Percent Passing, %**
	MCA
37.5	100
25	94
19	85
12.5	74
9.5	63
4.75	32
2.36	21
1.18	14
0.6	9
0.3	6
0.15	4
0.075	3.4

Table 3.4. HMA Mixtures and Volumetric Properties

Mix ID	Nominal Size, mm	Binder Type	Binder Content, %	Max. Specific Gravity (Gmm)
MCA-12.5-0.5	12.5	ERGON PG67-22	5.5	2.409
MCA-12.5-0.0	12.5	ERGON PG67-22	6.0	2.397
MCA-12.5+0.5	12.5	ERGON PG67-22	6.5	2.376
MCA-25.0-0.0	25.0	ERGON PG67-22	5.2	2.436

Table 3.5. Mixing and Compaction Temperatures for the Mixtures

Aggregate Source	Binder Type	Mixing Temperature, ^{o}C (^{o}F)	Compaction Temperature, ^{o}C (^{o}F)
MCA	ERGON PG67-22	152 (305)	143 (290)

The samples after mixing were compacted with a Pine Gyratory Compactor in a 150 mm diameter mold to 165 mm height. The bulk specific gravity and air void content for each specimen were measured after compaction. The target air void contents for the specimens after compaction were 6.5 ± 0.5 and 9.0 ± 0.5 percent. Since these specimens were compacted to a fixed height of 165 mm, the quantity of mixture for each specimen were determined from a trial compaction program in which two specimens were prepared for each testing combination, as presented in Table 3.6.

Table 3.6. Number of Trial Specimens

Mix ID	Nominal Size, mm	Binder Content, %	Trial Specimens for 6.5% air voids	Trial Specimens for 9.0% air voids
MCA-12.5-0.5	12.5	5.5	2	2
MCA-12.5-0.0	12.5	6.0	2	2
MCA-12.5+0.5	12.5	6.5	2	2
MCA-25.0-0.0	25.0	5.2	2	2
Total Number of Specimens Prepared			**16**	

Based on the quantity of mix determined in the trial compaction program, four specimens of 150 mm diameter and 165 mm height were prepared for each testing combination, as described in Table 3.7. Then, test specimens, 100 mm in diameter, were cored from the center of the gyratory compacted specimens and approximately 7 mm were sawed from each end of the test specimens. Figure 3.1 showed a test specimen of 100 mm diameter and 150 mm height next to a compacted specimen of 150 mm diameter and 165 mm height.

The bulk specific gravity and air void content for each gyratory-compacted specimen were measured before the specimen were sawed and cored, and the bulk specific gravity and air void content for each specimen of 100 mm diameter and 150 mm height were measured before the specimen was tested according to the SPT. The detailed measured air void data were presented in Appendix A of this report. The relation between the air void contents of gyratory-compacted specimens and those of their cored specimens was presented in Figure 3.2.

Table 3.7. Number of Test Specimens

Mix ID	Nominal Size, mm	Binder Content, %	Test Specimens for 4.5% air voids	Test Specimens for 7% air voids
MCA-12.5-0.5	12.5	5.5	4	4
MCA-12.5-0.0	12.5	6.0	4	4
MCA-12.5+0.5	12.5	6.5	4	4
MCA-25.0-0.0	25.0	5.2	4	4
Total Number of Specimens Prepared			**32**	

Figure 3.3 illustrated the procedure for preparing the testing specimens, and Table 3.8 provided the criteria for acceptance and rejection of testing specimens for *Standard Test Method for Dynamic Modulus of Asphalt Concrete Mixtures for Fatigue Cracking*.

Figure 3.1. Gyratory-Compacted and Cored Specimens

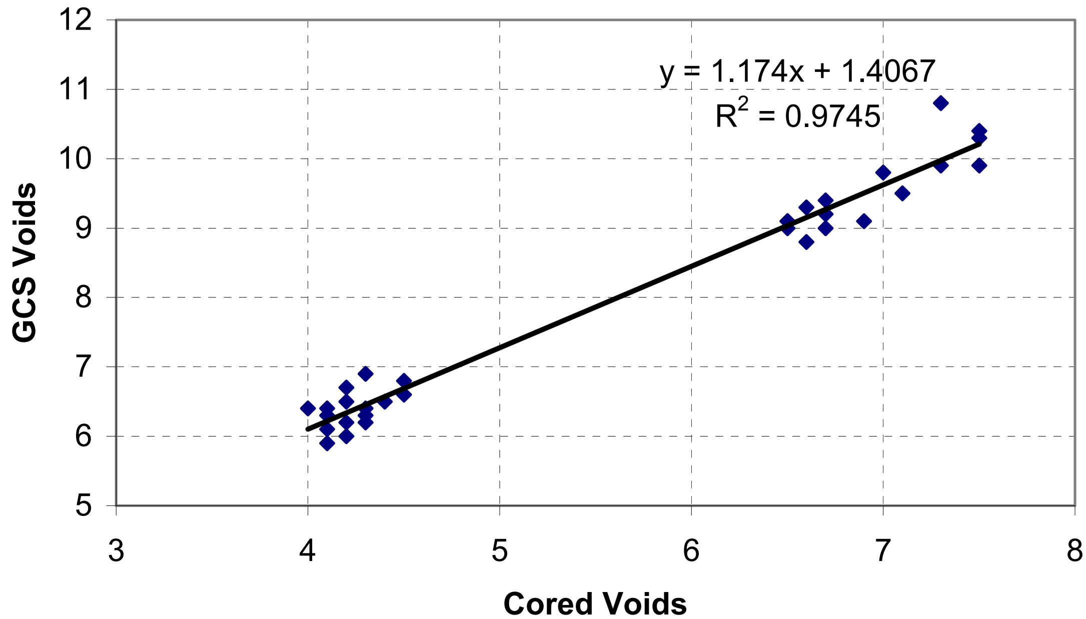

Figure 3.2. Relation Between Gyratory-Compacted and Cored Specimen Air Voids

3.3 SELECTION OF TEST PARAMETERS

This section described the parameters of the test, which were selected for this project. Even though the proposed test protocol for the SPT recommended conducting the test for dynamic modulus of HMA for fatigue cracking at one temperature, the tests were conducted at three temperatures in this project to determine the effects of temperature on dynamic modulus. Likewise, the test was conducted at six frequencies instead of one frequency, as required in the proposed test protocol. The other parameters, such as dynamic loads and cycles, were selected corresponding to the test temperatures and test frequencies, respectively. The parameters of the test were listed in Table 3.9.

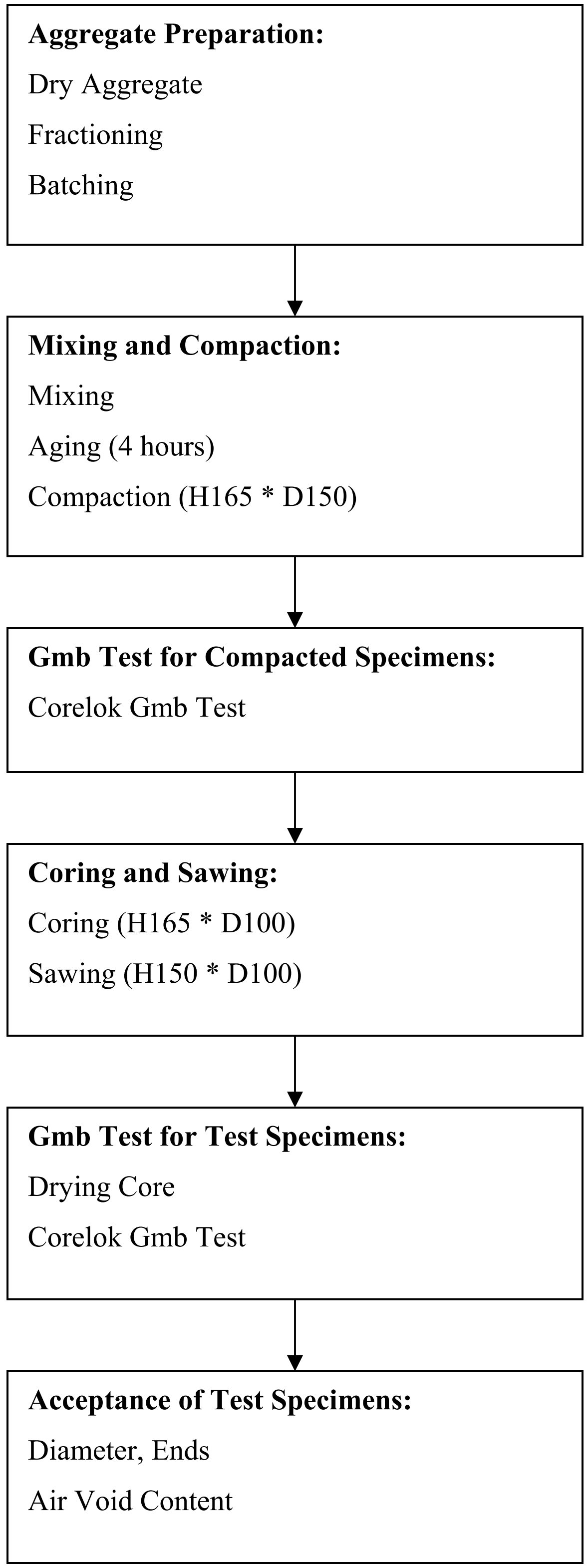

Figure 3.3. Preparation of Test Specimens [3]

Table 3.8. Criteria for Acceptance of Test Specimens [3]

Criterion Items	Requirements
Size	Size of sample: 100 mm in diameter by 150 mm in height
Coring	Nominal diameter of sample after coring: 100 mm Side of sample after coring: smooth, parallel, and free from steps, ridges, and grooves
Diameter (*)	Standard deviation of six measurements: not greater than 2.5 mm
Ends	Ends of sample after sawing: smooth and perpendicular to the axis Tolerance of a cut surface waviness height: ± 0.05 mm across any diameter Angle departing from perpendicular to axis of specimen: not more than 0.5 degrees
Air Void Content	Air Void Content of test Specimen: within 0.5 percent from the target air void content

Notes: (*) The diameters of a test specimen were measured at the mid height and third points along axes that are 90 degrees apart.

3.4 TEST PROCEDURE

Figure 3.4 illustrated the test procedure, and Figure 3.5 showed the test setup for dynamic modulus of HMA.

Table 3.9. Test Parameters [3]

Parameters	Values
Temperature (*)	At 4^o, 20^o, and 38^{o}C (40^o, 70^o, and 100^{o}F)
Frequency (**)	At 25, 10, 5, 1, 0.5, 0.1 Hz
Contact Load	5 percent of the dynamic load
Preconditioning	With 200 cycles at 25 Hz
Axial Strains	Between 50 and 150 microstrain
Dynamic Load (***)	At 4^{o}C (40^{o}F): 700 to 1400 kPa (100 to 200 psi)
	At 20^{o}C (70^{o}F): 350 to 700 kPa (50 to 100 psi)
	At 38^{o}C (100^{o}F): 140 to 250 kPa (20 to 50 psi)
Cycles	At 25 Hz: 200 cycles
	At 10 Hz: 200 cycles
	At 5 Hz: 100 cycles
	At 1 Hz: 20 cycles
	At 0.5 Hz: 15 cycles
	At 0.1Hz: 15 cycles

(*, **) The proposed standard required only one test at one effective pavement temperature T_{eff} in the range of 4^o to 20^{o}C (39^o to 70^{o}F), and at one design frequency in the range of 5 to 20Hz.

(***) The dynamic load should be adjusted to obtain axial strains between 50 and 150 microstrain.

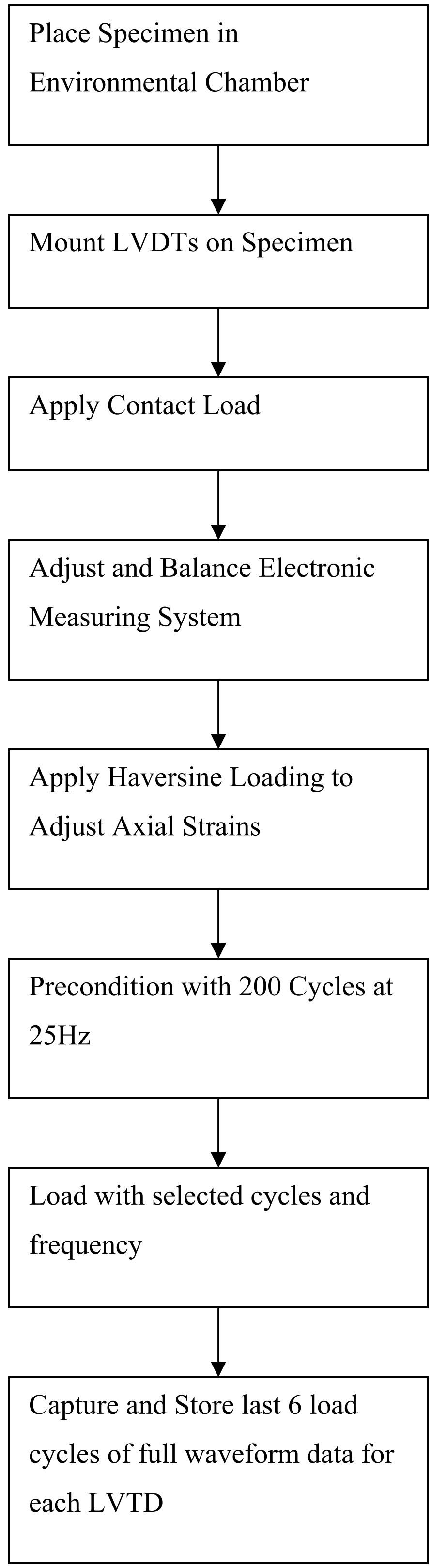

Figure 3.4. Test Procedure for Dynamic Modulus of HMA for Fatigue Cracking [3]

Figure 3.5. Test Setup for Dynamic Modulus of HMA for Fatigue Cracking

3.5 SUMMARY

One aggregate type with two nominal maximum sizes and one binder type were used in this study. The binder and air void contents were varied to determine the effects of binder and air void contents on the dynamic modulus or fatigue characteristics of HMA mixture. One type of asphalt binder and two primary HMA mixtures typical in the state of Arkansas were used in the research. The binder contents for the 12.5 mm mix were the optimum binder content and plus and minus 0.5 percent from the optimum binder content, and the binder content for the 25.0 mm mix was the optimum binder content.

The preparation of test specimens was in two steps. First, a trial compaction program was conducted to determine the quantity of mix with which the test specimens in 150 mm diameter and 165 mm height were prepared to meet the target air void contents of 6.5 ± 0.5 and 9.0 ± 0.5 percent. Then, the test specimens, 100 mm in diameter, were cored from the center of the gyratory compacted specimens and approximately 7 mm were sawed from each end of the test specimens.

Air void contents for each gyratory-compacted specimen and each cored specimen were measured, and the relation between the air void contents of gyratory-compacted specimens and those of their cored specimens was presented in this chapter.

The tests were conducted at three temperatures at six different frequencies in this project. The other parameters, such as dynamic loads, and cycles, were selected corresponding to the test temperatures and frequencies.

CHAPTER 4

LABORATORY TEST RESULTS AND ANALYSIS

4.1 DYNAMIC MODULUS TEST RESULTS

A sample of raw data over last six loading cycles of one test condition, which is obtained from the MTS data files, is presented in Figure 4.1. The dynamic modulus was then calculated from the raw data using a Microsoft Excel macro, which was programmed using Visual Basic for Applications. The macro was able to read the raw data into the spreadsheet and then fit the sinusoidal equations to the recoded loading, LVDT 1, and LVDT 2 data:

$$y = a\sin(\omega t - b) - c \qquad (4.1)$$

where:

y	= predicted value of loading or displacement
a, c	= fitting parameters, lbf or in.
ω, b	= fitting parameters, rad.
t	= time, sec

Figure 4.2 shows an example of the loading curve constructed using the sinusoidal function. In the figure, the raw data were also graphed for comparison.

The peak stress and peak strain were calculated from the peak loading and peak displacement obtained from the fitted sinusoidal functions. Likewise, the time lag between a cycle of stress and strain and the time for a stress cycle were determined from the fitted sinusoidal functions. The dynamic modulus and phase angle were then calculated using Equations 2.35 and 2.38, and the calculated dynamic moduli and phase angles were presented in Appendix A.

MTS793|MPT|ENU|1|2|.|/|:|1|0|0|A

Cyclic Acquisition		Time: 30.030762 Sec	
Stored at: 194 cycle		Stored for: 12 segments	
Points: 246			
Time	Load	LVDT 1	LVDT 2
Sec	lbf	in	in
7.7722168	-1692.3267	0.0004394897	0.0002474169
7.7731934	-1787.1628	0.00043454816	0.0003126676
7.7741699	-1865.2141	0.0004663594	0.00035208592
....	....	....	....

Figure 4.1. Sample of Raw Data Obtained from MTS Data Files

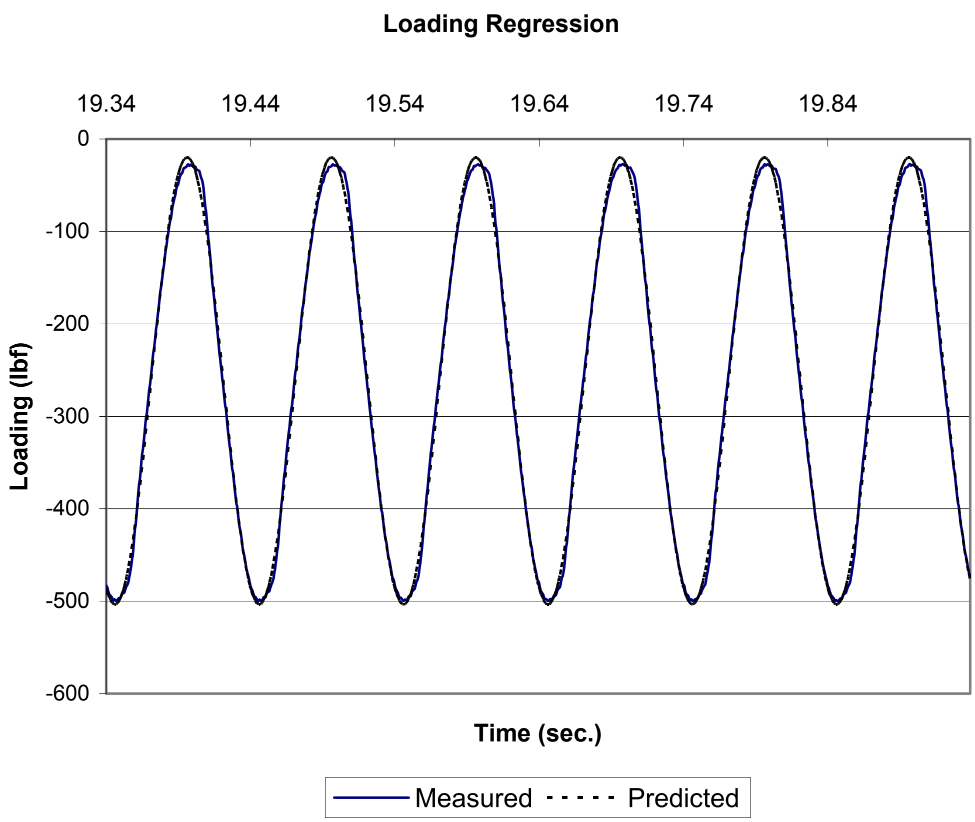

Figure 4.2. Example of Fitted Loading Curve

4.2 ANALYSIS PLAN

Based on the test results presented in Appendix A, the numerical descriptive measures such as mean, variance, standard deviation, and standard error for each set of four replicates were calculated in Appendices B and C. Moreover, the sample coefficient of variance was calculated to evaluate the accuracy of the average dynamic modulus as follows:

$$cv = \frac{s}{\bar{x}} \times 100 \tag{4.1}$$

where:

cv = sample coefficient of variance (%)

s = sample standard deviation

$\bar{x}$ = sample mean

Due to the time limitation of this project, only four types of mixes using one source of aggregate were tested, as listed in Table 4.1. Since the mixtures with the binder contents of plus and minus 0.5 percent from the optimum were not tested on 25.0 mm aggregate type, the full-scale ANOVA test could not be conducted on this source of aggregate. Therefore, in order to evaluate the effects of aggregate size, binder content, air void content, temperature and frequency on the dynamic modulus, there were three statistical tests conducted. The dynamic modulus data sets and main effects evaluated in each ANOVA test are listed in Table 4.2.

The ANOVA tests were first run on all test data without any transformation, and the normality check of test data showed that the test data did not exhibit normal distribution. Therefore, the rank transformation was used to normalize the test data prior to running ANOVA tests.

Table 4.1. Tested HMA Mixtures

Mix ID	Nominal Size, mm	Binder Content, %
MCA-12.5-0.5	12.5	5.5
MCA-12.5-0.0	12.5	6.0
MCA-12.5+0.5	12.5	6.5
MCA-25.0-0.0	25.0	5.2

Table 4.2. Data Sets and Main Effects of ANOVA Tests

ANOVA Test	Data Tested on	Main Effects	Variation Levels
No. 1	MCA-12.5-0.0	Aggregate size	12.5 and 25.0 mm
	MCA-25.0-0.0	Air voids	4.5 and 7.0%
		Temperature	40, 70, and 100^{o}F
		Frequency	25, 10, 5, 1, 0.5, and 0.1Hz
No. 2	MCA-12.5-0.5	Binder content	-0.5, Opt, and +0.5%
	MCA-12.5-0.0	Air voids	4.5 and 7.0%
	MCA-12.5+0.5	Temperature	40, 70, and 100^{o}F
		Frequency	25, 10, 5, 1, 0.5, and 0.1Hz
No. 3	MCA-12.5-0.5	Air voids	4.5 and 7.0%
	MCA-12.5-0.0	Temperature	40, 70, and 100^{o}F
	MCA-12.5+0.5	Frequency	25, 10, 5, 1, 0.5, and 0.1Hz
	MCA-25.0-0.0	Aggregate + Binder (block)	12-0.5, 12-0.0, 12+0.5, 25-0.0

- **ANOVA Test 1**

As afore-presented in Table 4.2, this ANOVA test is designed to evaluate the effects of aggregate size, air voids, temperature, and frequency on dynamic modulus. The test data used in this analysis are the dynamic moduli tested on 12.5 mm and 25.0 mm mixes at the optimum binder content.

- Analysis method

  The multi-factor ANOVA with rank transformation is used. The SAS program for Test 1 is presented in Appendix D.

- Fixed effect model

$$y_{ijklm} = \mu + a_i + b_j + (ab)_{ij} + c_k + (ac)_{ik} + (bc)_{jk} + (abc)_{ijk} + d_l + (ad)_{il} + (bd)_{jl} + (abd)_{ijl} + (cd)_{kl} + (acd)_{ikl} + (bcd)_{jkl} + (abcd)_{ijkl} + \varepsilon_{ijklm}$$

where:

y_{ijklm} = dynamic modulus

a = aggregate size varied at two levels (12.5 and 25.0 mm)

b = air voids varied at two levels (4.5 and 7.0%)

c = temperature varied at three levels (40, 70, and 100^{o}F)

d = frequency varied at six levels (25, 10, 5, 1, 0.5, and 0.1Hz)

m = number of replicates (4)

- Assumption

  ε_{ijklm} are NID(0, σ^2)

- Significance level

  $\alpha = 0.05$

- **ANOVA Test 2**

As afore-presented in Table 4.2, this ANOVA test is designed to evaluate the effects of binder content, air voids, temperature, and frequency on dynamic modulus. The test data used in this analysis are the dynamic moduli tested on 12.5 mm mixes at the optimum binder content, as well as plus and minus 0.5 % from the optimum.

- Analysis method

  The multi-factor ANOVA with rank transformation is used. The SAS program for Test 2 is presented in Appendix E.

- Fixed effect model

$$y_{ijklm} = \mu + a_i + b_j + (ab)_{ij} + c_k + (ac)_{ik} + (bc)_{jk} + (abc)_{ijk} + d_l + (ad)_{il} + (bd)_{jl} + (abd)_{ijl} + (cd)_{kl} + (acd)_{ikl} + (bcd)_{jkl} + (abcd)_{ijkl} + \varepsilon_{ijklm}$$

where:

y_{ijklm} = dynamic modulus

a = binder content varied at three levels (-0.5% , opt., and +0.5%)

b = air voids varied at two levels (4.5 and 7.0%)

c = temperature varied at three levels (40, 70, and 100^{o}F)

d = frequency varied at six levels (25, 10, 5, 1, 0.5, and 0.1Hz)

m = number of replicates (4)

- Assumption

  ε_{ijklm} are NID(0, σ^2)

- Significance level

  $\alpha = 0.05$

- **ANOVA Test 3**

As afore-presented in Table 4.2, this ANOVA test is designed to evaluate the effects of air voids, temperature, and frequency on dynamic modulus. The test data used in this analysis are all of dynamic moduli tested. However, the aggregate size and binder content are the factors that also affect the magnitude of dynamic modulus, but they are not the main effects that are evaluated in this analysis because of missing of data. Therefore, these factors are considered as the blocked factors in this analysis.

- Analysis method

  The multi-factor ANOVA with rank transformation is used. The SAS program for Test 3 is presented in Appendix F.

- Fixed effect model

  $$y_{ijklm} = \mu + a_i + b_j + (ab)_{ij} + c_k + (ac)_{ik} + (bc)_{jk} + (abc)_{ijk} + d_l + \varepsilon_{ijklm}$$

  where:

y_{ijklm}	= dynamic modulus
a	= air voids varied at two levels (4.5 and 7.0%)
b	= temperature varied at three levels (40, 70, and 100^{o}F)
c	= frequency varied at six levels (25, 10, 5, 1, 0.5, and 0.1Hz)
d	= mix type varied at four levels (12.5-0.5, 12.5opt, 12.5+0.5, 25opt)
m	= number of replicates (4)

- Assumption

  ε_{ijklm} are NID(0, σ^2)

- Significance level

  $\alpha = 0.05$

4.3 DATA ANALYSIS

This section summarizes the findings about the test accuracy and the effects of aggregate size, binder content, air void content, temperature and frequency on the dynamic modulus.

4.3.1 Test Accuracy

The accuracy of the average dynamic modulus evaluated by the sample coefficient of variance, which was calculated using Equation 4.1, should be within ± 15 % as required by the test method specification. According to the detailed calculation, as presented in Appendix B, most of the sample coefficients of variance are within the limit. Table 4.3 shows the summary of the sample coefficients of variance of test results. However, the occurrence of data sets, whose coefficient of variance is slightly out of limit, seems to be random in this analysis.

Table 4.3. Summary of Sample Coefficients of Variance of Test Results

Accuracy Limit	No. of Coefficients	Percentage
≤ 15 %	124	86.11 %
> 15 % and < 16 %	20	13.89 %
Total	**144**	**100 %**

Figure 4.3 shows the relation between coefficients of variance and test temperatures, and Figure 4.4 shows the relation between coefficients of variance and frequencies. The coefficients of variances are higher when the dynamic modulus tests are run at high temperatures or high frequencies. This occurrence can be explained by the working mechanism of asphalt mixtures at different temperatures. At low temperatures, the stiffness of mixture is dependent of the stiffness of the binder. At high temperatures, the aggregate skeleton develops its effects on the stiffness of

the mixture, and the aggregate skeleton is changeable for different mixtures. Therefore, the variance of mix stiffness is higher at high temperatures.

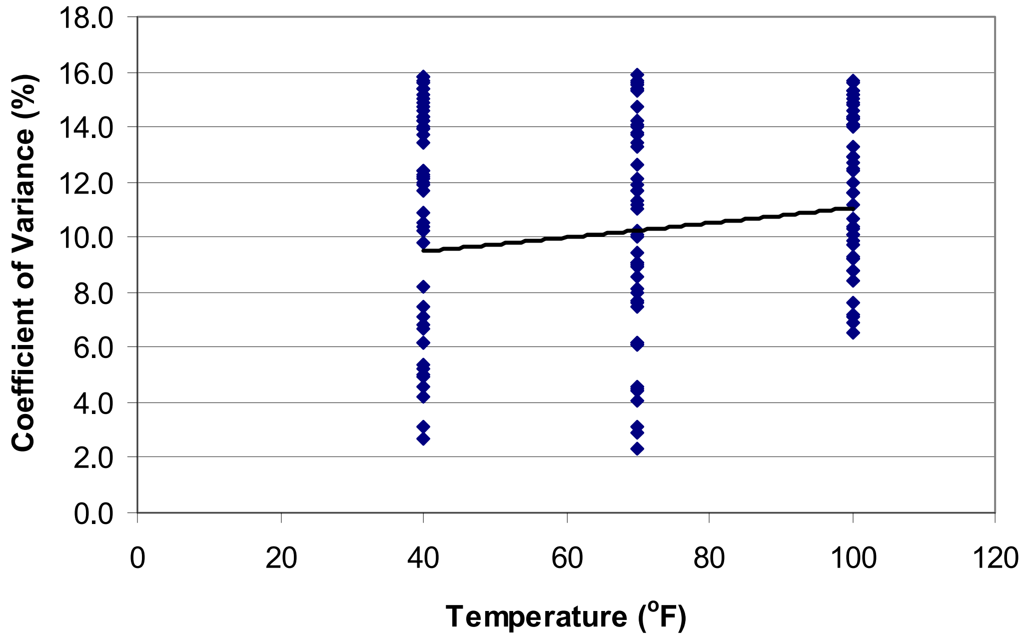

Figure 4.3. Coefficient of Variance vs. Test Temperature

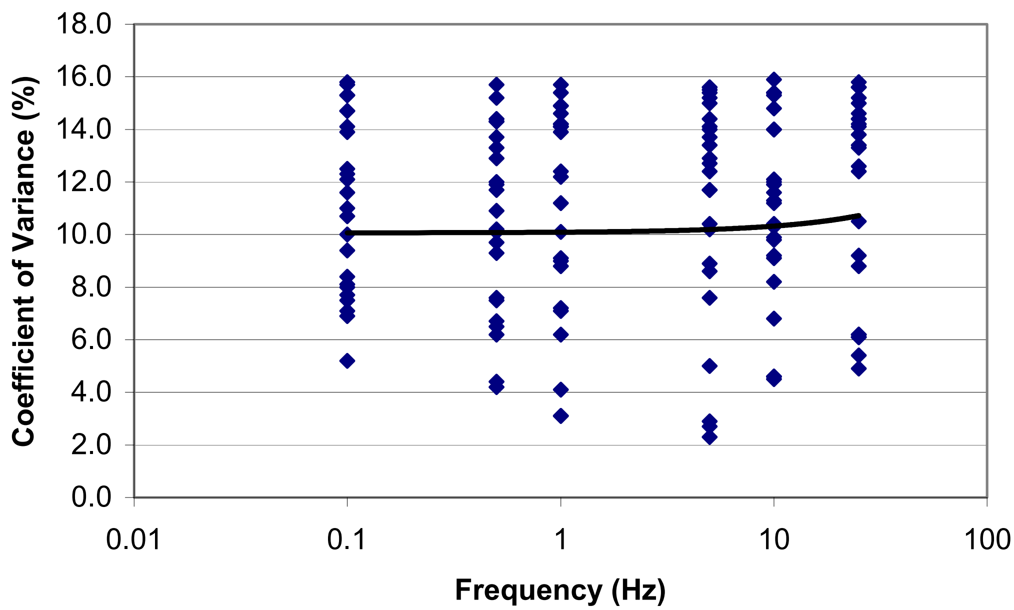

Figure 4.4. Coefficient of Variance vs. Frequency

4.3.2 ANOVA Test 1

The ANOVA table for test 1 is shown in Table 4.5. The test statistic is significant when the P-value is smaller than the level of significance $\alpha = 0.05$ as follows:

- There is a significant four-way interaction between aggregate size, air void content, test temperature, and test frequency.
- There is a significant three-way interaction between air void content, test temperature, and test frequency.
- There are three significant two-way interactions between test temperature and test frequency, between air void content and test frequency, and between aggregate size and air void content.
- All main effects of aggregate size, air void content, test temperature, and test frequency are also significant.

The Duncan's test results for test 1 are summarized in Table 4.4. The Duncan's test results confirm the significance of every test variation level for all main effects.

Table 4.4. Duncan's Test for ANOVA Test 1

Factors	**Duncan's Test**					
Aggregate Size	12.5	25.0				
Air Void Content	4.5	7.0				
Test Temperature	40	70	100			
Test Frequency	25	10	5	1	0.5	0.1

Table 4.5. ANOVA Table for ANOVA Test 1

Source	DF	Type I SS	Mean Square	F Value	P-value	
AGGSZ	1	22120.1	22120.1	117.54	<.0001	*
AVOID	1	23871.1	23871.1	126.84	<.0001	*
AGGSZ*AVOID	1	36405.0	36405.0	193.44	<.0001	*
TEMP	2	1229045.7	614522.8	3265.28	<.0001	*
AGGSZ*TEMP	2	13.8	6.9	0.04	0.9640	
AVOID*TEMP	2	713.3	356.6	1.89	0.1528	
AGGSZ*AVOID*TEMP	2	542.7	271.4	1.44	0.2388	
FREQ	5	595986.8	119197.4	633.36	<.0001	*
AGGSZ*FREQ	5	787.6	157.5	0.84	0.5247	
AVOID*FREQ	5	3051.3	610.3	3.24	0.0076	*
AGGSZ*AVOID*FREQ	5	226.3	45.3	0.24	0.9442	
TEMP*FREQ	10	27467.4	2746.7	14.59	<.0001	*
AGGSZ*TEMP*FREQ	10	1481.0	148.1	0.79	0.6414	
AVOID*TEMP*FREQ	10	3902.9	390.3	2.07	0.0277	*
AGGS*AVOID*TEMP*FREQ	10	4366.1	436.6	2.32	0.0130	*

From ANOVA test 1, the effects of the main effects are concluded as follows:

- 25 mm HMA has a higher dynamic modulus than 12.5 mm HMA, as shown in Figure 4.5.
- Specimens compacted at 4.5 percent air voids have higher dynamic moduli than specimens at 7 percent air voids, as shown in Figure 4.6.
- HMA is stiffer at lower temperatures, as shown in Figure 4.7.
- HMA has higher dynamic moduli at higher frequencies, as shown in Figure 4.8.

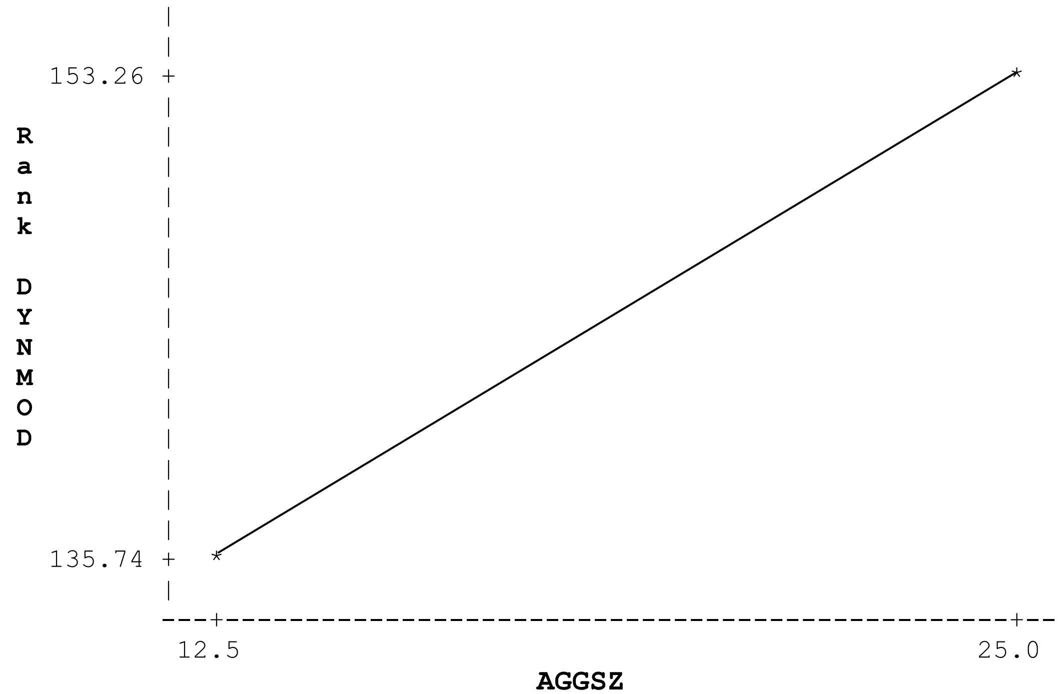

Figure 4.5. Effects of Aggregate Size on Dynamic Modulus

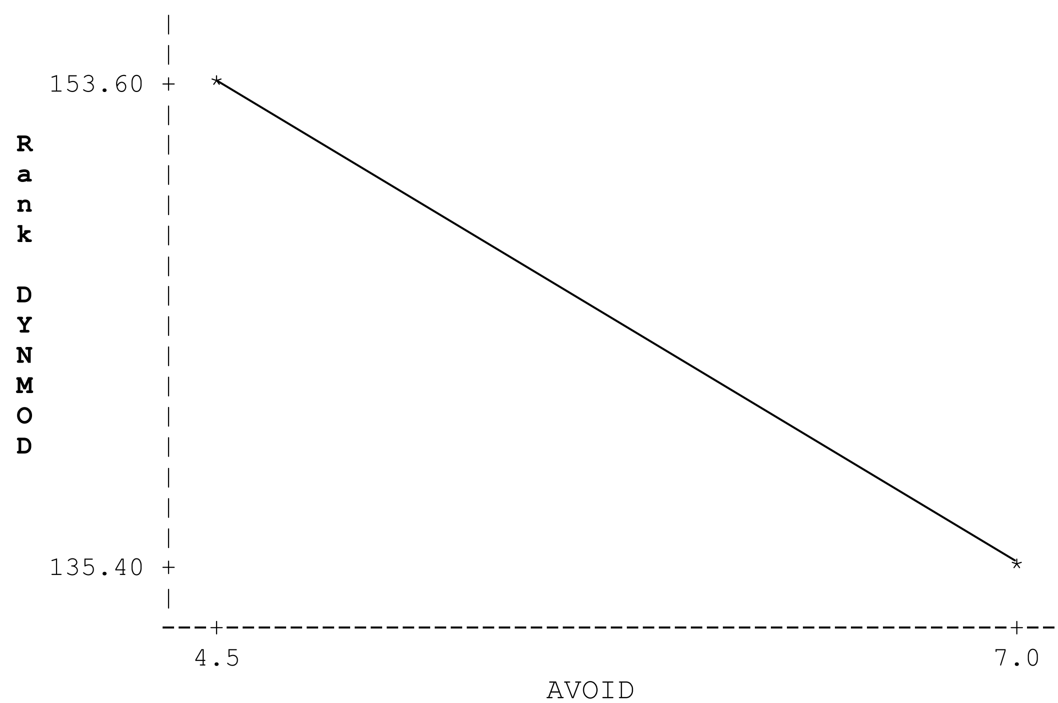

Figure 4.6. Effects of Air Voids on Dynamic Modulus

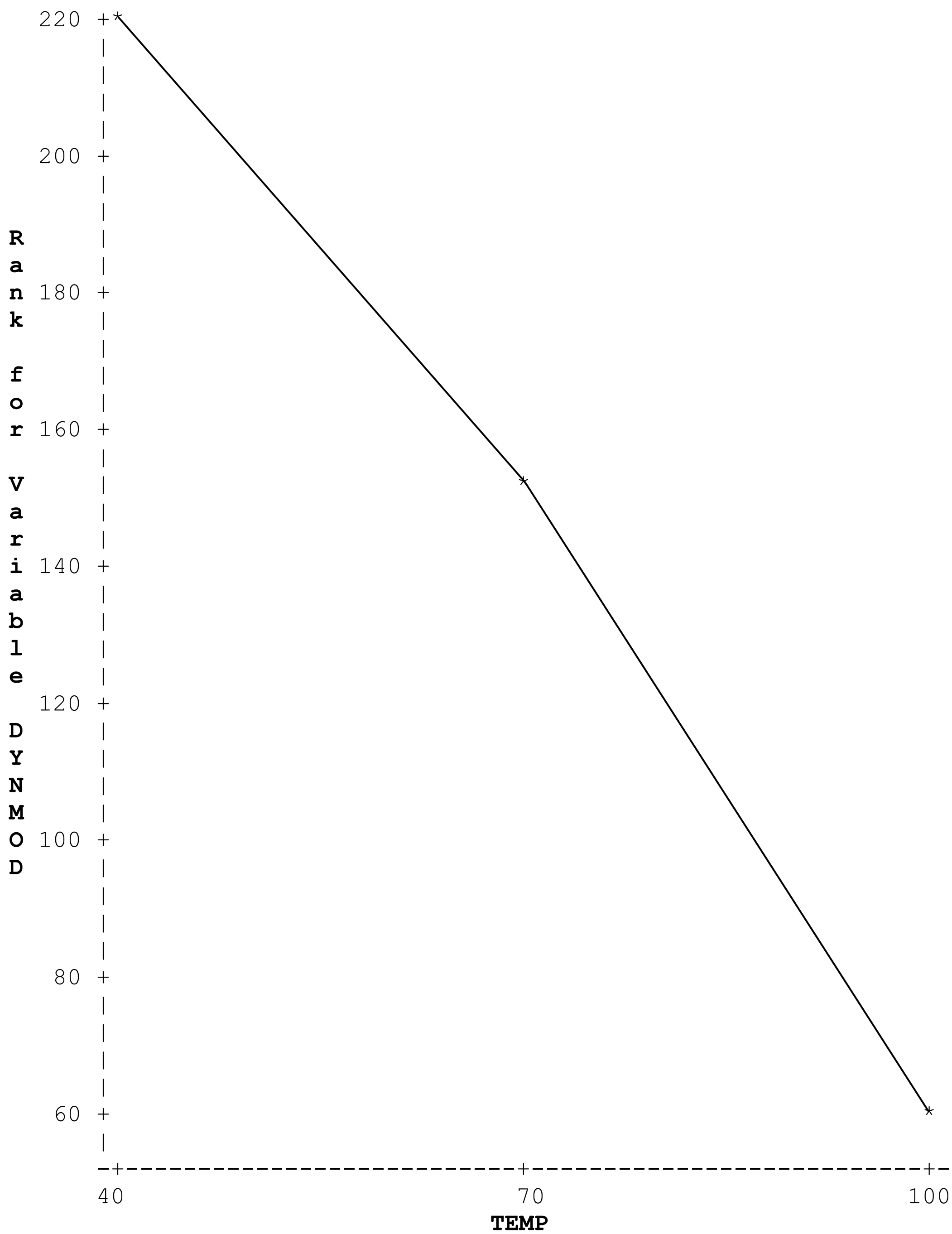

Figure 4.7. Effects of Temperature on Dynamic Modulus

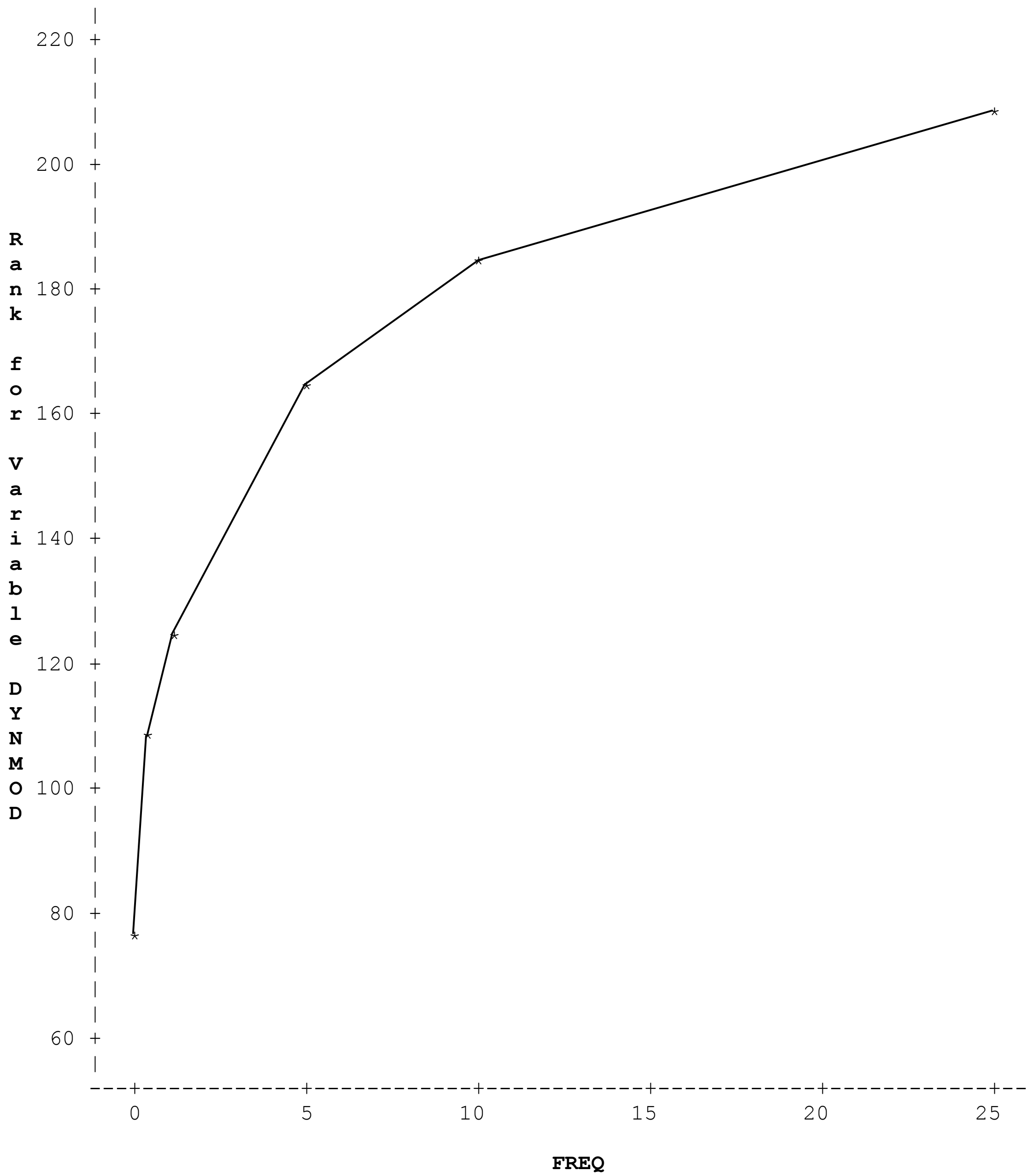

Figure 4.8. Effects of Frequency on Dynamic Modulus

A check of the normality assumption may be made by constructing a normal probability plot of the residuals. If the error distribution is normal, this plot will resemble a straight line. In visualizing the straight line, place more emphasis on the central values of the plot than on the extremes. Therefore, even though there are some points standing out on the extremes of the normal probability plot, as presented in Figure 4.9, there is no big trouble with the central part of the graph, so the normality assumption is justified. Moreover, the plot of residuals versus time and plot of residuals versus fitted values do not reveal any obvious pattern, so the independent assumption and the constant variance are justified.

```
     37.5+                                                  *
         |                                              ** *
         |                                          **** ++++
     22.5+                                        ***++++
         |                                      +**+
         |                                  +****
      7.5+                              +*****
         |                         *******
         |                    ******
     -7.5+                *****
         |            *****
         |       *****+
    -22.5+    ***++
         |+++*
         | *
    -37.5+*
          +----+----+----+----+----+----+----+----+----+----+
              -2        -1         0        +1        +2
```

Figure 4.9. Normal Probability Plot of ANOVA Test 1

4.3.3 ANOVA Test 2

The ANOVA table for test 2 is shown in Table 4.6. The test statistic is significant when the P-value is smaller than the level of significance $\alpha = 0.05$ as follows:

- There is a significant three-way interaction between binder content, test temperature, and test frequency.

- There are four significant two-way interactions between test temperature and test frequency, between air void content and test temperature, between binder content and test temperature, and between binder content and air void content.
- All main effects of binder content, air void content, test temperature, and test frequency are also significant.

Table 4.6. ANOVA Table for ANOVA Test 2

Source	DF	Type I SS	Mean Square	F Value	P-value	
BINDC	2	157720.4	78860.2	189.26	<.0001	*
AVOID	1	3663.3	3663.3	8.79	0.0033	*
BINDC*AVOID	2	11933.8	5966.9	14.32	<.0001	*
TEMP	2	4373336.6	2186668.3	5247.79	<.0001	*
BINDC*TEMP	4	15805.8	3951.4	9.48	<.0001	*
AVOID*TEMP	2	6584.6	3292.3	7.90	0.0004	*
BINDC*AVOID*TEMP	4	2010.3	502.6	1.21	0.3080	
FREQ	5	1908313.6	381662.7	915.95	<.0001	*
BINDC*FREQ	10	1868.9	186.9	0.45	0.9215	
AVOID*FREQ	5	3589.6	717.9	1.72	0.1288	
BINDC*AVOID*FREQ	10	1740.9	174.1	0.42	0.9378	
TEMP*FREQ	10	77428.1	7742.8	18.58	<.0001	*
BINDC*TEMP*FREQ	20	14917.1	745.9	1.79	0.0207	*
AVOID*TEMP*FREQ	10	937.0	93.7	0.22	0.9938	
BIND*AVOID*TEMP*FREQ	20	3572.4	178.6	0.43	0.9862	

The Duncan's test results for test 2 are summarized in Table 4.7. The Duncan's test results confirm the significance of every test variation level for all main effects.

Table 4.7. Duncan's Test for ANOVA Test 2

Factors	**Duncan's Test**					
Binder Content	-0.5	Opt	+0.5			
Air Voids	4.5	7.0				
Temperature	40	70	100			
Frequency	25	10	5	1	0.5	0.1

From ANOVA test 2, the effects of the main effects are concluded as follows:

- For this 12.5 mm HMA, the mix is stiffer when the binder content is 0.5 percent lower than the optimum, and the mix is less stiff when the binder content is 0.5 percent higher than the optimum, as shown in Figure 4.10.
- The conclusions on the effects of air voids, temperature and frequency from ANOVA test 2 are same as those from ANOVA test 1.

Even though there are some points standing out in the normal probability plot, as presented in Figure 4.11, there is no big trouble with the central part of the graph, so the normality assumption is justified. The independent assumption and constant variance are also justified using the plot of residuals versus time and the plot of residuals versus fitted values.

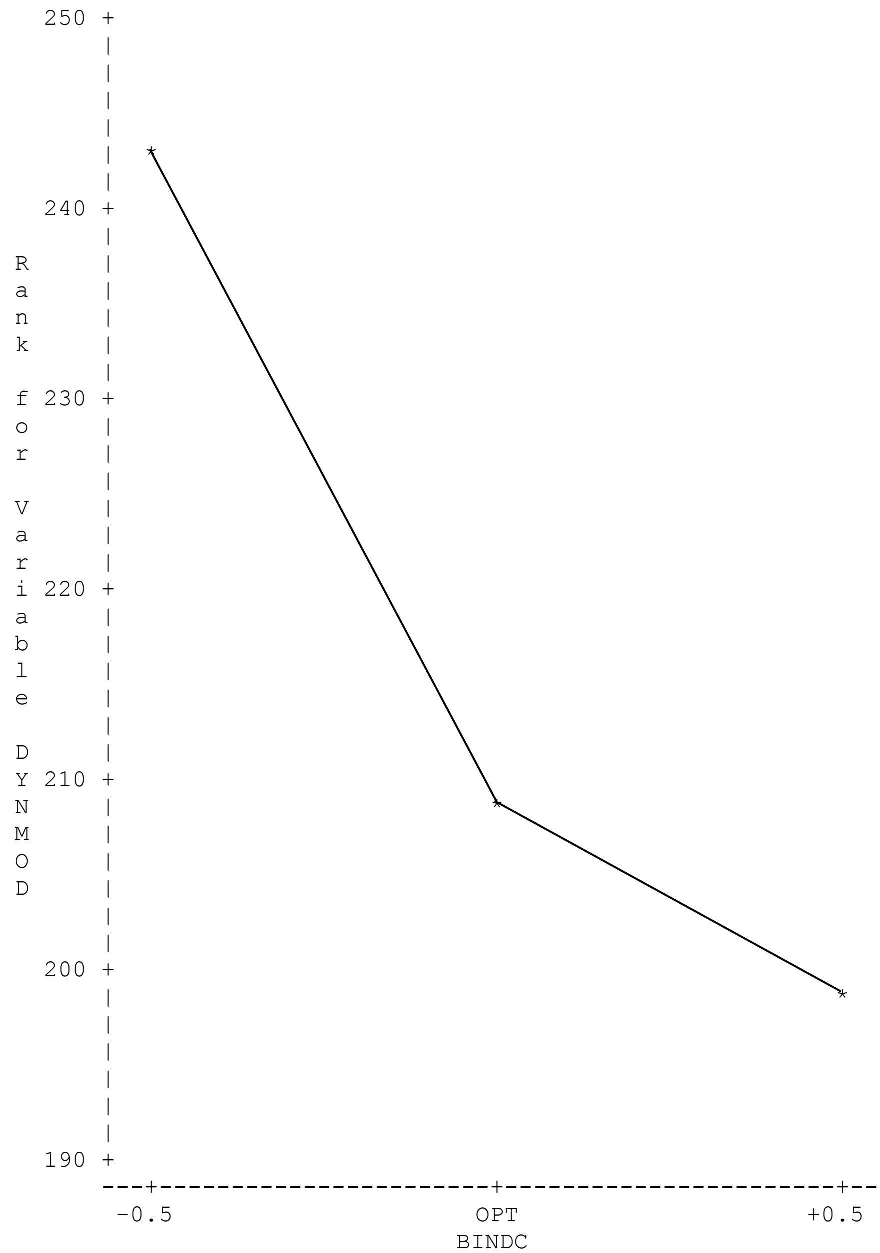

Figure 4.10. Effects of Binder Content on Dynamic Modulus

```
 57.5+                                                  *
     |                                                  *
     |                                                 *
     |                                            *****++
     |                                          ***+++
     |                                        **+++
     |                                      ***+
 22.5+                                     **+
     |                                  +***
     |                               +****
     |                            +****
     |                         *****
     |                      ****
     |                   ****
-12.5+                ****
     |            *****
     |          ***+
     |       ****
     |    ****+
     |   **+
     |****
-47.5+*
      +----+----+----+----+----+----+----+----+----+----+
          -2        -1         0        +1        +2
```

Figure 4.11. Normal Probability Plot of ANOVA Test 2

4.3.4 ANOVA Test 3

The ANOVA table for test 3 is shown in Table 4.8. The test statistic is significant when the P-value is smaller than the level of significance $\alpha = 0.05$ as follows:

- There are two significant two-way interactions between test temperature and test frequency, between air void content and test temperature.
- All main effects of air void content, test temperature, and test frequency are also significant.

The Duncan's test results for test 3 are summarized in Table 4.9. The Duncan's test results confirm the significance of every test variation level for all main effects.

The conclusions on the effects of air voids, temperature and frequency from ANOVA test 3 are same as those from ANOVA tests 1 and 2.

Table 4.8. ANOVA Table for ANOVA Test 3

Source	DF	Type I SS	Mean Square	F Value	P-value	
AVOID	1	96980.3	96980.3	86.53	<.0001	*
TEMP	2	10080452.0	5040226.0	4497.29	<.0001	*
AVOID*TEMP	2	7770.5	3885.3	3.47	0.0319	*
FREQ	5	4586260.6	917252.1	818.45	<.0001	*
AVOID*FREQ	5	12003.9	2400.8	2.14	0.0591	
TEMP*FREQ	10	190035.0	19003.5	16.96	<.0001	*
AVOID*TEMP*FREQ	10	11069.2	1106.9	0.99	0.4529	
MIX	3	338799.7	112933.2	100.77	<.0001	*

Table 4.9. Duncan’s Test for ANOVA Test 3

Factors	Duncan’s Test					
Air Voids	4.5	7.0				
Temperature	40	70	100			
Frequency	25	10	5	1	0.5	0.1

Even though there are some points standing out in the normal probability plot, as presented in Figure 4.12, there is no big trouble with the central part of the graph, so the normality assumption is justified. The independent assumption and constant variance are also justified using the plot of residuals versus time and the plot of residuals versus fitted values.

```
135+                                                  *
   |
   |                                                  *
   |                                                **
   |                                              *** +
   |                                             **+++
   |                                           **++
   |                                        ****
   |                                      +**
   |                                  ******
 25+                                ***
   |                            *****
   |                         ****
   |                      ****
   |                   ****
   |                ****
   |             ****
   |        ******
   |    *****+
   |  ***++
   |***+
-85+*
    +----+----+----+----+----+----+----+----+----+----+
        -2        -1         0        +1        +2
```

Figure 4.12. Normal Probability Plot of ANOVA Test 3

4.4 ENGINEERING EVALUATION OF DATA ANALYSIS

The coefficients of variances are higher when the dynamic modulus tests are run at high temperatures or high frequencies. Since most of the sample coefficients of variance are within the limit, the performance of dynamic modulus test using available test equipments may be considered acceptable. The accuracy of the test results will be enhanced with the improvements of specimen preparation procedures and testing equipments in the future project.

All main affects of aggregate size, binder content, air void content, test temperature, and test frequency are significant as follows:

- 25 mm HMA has a higher dynamic modulus than 12.5 mm HMA.
- For this 12.5 mm HMA, the mix is stiffer when the binder content is 0.5 percent lower than the optimum, and the mix is less stiff when the binder content is 0.5 percent higher than the optimum.
- Specimens compacted at 4.5 percent air voids have higher dynamic moduli than specimens at 7 percent air voids.
- HMA is stiffer at lower temperatures.
- HMA has higher dynamic moduli at higher frequencies.

The above statistical analysis results show reasonable tendencies of asphalt mixture stiffness to change due to the changes of test parameters. Since all of test parameters varied in the experimental plan are significant, no test parameter may be eliminated from future research efforts.

CHAPTER 5

GRAPHIC PRESENTATION OF DYNAMIC MODULUS

5.1 ISOTHERMAL AND ISOCHRONAL CURVES

Dynamic modulus test results can be presented in the graphs of isothermal curves and isochronal curves [15]. Figures 5.1, 5.2, 5.3 and 5.4 shows the isothermal curves of dynamic modulus test results. Figures 5.5, 5.6, 5.7 and 5.8 shows the isochronal curves of dynamic modulus test results.

From the graphs of isothermal and isochronal curves, the conclusions on the effects of air voids, temperature and frequency on dynamic modulus can be verified as follows:

- Specimens compacted at 4.5 percent air voids have higher dynamic moduli than specimens at 7 percent air voids.
- HMA is stiffer at lower temperatures.
- HMA has higher dynamic moduli at higher frequencies.

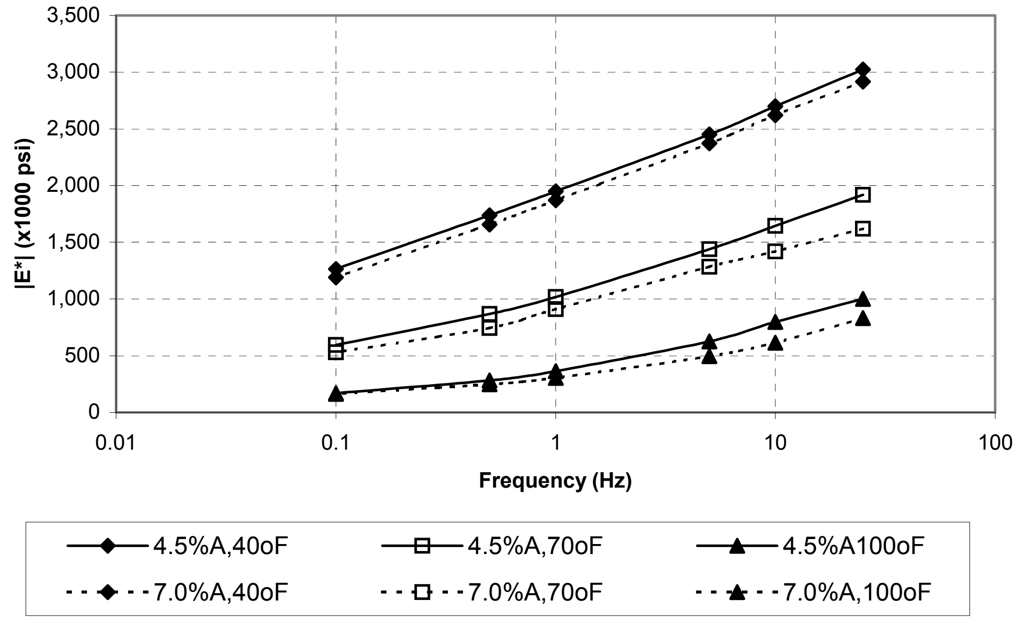

Figure 5.1. Isothermal Curves of Dynamic Modulus Test Results

of 12.5 mm Mix @ Opt - 0.5 Percent Binder Content

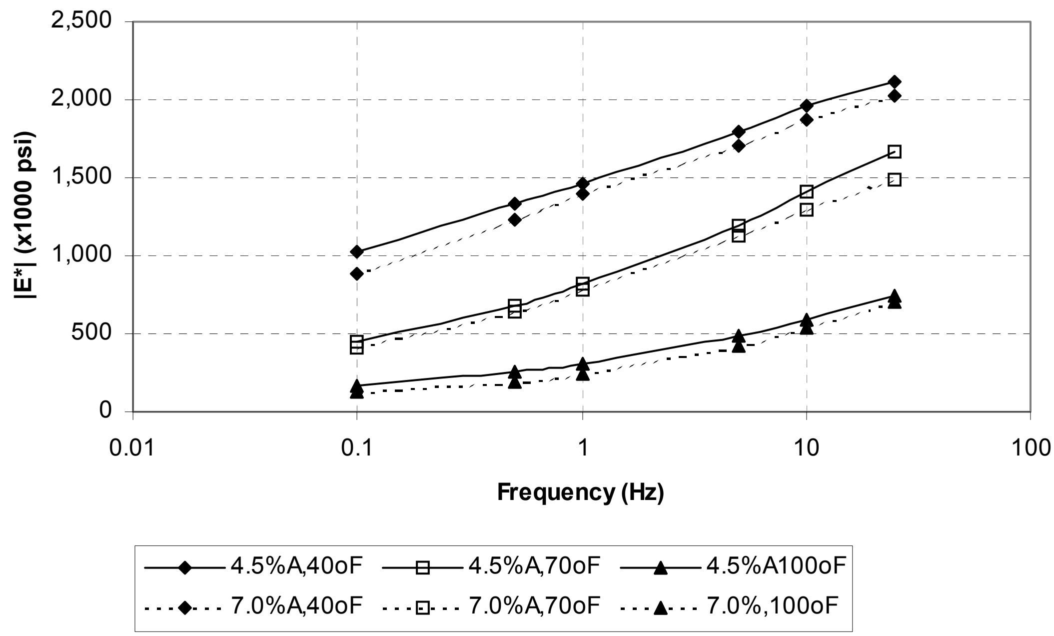

Figure 5.2. Isothermal Curves of Dynamic Modulus Test Results

of 12.5 mm Mix @ Optimum Binder Content

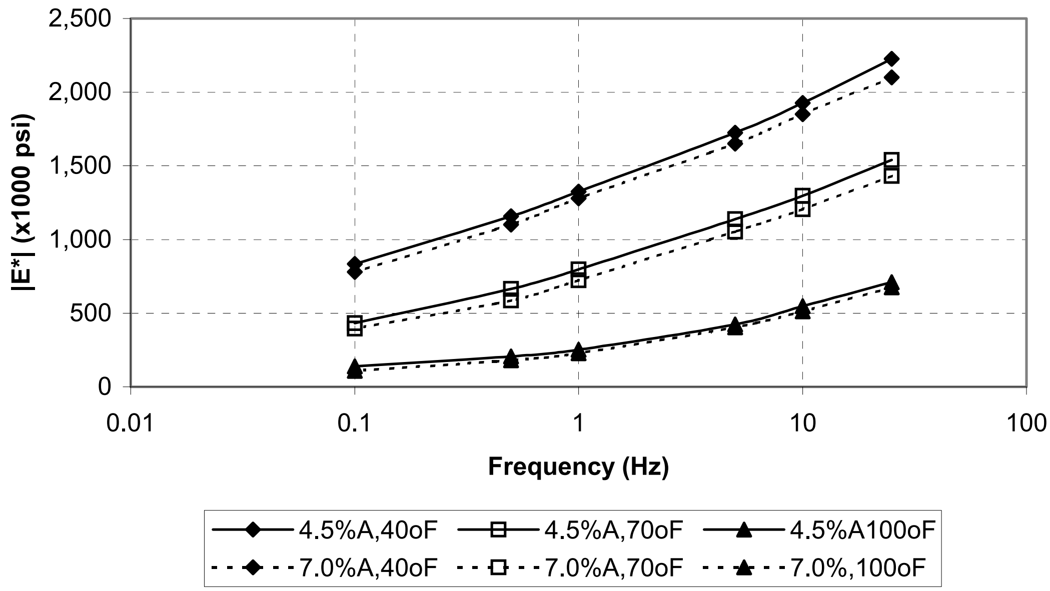

Figure 5.3. Isothermal Curves of Dynamic Modulus Test Results of 12.5 mm Mix @ Opt + 0.5 Percent Binder Content

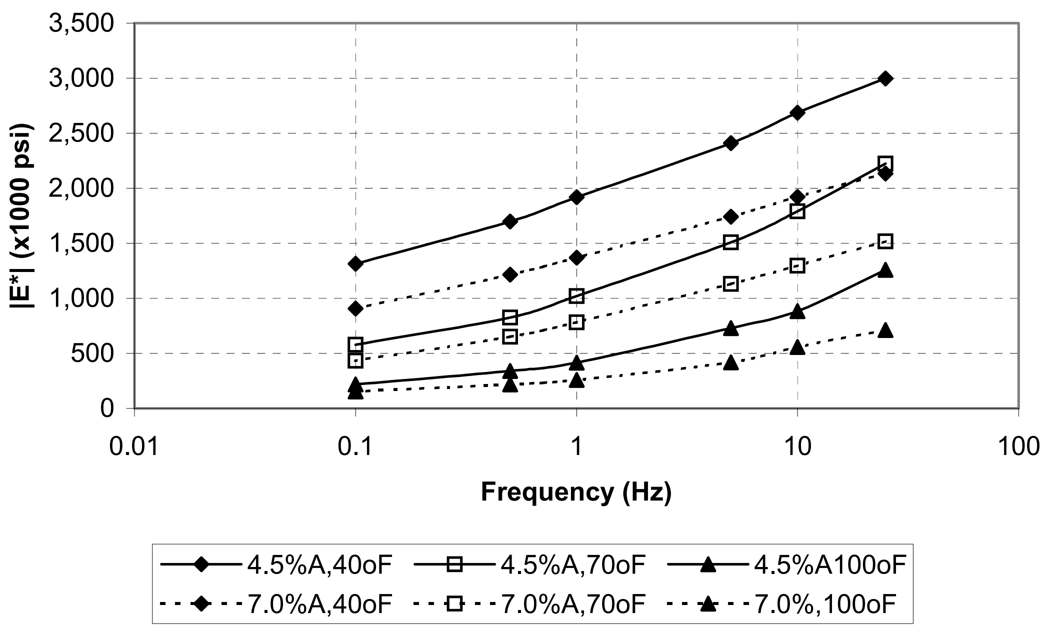

Figure 5.4. Isothermal Curves of Dynamic Modulus Test Results of 25 mm Mix @ Optimum Binder Content

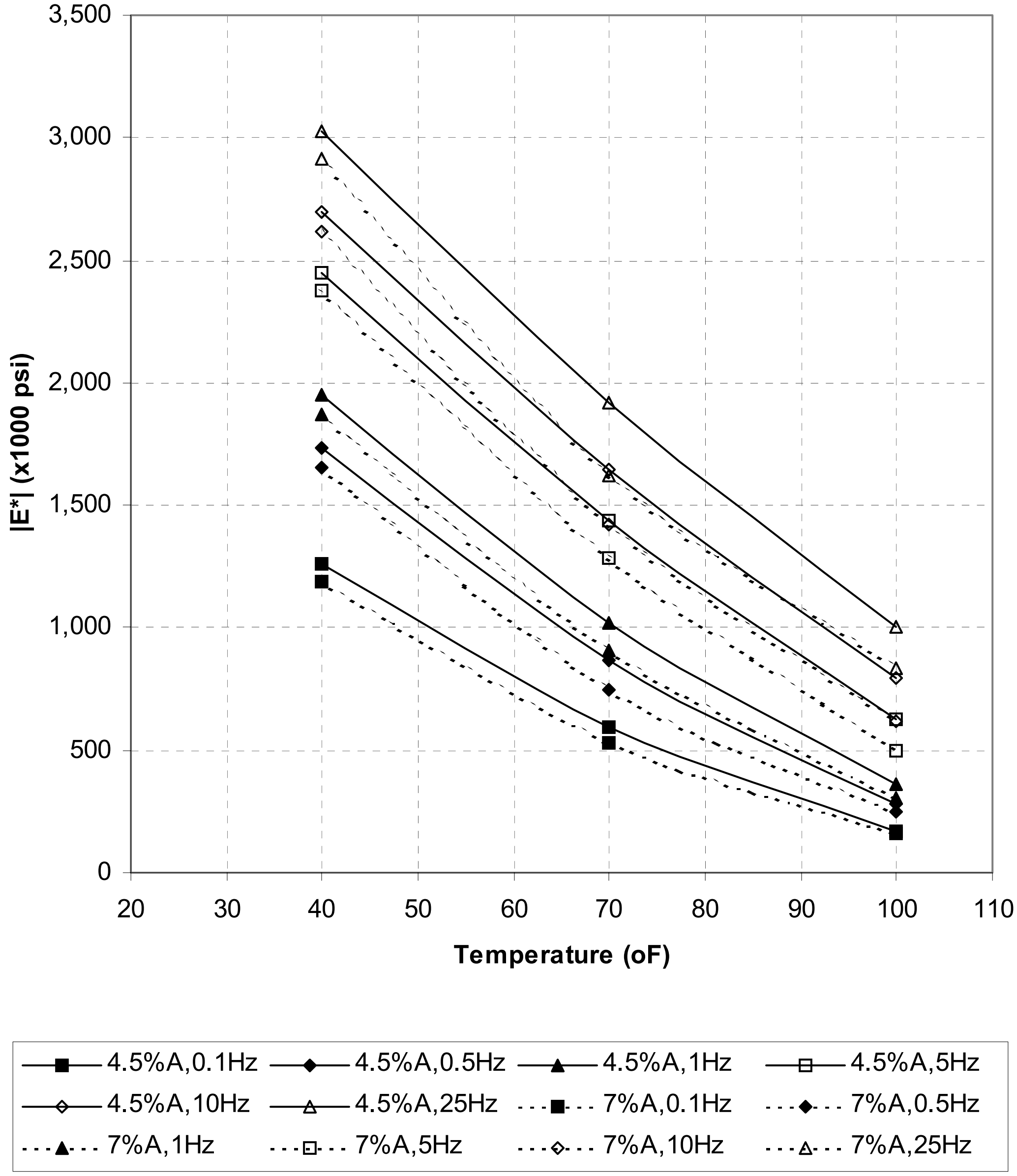

Figure 5.5. Isochronal Curves of Dynamic Modulus Test Results

of 12.5 mm Mix @ Opt - 0.5 Percent Binder Content

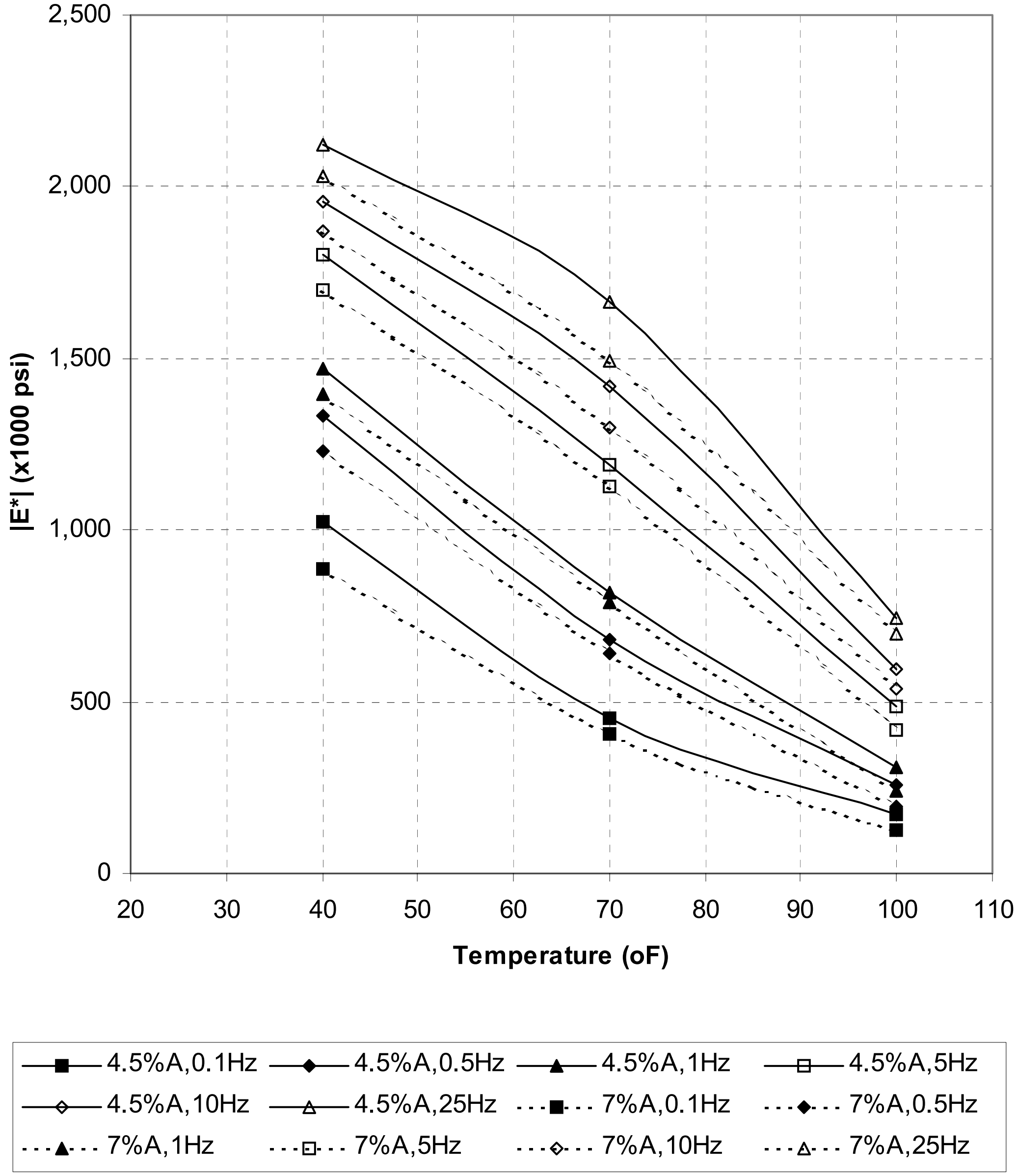

Figure 5.6. Isochronal Curves of Dynamic Modulus Test Results of 12.5 mm Mix @ Optimum Binder Content

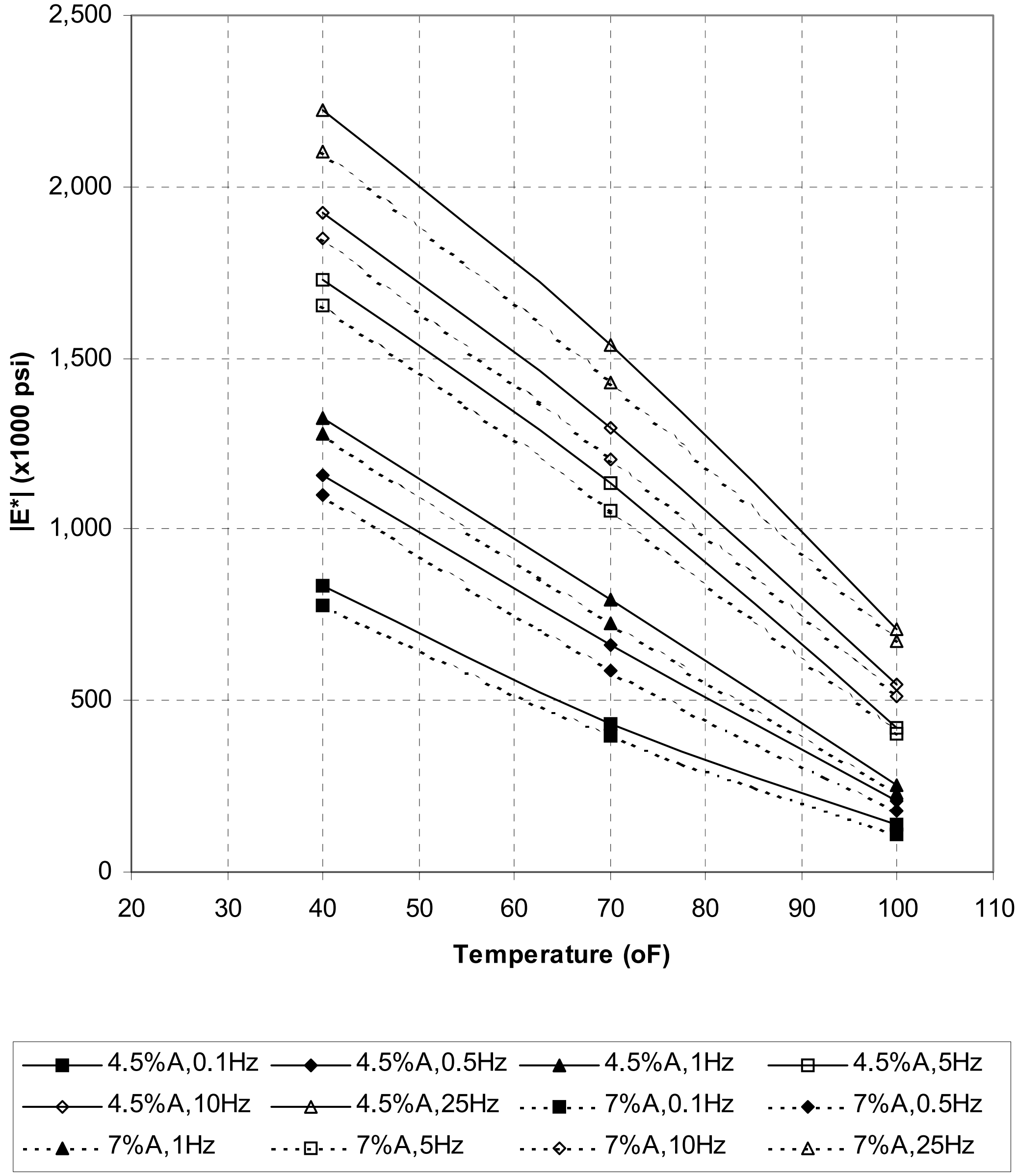

Figure 5.7. Isochronal Curves of Dynamic Modulus Test Results

of 12.5 mm Mix @ Opt + 0.5 Percent Binder Content

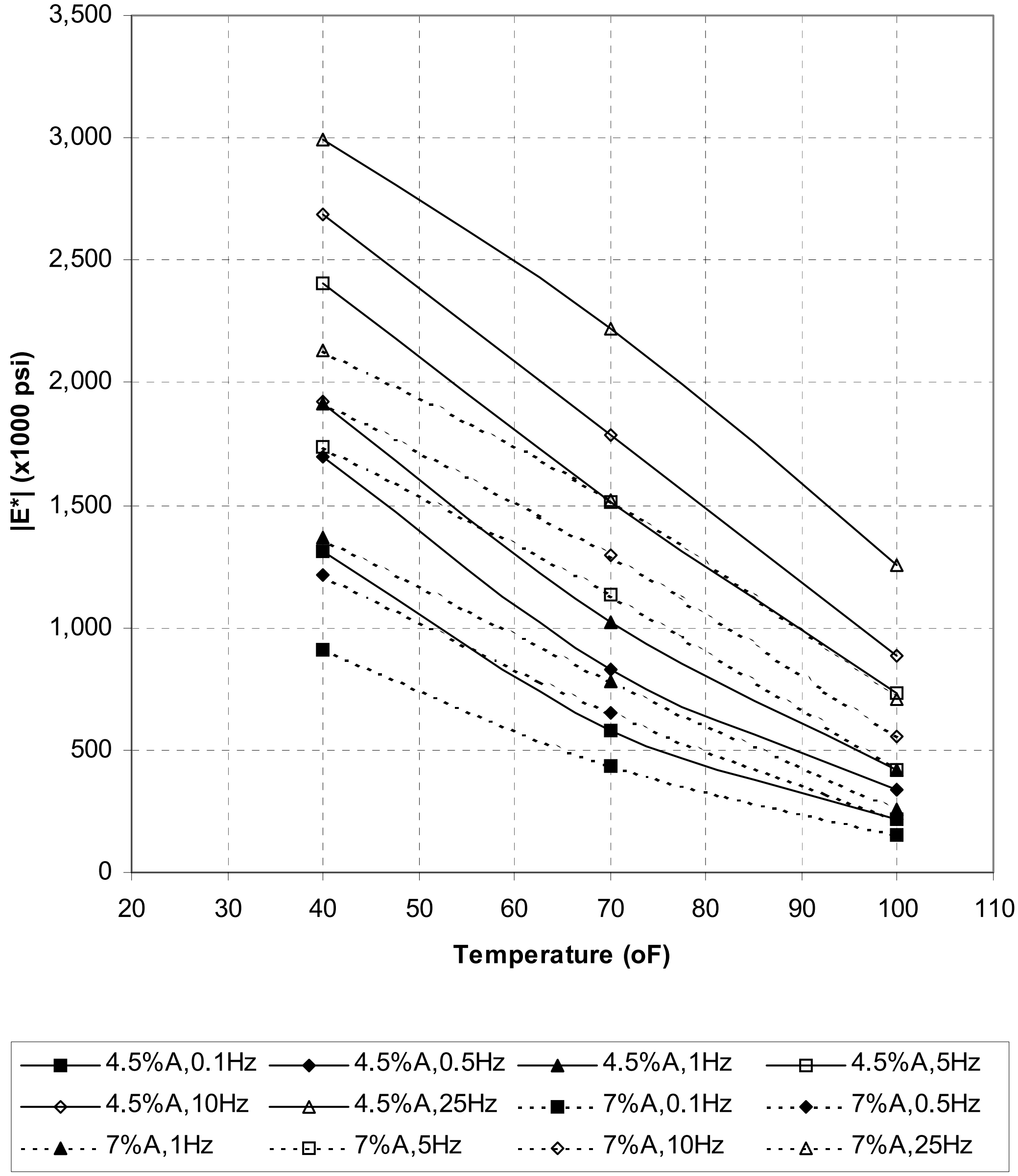

Figure 5.8. Isochronal Curves of Dynamic Modulus Test Results

of 25 mm Mix @ Optimum Binder Content

5.2 MASTER CURVES

A master curve of an asphalt mix allows comparison of linear visco-elastic materials tested at different frequencies and temperatures, and it can be constructed using the time-temperature superposition principle.

5.2.1 Time-Temperature Superposition Principle

Since the isothermal curves of dynamic modulus test results have similar shapes, they can be shifted relative to the frequency, so the various curves can be aligned to form a single master curve. The shift factor, *a(T),* defines the required shift at a given temperature, so these curves can be connected for a master curve at reference temperature T_R [16]:

$$a(T) = \frac{f_r}{f} \tag{5.1}$$

where

$a(T)$ = shift factor

f_r = reduced frequency at reference temperature T_R

f = frequency at temperature T

5.2.2 Polynomial Power Function Procedure

The method used to construct the master curve of a visco-elastic material uses Arrhenius equation as the basic expression for the shift factor [17]:

$$\log[a(T)] = 0.4343\frac{\delta H}{R}\left(\frac{1}{T} - \frac{1}{T_R}\right) \tag{5.2}$$

where

$a(T)$ = shift factor

δH = apparent activation energy, kcal/mole

R = universal gas constant, 1.98 cal/mole/K

T = shifted temperature, ^oK

T_R = reference temperature, ^oK

The reduced frequency in a decimal logarithmic scale is then calculated using Equation 5.1 as follows:

$$\log(f_r) = \log(f) + \log[a(T)] \tag{5.3}$$

The curve obtained after shifting can be approximated by a polynomial power function of the form [17]:

$$\log(|E^*|) = C_1 + \sum_{i=1}^{D} C_{i+1} \log(f_r) \tag{5.4}$$

where

$|E^*|$ = dynamic modulus

C_i = adjusting factor

D = power to be chosen by users

5.2.3 Sigmoidal Function Procedure

The method developed at the University of Maryland uses sigmoidal function as the fitting equation for master curve construction. The shifting factor is solved simultaneously with the coefficients of the sigmoidal function, without assuming any functional form for the relationship of a(T) versus temperature. The sigmoidal function is defined as follows [16]:

$$\log(|E^*|) = \delta + \frac{\alpha}{1 + e^{\beta - \gamma \log(f_r)}} \tag{5.5}$$

where

$|E^*|$ = dynamic modulus

δ = minimum value of $|E^*|$

α = span between maximum and minimum value of $|E^*|$

β, γ = parameters describing the shape of the sigmoidal function

f_r = reduced frequency at T_R

5.2.4 Master Curve Construction Procedure

In this study, since the tests were conducted at the intermediate temperatures, i.e., 40, 70, and 100 $^{\circ}$F, the polynomial and sigmoidal fitting functions described above do not fit well to the measured dynamic modulus test data. Figure 5.9 shows an example of fitting those equations to one set of measured dynamic modulus data. Therefore, the mater curve construction procedure is modified, and it is described in this section.

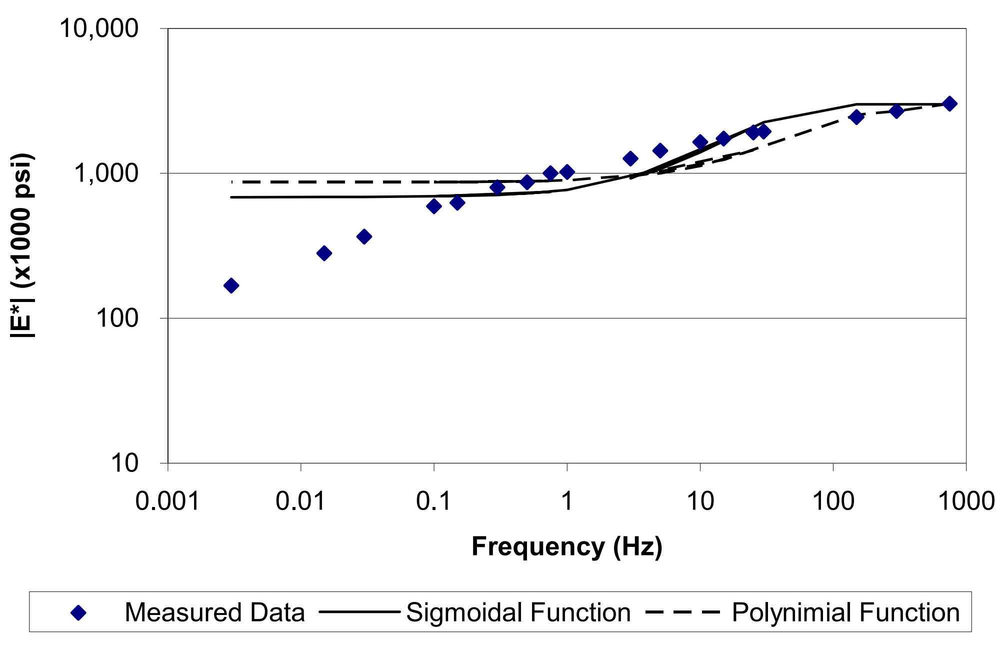

Figure 5.9. Example of Fitting Sigmoidal and Polynomial Functions

The method uses Arrhenius equation as the basic expression for the shift factor:

$$a(T) = \exp\left[\frac{\delta H}{R}\left(\frac{1}{T} - \frac{1}{T_R}\right)\right] \tag{5.6}$$

where

a(T)	= shift factor
δH	= apparent activation energy, kcal/mole
R	= universal gas constant, 1.98 cal/mole/K
T	= shifted temperature, ^oK
T_R	= reference temperature, ^oK

The reduced frequency is then calculated as follows:

$$f_r = a(T) * f \tag{5.7}$$

where

$a(T)$	= shift factor
f_r	= reduced frequency at reference temperature T_R
f	= frequency at temperature T

The master curve is finally constructed by fitting the following power function to the shifted test data:

$$|E^*| = C_1 + C_2\left(\frac{f_r}{C_3}\right)^{C_4} + C_5\left(\frac{C_6}{f_r}\right)^{C_7} \tag{5.8}$$

where

$\|E^*\|$	= dynamic modulus, 10^3 psi
C_i	= adjusting factors
f_r	= reduced frequency, Hz

In this procedure, the apparent activation energy, δH, is solved simultaneously with the adjusting factors of the fitting equation using the Solver Equation in the Excel spreadsheet. Table 5.1 shows the fitting coefficients calculated for each asphalt mixture. It is evident from the data shown in Table 5.1 that no consistent pattern exists for establishing the coefficients necessary to construct a master curve for a given data set. Therefore, master curves must be experimentally determined for each HMA mixture.

Table 5.1. Fitting Coefficients

Mixture	a(40°F)	a(100°F)	C_1	C_2	C_3	C_4	C_5	C_6	C_7
12.5-0.5-4.5	27.390	0.028	-48725.2	47273.5	1.00	0.010	2493.8	1.00	0.090
12.5-0.5-7.0	50.560	0.020	38339.8	15970.3	0.40	0.041	-53724.9	0.54	-0.009
12.5-0.0-4.5	14.988	0.019	52351.3	22417.5	3.28	-0.036	-79590.8	0.01	0.014
12.5-0.0-7.0	15.052	0.019	7070.8	-84639.5	1.30	-0.084	59446.8	29.56	0.089
12.5+0.5-4.5	10.655	0.019	35006.0	-55496.4	1.00	-0.022	20771.5	1.68	0.049
12.5+0.5-7.0	12.689	0.023	23834.0	20376.6	1.34	-0.054	-44820.9	0.46	0.030
25.0-0.0-4.5	15.025	0.050	-23028.4	145.6	1.00	-0.354	23987.2	1.00	-0.014
25.0-0.0-7.0	14.546	0.018	31329.8	38943.9	1.00	-0.041	-63628.7	31.95	0.025

Figures 5.10 to 5.17 show the master curves and shift factors for samples tested in this study. Figures 5.18 and 5.19 present the master curves of mixtures in the statistical tests 1 and 2, respectively. From the master curves, the conclusions on the effects of aggregate size and binder content on the dynamic modulus can be verified as follows:

- 25 mm HMA has a higher dynamic modulus than 12.5 mm HMA.
- For the 12.5 mm HMA, the mix is stiffer when the binder content is 0.5 percent lower than the optimum, and the mix is less stiff when the binder content is 0.5 percent higher than the optimum.

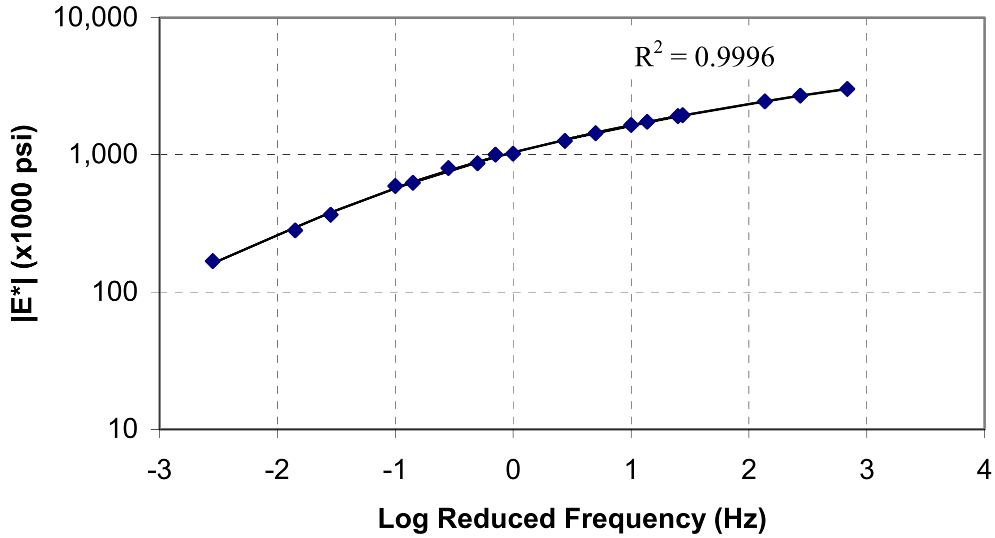

(a) Master Curve (Reference Temperature 40 °F)

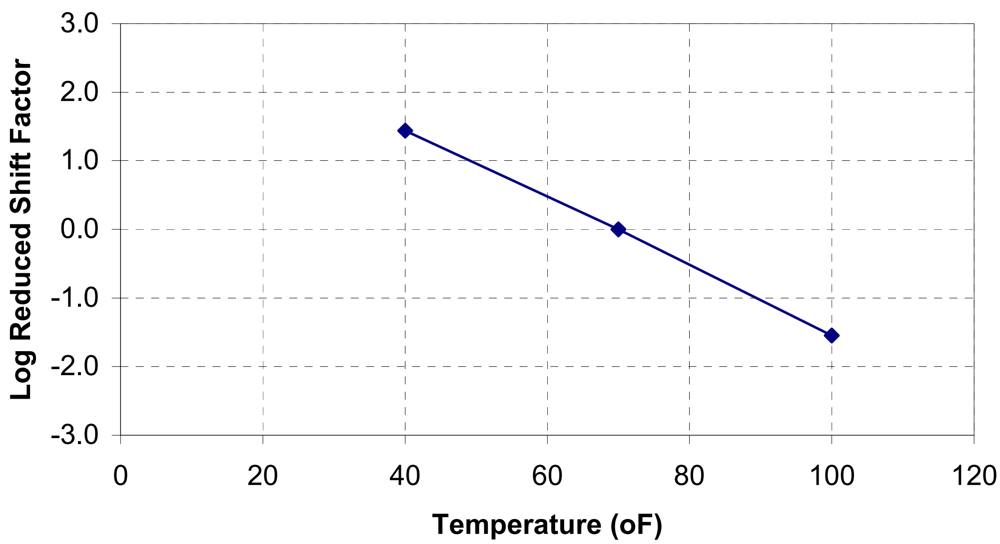

(b) Shift Factor *a(T)*

Figure 5.10. Master Curve of 12.5-0.5-4.5 Samples

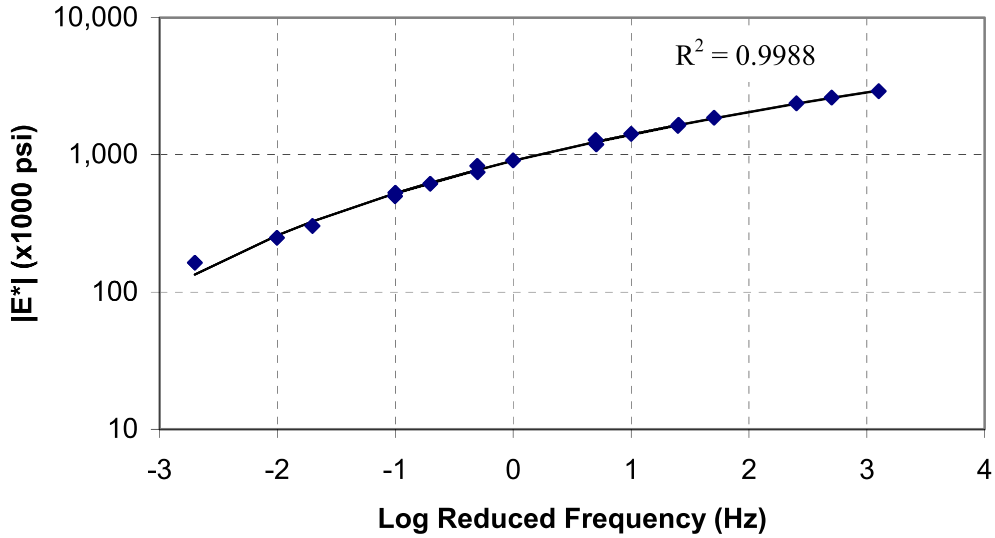

(a) Master Curve (Reference Temperature 40 ^{o}F)

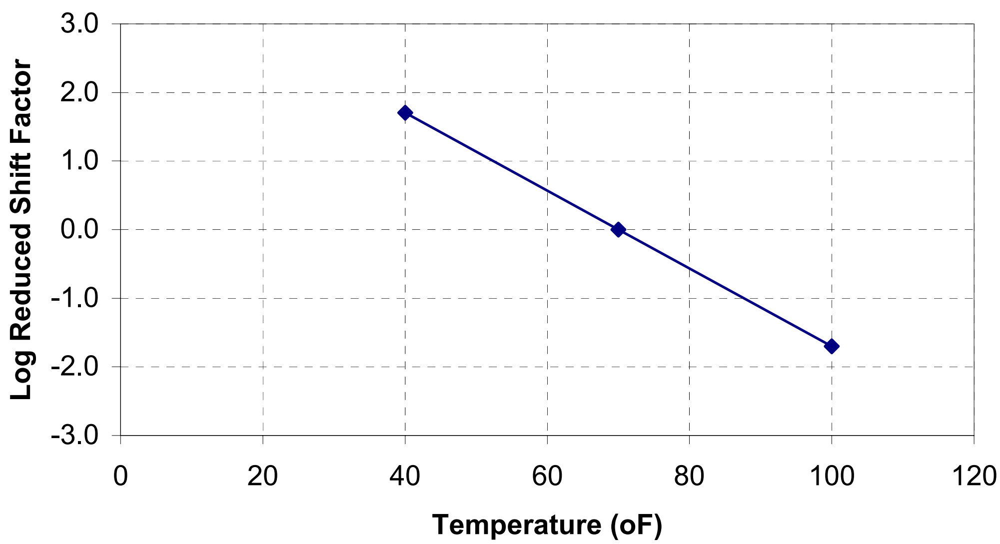

(b) Shift Factor *a(T)*

Figure 5.11. Master Curve of 12.5-0.5-7.0 Samples

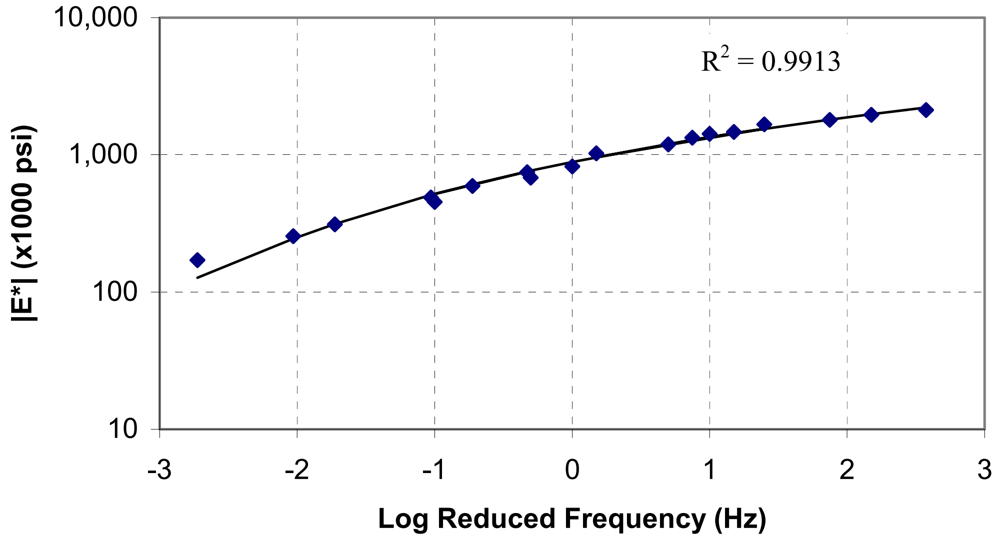

(a) Master Curve (Reference Temperature 40 ^oF)

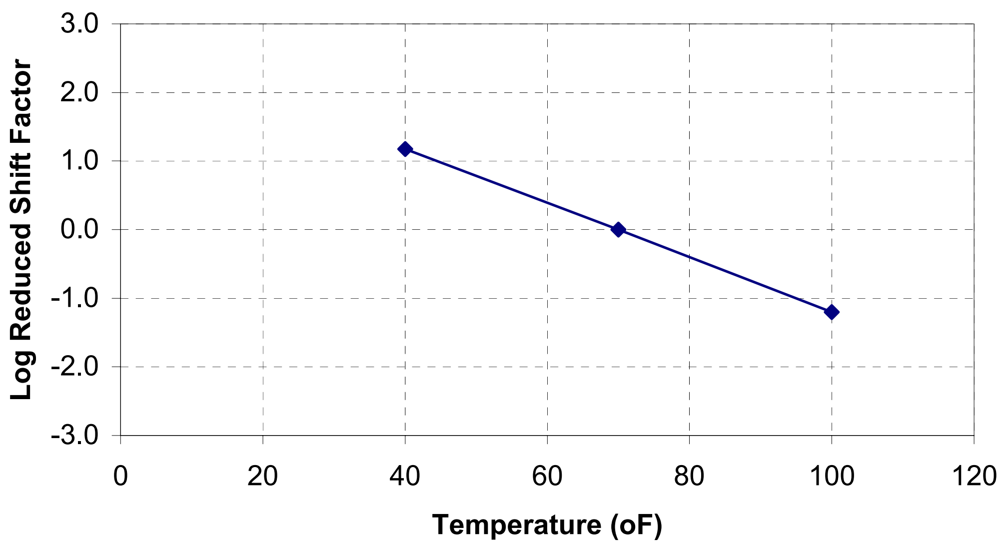

(b) Shift Factor *a(T)*

Figure 5.12. Master Curve of 12.5-0.0-4.5 Samples

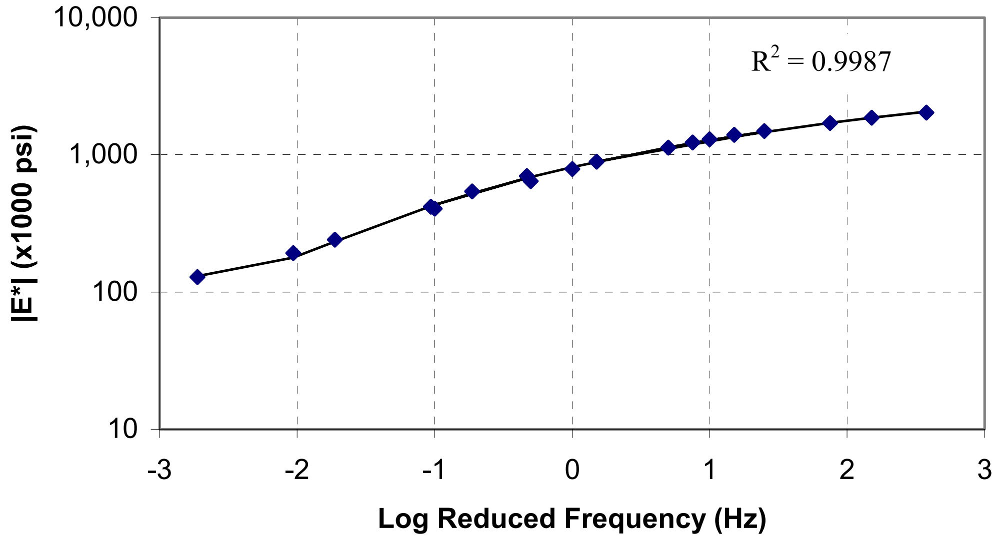

(a) Master Curve (Reference Temperature 40 °F)

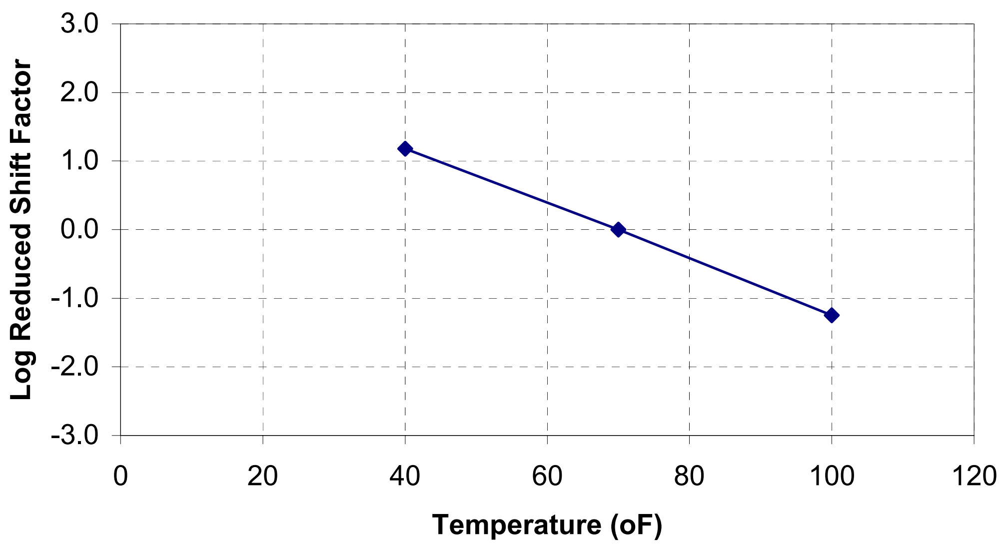

(b) Shift Factor *a(T)*

Figure 5.13. Master Curve of 12.5-0.0-7.0 Samples

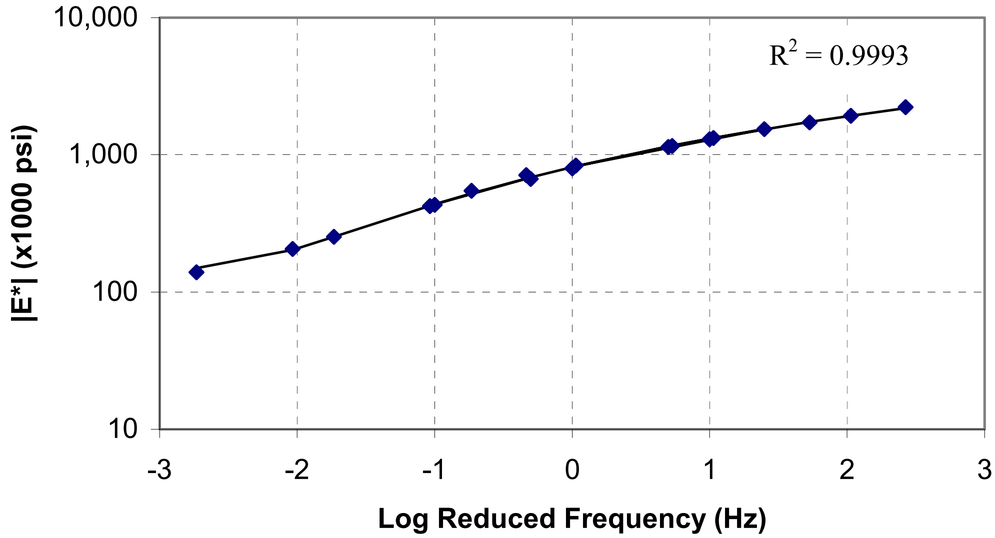

(a) Master Curve (Reference Temperature 40 °F)

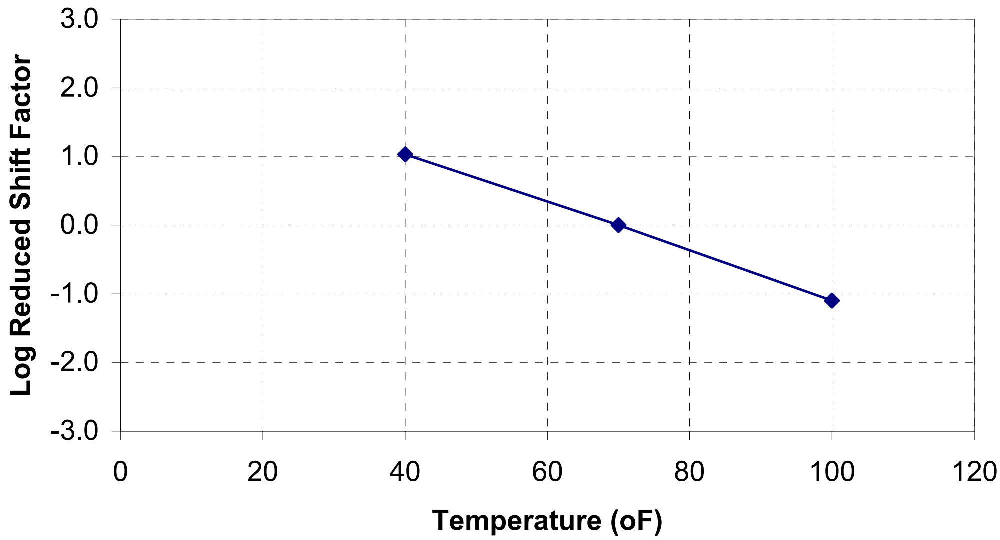

(b) Shift Factor *a(T)*

Figure 5.14. Master Curve of 12.5+0.5-4.5 Samples

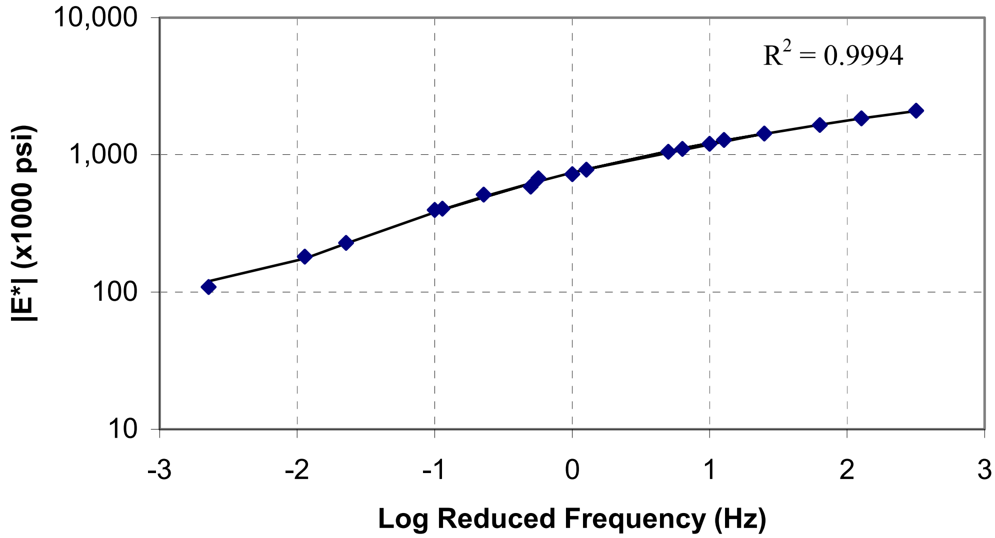

(a) Master Curve (Reference Temperature 40 °F)

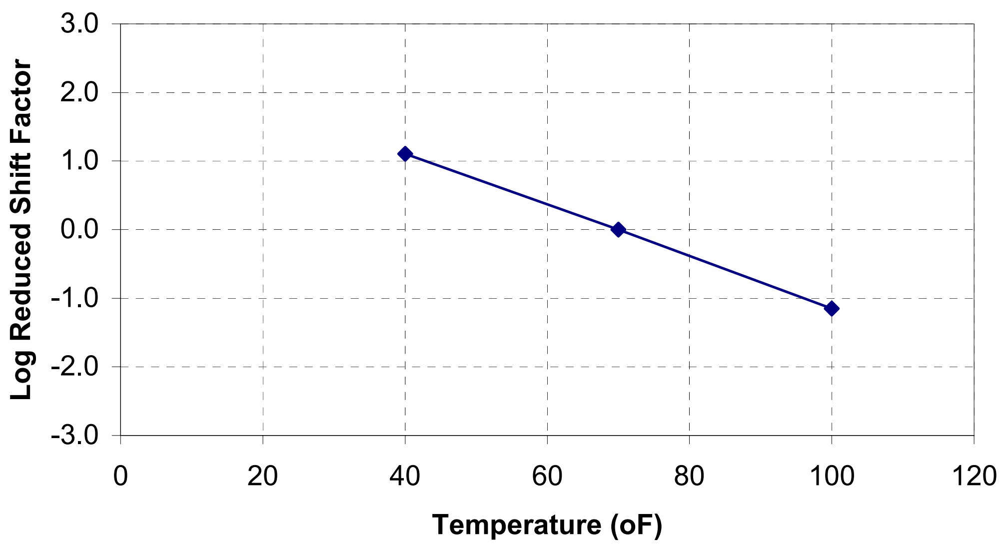

(b) Shift Factor *a(T)*

Figure 5.15. Master Curve of 12.5+0.5-7.0 Samples

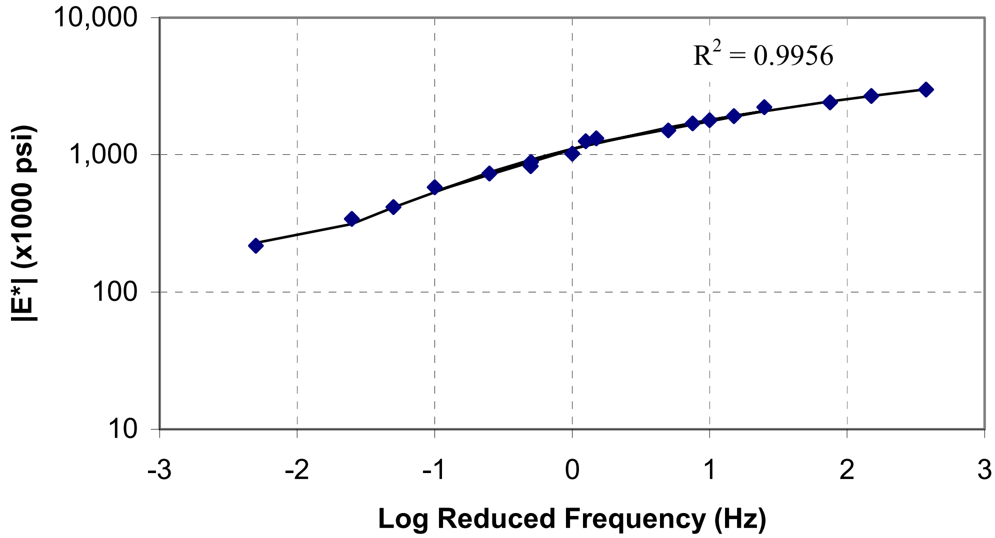

(a) Master Curve (Reference Temperature 40 °F)

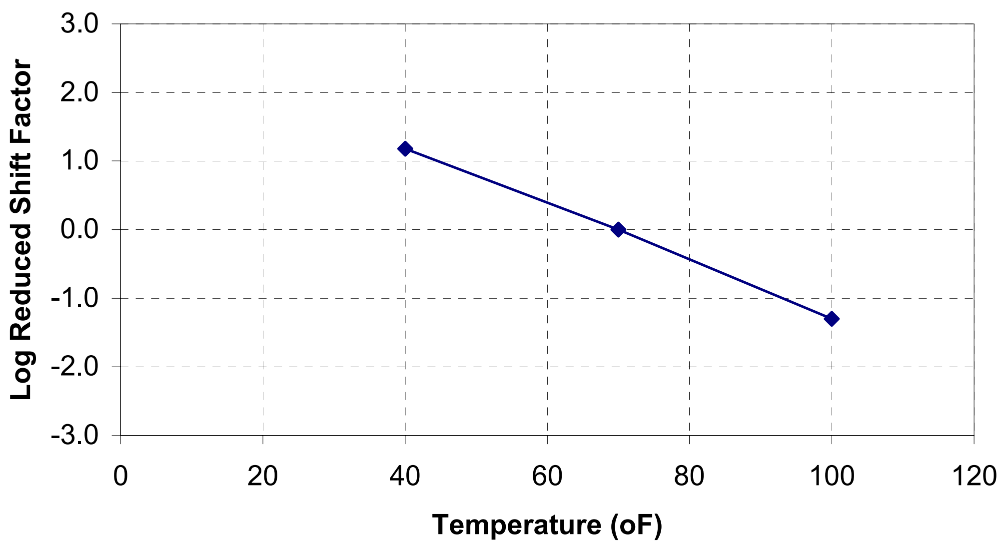

(b) Shift Factor *a(T)*

Figure 5.16. Master Curve of 25.0-0.0-4.5 Samples

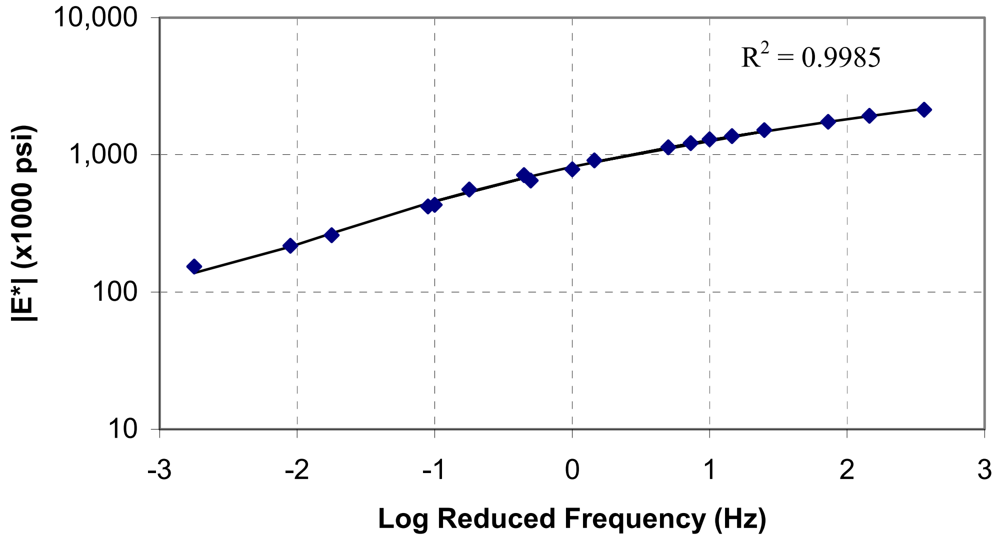

(a) Master Curve (Reference Temperature 40 °F)

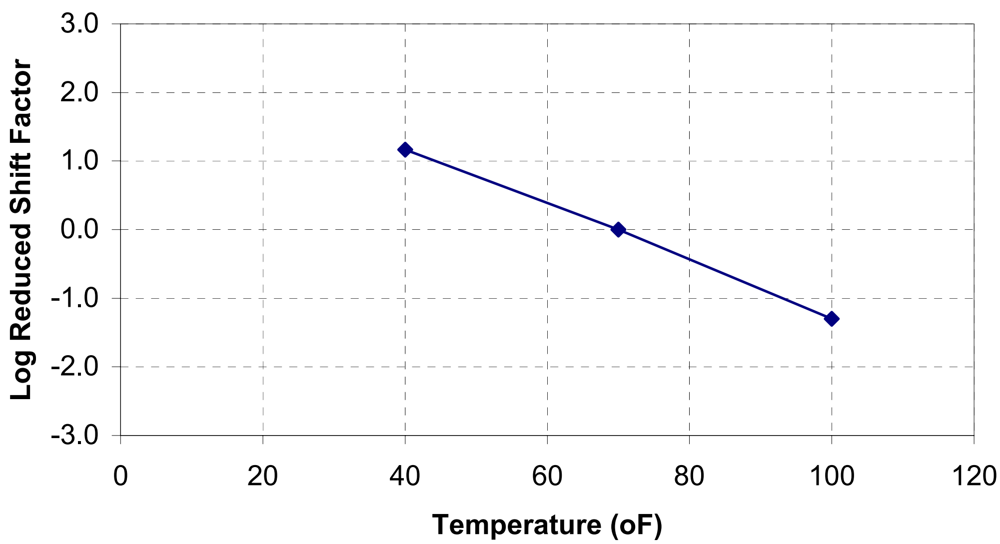

(b) Shift Factor *a(T)*

Figure 5.17. Master Curve of 25.0-0.0-7.0 Samples

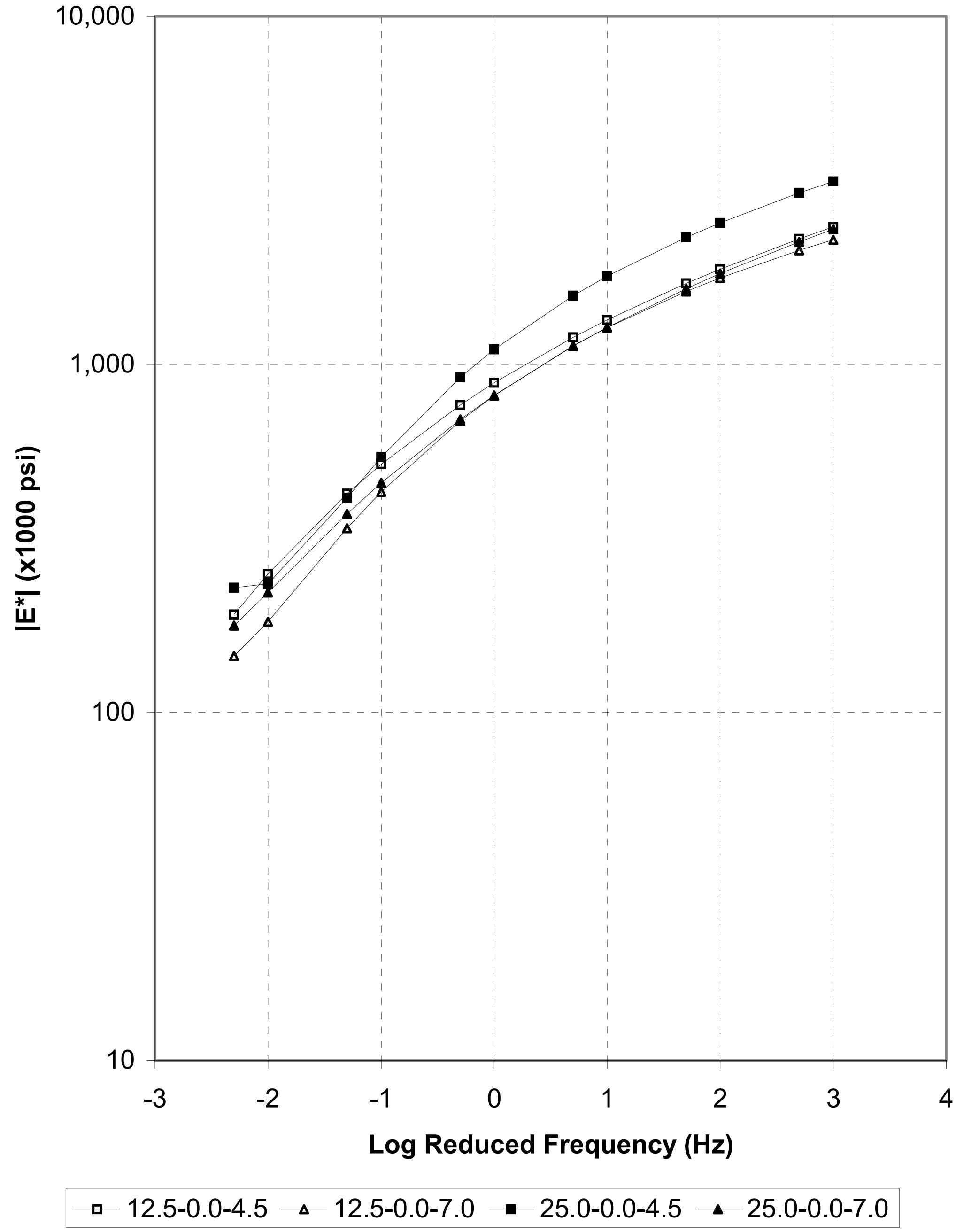

Figure 5.18. Master Curves of Mixtures

in Statistical Test No. 1

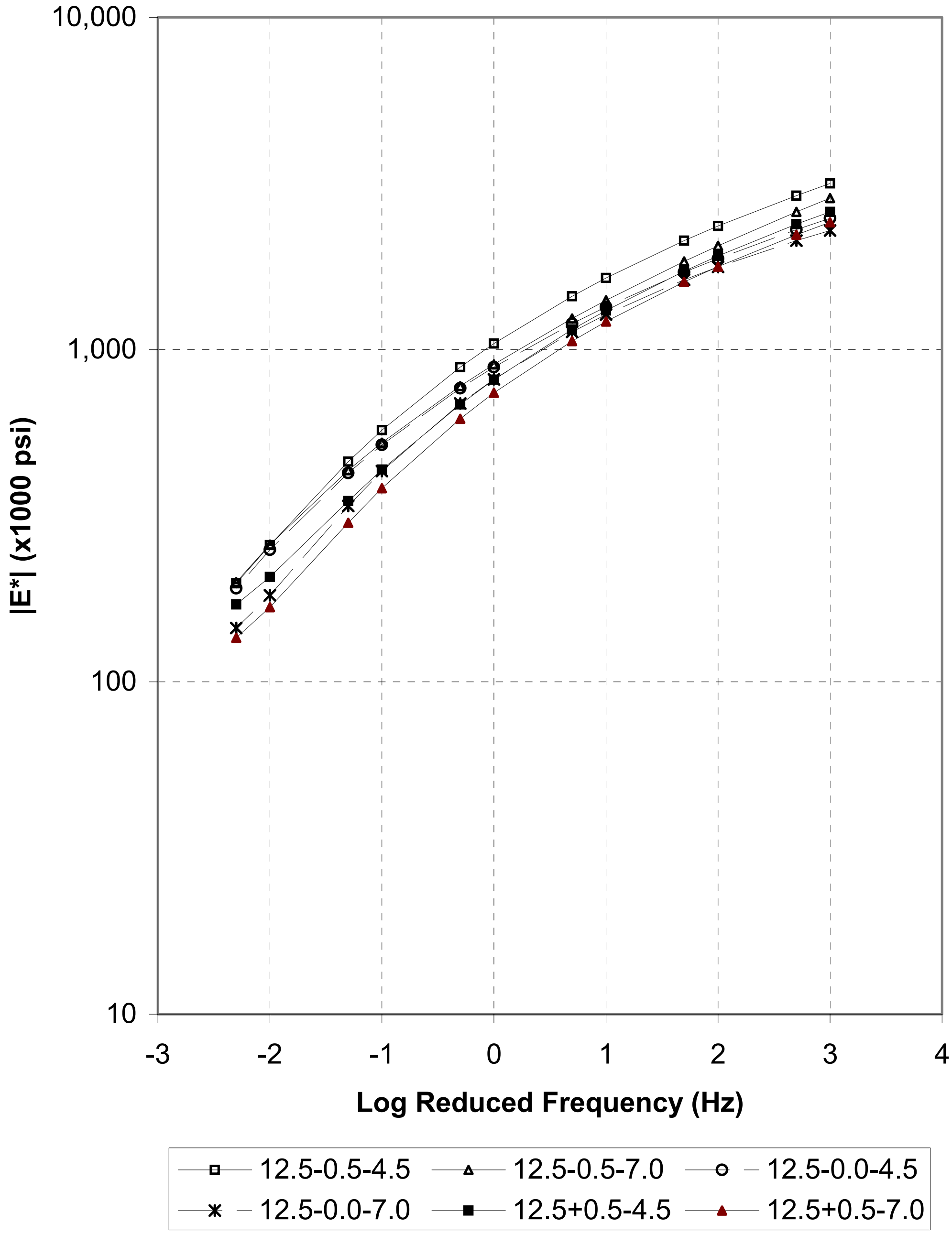

Figure 5.19. Master Curves of Mixtures

in Statistical Test No. 2

CHAPTER 6

CONCLUSIONS

This project provides an extensive search of historic and current literature relating to the analysis and performance-based test procedures of HMA fatigue characteristics, and the role of the performance-based tests in the quality control and pavement performance predictions in flexible pavement design. Through the literature review, the candidate test for fatigue cracking selected for this project is *Standard Test Method for Dynamic Modulus of Asphalt Concrete Mixtures for Fatigue Cracking* proposed in the SPT developed under the NCHRP 9-19 project.

The testing program of this project is designed to conduct the dynamic modulus test. The results of the test are analyzed to determine the accuracy of average dynamic modulus using available equipments. Furthermore, the effects of aggregate size, binder content, air void content, test temperature, and test frequency on the dynamic modulus of asphalt concrete are also evaluated.

The relationship between the air void contents of gyratory-compacted samples and cored specimens are developed using linear regression.

The sample coefficient of variance is calculated to evaluate the accuracy of the average dynamic modulus, and the coefficients of variances are higher when the dynamic modulus tests are run at high temperatures or high frequencies.

Three statistical tests are conducted using multi-factorial ANOVA to evaluate the effects of aggregate size, binder content, air void content, test temperature and test frequency on the dynamic modulus.

The dynamic modulus test data are then presented in the graphs of isothermal, isochronal and master curves to verify the conclusions from the statistical tests. In this research, since the tests were run at intermediate temperatures, the polynomial and sigmoidal equations do not fit well to the measured dynamic modulus data. However, the use of power equation gains a good result.

From the statistical tests, the conclusions on the effects of aggregate size and binder content, which are also verified using the master curves, are as follows:

- 25 mm HMA has a higher dynamic modulus than 12.5 mm HMA.
- For this 12.5 mm HMA, the mix is stiffer when the binder content is 0.5 percent lower than the optimum, and the mix is less stiff when the binder content is 0.5 percent higher than the optimum.

The effects of air voids, temperature, and frequency on dynamic modulus are concluded in the statistical tests and verified using isothermal and isochronal curves of dynamic modulus as follows:

- Specimens compacted at 4.5 percent air voids had higher dynamic moduli than specimens at 7 percent air voids.
- HMA is stiffer at lower temperatures.
- HMA has higher dynamic moduli at higher frequencies.

The above conclusions show reasonable tendencies of asphalt mixture stiffness to change due to the variation of test parameters. Since all of test parameters varied in the experimental plan are significant, no test parameter may be eliminated from future research efforts.

REFERENCES

[1] Federal Highway Administration, & Asphalt Institute. (1994). Superpave: Asphalt Mixture Design and Analysis. Washington D.C., & Kentucky: Authors.

[2] Asphalt Institute. (1996). Superpave Mix Design: Superpave Series No. 2 (SP-2). Kentucky: Author.

[3] Witczak, M. W., & et al. (2000). Simple Performance Test: Test Results and Recommendations. Interim Report. Arizona: Arizona State University.

[4] Witczak, M. W., & et al. (1996). Evaluation and Management of Performance Models: Key Findings and Recommendations. Draft Report. Maryland: University of Maryland.

[5] NCHRP. (2001). Project 9-19, FY 1998: Superpave Support and Performance Models Management [Online]. Available: http://www4.nationalacademies.org/trb/crp.nsf/All+Projects/NCHRP+9-19

[6] Lytton, R. L., & et al. (1993). Development and Validation of Performance Prediction Models and Specifications for Asphalt Binders and Paving Mixes. SHRP-A-357. Washington D.C: Strategic Highway Research Program.

[7] Monismith, C. L., & et al. (1994). Accelerated Performance-Related Tests for Asphalt-Aggregate Mixes and Their Use in Mix Design and Analysis Systems. SHRP-A-417. Washington D.C: Strategic Highway Research Program.

[8] Tayebali, A. A., & et al. (1994). Fatigue Response of Asphalt-Aggregate Mixes. SHRP-A-404. Washington D.C: Strategic Highway Research Program.

[9] Witczak, M. W., & et al. (1997). Superpave Support and Performance Models Management: Evaluation of the SHRP Performance Models System. Proceedings of Eight International Conference on Asphalt Pavements, Volume III. Washington: University of Washington.

[10] Thompson, M. R., & et al. (1990). Calibrated Mechanistic Structural Analysis Procedures for Pavements. Volume I, Final Report. NCHRP 1-26. Illinois: University of Illinois.

[11] Thompson, M. R., & et al. (1990). Calibrated Mechanistic Structural Analysis Procedures for Pavements. Volume II, Final Report. NCHRP 1-26. Illinois: University of Illinois.

[12] Tayebali, A. A., & et al. (1994). Stiffness of Asphalt-Aggregate Mixes. SHRP-A-388. Washington D.C: Strategic Highway Research Program.

[13] Sousa, J. B., & et al. (1994). Permanent Deformation of Asphalt-Aggregate Mixes. SHRP-A-415. Washington D.C: Strategic Highway Research Program.

[14] LAW PCS. (2000). Protocol P07: Test Method for Determining the Creep Compliance, Resilient Modulus and Strength of Asphalt Materials Using the Indirect Tensile test Device. LTPP. Washington D.C: FHWA.

[15] Di Benedetto, H., & de la Roche, S. (1998). State of the Art of Stiffness Modulus and Fatigue of Bituminous Mixtures, RILEM Report 17, Bituminous Binders and Mixes, Edited by L.Francen, NY.

[16] Pellinen, T. (2001). Investigation of the Use of Dynamic Modulus As an Indicator of Hot-Mix Asphalt Performance. Ph.D. dissertation. Arizona State University, Tempe, AZ.

[17] Francken, L., & Vanelstraete, A. (1997). Complex Moduli of Bituminous Materials: A Rational Method for the Interpretation of Test Results. Mechanical Test for Bituminous Materials. Edited by Di Benedetto & Francken. 1997 RILEM.

APPENDIX A

DYNAMIC MODULUS TEST RESULTS

DYNAMIC MODULUS TEST RESULTS
Sample Size: H150*D100

Spec. ID	Agg. Source	Nom. Size (mm)	Binder Grade	Binder Cont. (%)	A.Void Gyr. (%)	A.Void Core (%)	Dynamic Modulus Test Tem. (D.F)	Freq (Hz)	Stress (psi)	|E*| (psi)	PhAng (Deg)
201	MCA	12.5	PG67-22	5.5	6.7	4.2	40	25	150	3,199,716	13.05
							40	10	150	2,981,345	11.10
							40	5	150	2,760,132	12.76
							40	1	150	2,304,990	13.40
							40	0.5	150	1,854,251	14.28
							40	0.1	150	1,531,404	16.26
							70	25	75	2,030,906	25.26
							70	10	75	1,735,194	22.97
							70	5	75	1,478,252	23.44
							70	1	75	1,017,167	24.01
							70	0.5	75	854,929	24.63
							70	0.1	75	565,695	25.46
							100	25	40	1,035,685	34.31
							100	10	40	920,835	33.09
							100	5	40	750,863	33.75
							100	1	40	430,000	32.86
							100	0.5	40	298,058	31.93
							100	0.1	40	185,058	26.15
202	MCA	12.5	PG67-22	5.5	6.2	4.3	40	25	150	2,979,511	15.05
							40	10	150	2,520,074	11.30
							40	5	150	2,241,950	11.54
							40	1	150	1,825,738	12.78
							40	0.5	150	1,432,607	14.05
							40	0.1	150	1,141,575	15.81
							70	25	75	1,951,044	22.13
							70	10	75	1,675,293	17.88
							70	5	75	1,467,477	18.27
							70	1	75	1,043,235	20.31
							70	0.5	75	887,163	21.23
							70	0.1	75	627,539	22.82
							100	25	40	967,201	29.74
							100	10	40	745,061	28.38
							100	5	40	583,473	28.90
							100	1	40	385,920	24.00
							100	0.5	40	326,485	23.18
							100	0.1	40	193,918	19.72

DYNAMIC MODULUS TEST RESULTS (CON'T)
Sample Size: H150*D100

Spec. ID	Agg. Source	Nom. Size (mm)	Binder Grade	Binder Cont. (%)	A.Void Gyr. (%)	A.Void Core (%)	Dynamic Modulus Test Tem. (D.F)	Freq (Hz)	Stress (psi)	|E*| (psi)	PhAng (Deg)
203	MCA	12.5	PG67-22	5.5	6.2	4.2	40	25	150	2,848,369	12.25
							40	10	150	2,531,700	10.86
							40	5	150	2,317,979	12.06
							40	1	150	1,875,158	13.33
							40	0.5	150	1,682,230	14.46
							40	0.1	150	1,247,364	17.32
							70	25	75	1,754,807	20.07
							70	10	75	1,561,692	17.37
							70	5	75	1,405,038	18.24
							70	1	75	1,041,207	19.19
							70	0.5	75	910,635	19.37
							70	0.1	75	637,518	20.69
							100	25	40	842,613	31.04
							100	10	40	653,557	29.64
							100	5	40	548,258	28.99
							100	1	40	337,152	28.21
							100	0.5	40	263,614	27.61
							100	0.1	40	157,527	24.85
204	MCA	12.5	PG67-22	5.5	6.1	4.1	40	25	150	3,069,441	16.50
							40	10	150	2,599,508	13.50
							40	5	150	2,264,860	15.72
							40	1	150	1,784,878	16.61
							40	0.5	150	1,574,637	17.48
							40	0.1	150	1,135,476	19.92
							70	25	75	1,932,707	18.50
							70	10	75	1,609,054	18.30
							70	5	75	1,397,212	20.00
							70	1	75	975,652	20.89
							70	0.5	75	822,937	21.71
							70	0.1	75	544,597	23.27
							100	25	40	1,162,898	35.95
							100	10	40	875,252	34.86
							100	5	40	623,362	37.71
							100	1	40	306,035	32.50
							100	0.5	40	234,580	33.46
							100	0.1	40	136,249	27.80

DYNAMIC MODULUS TEST RESULTS (CON'T)
Sample Size: H150*D100

Spec. ID	Agg. Source	Nom. Size (mm)	Binder Grade	Binder Cont. (%)	A.Void Gyr. (%)	A.Void Core (%)	Dynamic Modulus Test Tem. (D.F)	Freq (Hz)	Stress (psi)	|E*| (psi)	PhAng (Deg)
211	MCA	12.5	PG67-22	5.5	9	6.5	40	25	150	2,690,758	12.30
							40	10	150	2,457,337	10.92
							40	5	150	2,424,586	10.55
							40	1	150	1,758,993	13.57
							40	0.5	150	1,530,931	14.57
							40	0.1	150	1,098,147	16.68
							70	25	75	1,741,646	20.10
							70	10	75	1,607,403	17.21
							70	5	75	1,360,660	18.37
							70	1	75	965,774	21.33
							70	0.5	75	792,365	22.69
							70	0.1	75	493,536	25.22
							100	25	40	997,102	35.40
							100	10	40	724,100	27.29
							100	5	40	584,512	30.80
							100	1	40	352,485	21.33
							100	0.5	40	289,452	27.98
							100	0.1	40	185,021	23.70
212	MCA	12.5	PG67-22	5.5	9.9	7.5	40	25	150	3,211,148	12.80
							40	10	150	3,058,520	10.80
							40	5	150	2,565,954	10.56
							40	1	150	2,251,651	12.03
							40	0.5	150	2,021,543	15.54
							40	0.1	150	1,405,369	16.53
							70	25	75	1,902,151	16.08
							70	10	75	1,545,615	14.81
							70	5	75	1,512,051	15.84
							70	1	75	1,050,054	22.59
							70	0.5	75	802,158	20.32
							70	0.1	75	640,402	24.47
							100	25	40	757,847	28.83
							100	10	40	592,084	27.48
							100	5	40	495,566	26.72
							100	1	40	316,026	25.60
							100	0.5	40	261,896	24.37
							100	0.1	40	180,624	20.89

DYNAMIC MODULUS TEST RESULTS (CON'T)
Sample Size: H150*D100

Spec. ID	Agg. Source	Nom. Size (mm)	Binder Grade	Binder Cont. (%)	A.Void Gyr. (%)	A.Void Core (%)	Dynamic Modulus Test Tem. (D.F)	Freq (Hz)	Stress (psi)	|E*| (psi)	PhAng (Deg)
213	MCA	12.5	PG67-22	5.5	9.4	6.7	40	25	150	3,381,360	16.50
							40	10	150	2,817,689	13.83
							40	5	150	2,473,813	13.65
							40	1	150	1,847,751	16.59
							40	0.5	150	1,617,779	19.10
							40	0.1	150	1,151,441	20.34
							70	25	75	1,336,429	20.05
							70	10	75	1,168,182	15.20
							70	5	75	1,053,864	18.89
							70	1	75	749,297	21.88
							70	0.5	75	638,452	22.23
							70	0.1	75	451,626	23.01
							100	25	40	729,927	33.70
							100	10	40	567,572	32.19
							100	5	40	443,355	33.22
							100	1	40	249,901	28.15
							100	0.5	40	205,125	28.54
							100	0.1	40	130,349	23.48
214	MCA	12.5	PG67-22	5.5	9.5	7.1	40	25	150	2,381,872	14.45
							40	10	150	2,142,016	13.08
							40	5	150	2,024,558	12.44
							40	1	150	1,616,379	13.67
							40	0.5	150	1,455,461	14.17
							40	0.1	150	1,102,256	16.53
							70	25	75	1,495,870	18.90
							70	10	75	1,355,616	17.57
							70	5	75	1,205,956	18.32
							70	1	75	874,365	19.84
							70	0.5	75	745,907	20.95
							70	0.1	75	535,964	22.20
							100	25	40	842,110	28.14
							100	10	40	573,281	27.62
							100	5	40	467,187	27.04
							100	1	40	295,537	25.34
							100	0.5	40	237,232	24.06
							100	0.1	40	158,803	19.94

DYNAMIC MODULUS TEST RESULTS (CON'T)
Sample Size: H150*D100

Spec. ID	Agg. Source	Nom. Size (mm)	Binder Grade	Binder Cont. (%)	A.Void		Dynamic Modulus Test				
					Gyr. (%)	Core (%)	Tem. (D.F)	Freq (Hz)	Stress (psi)	|E*| (psi)	PhAng (Deg)
221	MCA	12.5	PG67-22	6	6.4	4.3	40	25	150	1,896,988	23.85
							40	10	150	1,798,556	14.53
							40	5	150	1,614,805	14.29
							40	1	150	1,280,157	15.83
							40	0.5	150	1,143,183	16.74
							40	0.1	150	844,363	19.86
							70	25	75	1,518,234	24.14
							70	10	75	1,255,990	22.64
							70	5	75	1,062,831	23.03
							70	1	75	691,503	25.47
							70	0.5	75	570,189	25.20
							70	0.1	75	354,775	23.84
							100	25	40	763,291	39.78
							100	10	40	520,907	38.11
							100	5	40	384,524	36.00
							100	1	40	223,995	30.65
							100	0.5	40	170,739	27.00
							100	0.1	40	114,874	21.55
222	MCA	12.5	PG67-22	6	6.8	4.5	40	25	150	1,887,117	19.54
							40	10	150	1,767,598	13.28
							40	5	150	1,625,431	12.82
							40	1	150	1,297,612	13.91
							40	0.5	150	1,167,825	14.47
							40	0.1	150	868,751	16.92
							70	25	75	1,715,203	21.75
							70	10	75	1,556,025	17.52
							70	5	75	1,286,054	23.33
							70	1	75	815,566	26.48
							70	0.5	75	669,188	27.44
							70	0.1	75	432,001	27.88
							100	25	40	801,373	28.79
							100	10	40	608,927	32.04
							100	5	40	479,094	32.69
							100	1	40	264,567	30.07
							100	0.5	40	211,108	27.99
							100	0.1	40	135,060	22.32

DYNAMIC MODULUS TEST RESULTS (CON'T)
Sample Size: H150*D100

Spec. ID	Agg. Source	Nom. Size (mm)	Binder Grade	Binder Cont. (%)	A.Void Gyr. (%)	A.Void Core (%)	Dynamic Modulus Test Tem. (D.F)	Freq (Hz)	Stress (psi)	|E*| (psi)	PhAng (Deg)
223	MCA	12.5	PG67-22	6	6.4	4.1	40	25	150	2,166,075	22.40
							40	10	150	1,924,679	14.70
							40	5	150	1,732,600	15.34
							40	1	150	1,315,386	17.22
							40	0.5	150	1,159,006	18.04
							40	0.1	150	851,999	20.13
							70	25	75	1,682,212	25.54
							70	10	75	1,381,347	22.19
							70	5	75	1,150,843	22.82
							70	1	75	783,406	23.54
							70	0.5	75	657,209	23.79
							70	0.1	75	386,999	23.88
							100	25	40	650,238	35.95
							100	10	40	466,998	34.43
							100	5	40	363,602	32.71
							100	1	40	221,582	27.20
							100	0.5	40	180,158	24.42
							100	0.1	40	124,205	19.14
224	MCA	12.5	PG67-22	6	6.6	4.5	40	25	150	2,535,051	18.35
							40	10	150	2,205,150	13.46
							40	5	150	2,158,412	15.25
							40	1	150	1,684,922	18.84
							40	0.5	150	1,450,254	15.46
							40	0.1	150	987,254	18.32
							70	25	75	1,751,283	20.46
							70	10	75	1,471,639	17.45
							70	5	75	1,259,583	19.95
							70	1	75	859,039	22.57
							70	0.5	75	673,817	23.56
							70	0.1	75	441,667	24.85
							100	25	40	764,249	33.55
							100	10	40	564,905	32.71
							100	5	40	443,442	32.85
							100	1	40	252,848	30.17
							100	0.5	40	205,084	27.75
							100	0.1	40	138,570	22.06

DYNAMIC MODULUS TEST RESULTS (CON'T)
Sample Size: H150*D100

Spec. ID	Agg. Source	Nom. Size (mm)	Binder Grade	Binder Cont. (%)	A.Void Gyr. (%)	A.Void Core (%)	Dynamic Modulus Test Tem. (D.F)	Freq (Hz)	Stress (psi)	|E*| (psi)	PhAng (Deg)
231	MCA	12.5	PG67-22	6	9	6.7	40	25	150	1,994,560	11.99
							40	10	150	1,818,508	12.94
							40	5	150	1,698,569	12.54
							40	1	150	1,447,651	12.54
							40	0.5	150	1,342,462	11.92
							40	0.1	150	1,063,650	16.59
							70	25	75	1,486,469	16.40
							70	10	75	1,290,460	20.48
							70	5	75	1,112,131	21.11
							70	1	75	747,098	23.53
							70	0.5	75	626,827	24.09
							70	0.1	75	408,148	25.25
							100	25	40	645,450	29.02
							100	10	40	512,852	27.63
							100	5	40	432,233	27.78
							100	1	40	267,657	26.85
							100	0.5	40	221,303	25.75
							100	0.1	40	148,704	22.54
232	MCA	12.5	PG67-22	6	9.1	6.9	40	25	150	2,041,113	15.44
							40	10	150	1,876,836	15.54
							40	5	150	1,735,808	14.20
							40	1	150	1,366,229	15.74
							40	0.5	150	1,224,551	14.56
							40	0.1	150	925,446	18.94
							70	25	75	1,387,699	19.11
							70	10	75	1,200,722	17.61
							70	5	75	1,054,179	17.31
							70	1	75	761,614	20.00
							70	0.5	75	650,871	20.96
							70	0.1	75	444,160	23.20
							100	25	40	775,071	29.80
							100	10	40	616,432	28.84
							100	5	40	499,223	29.49
							100	1	40	308,911	27.61
							100	0.5	40	254,738	26.34
							100	0.1	40	162,726	23.30

DYNAMIC MODULUS TEST RESULTS (CON'T)
Sample Size: H150*D100

Spec. ID	Agg. Source	Nom. Size (mm)	Binder Grade	Binder Cont. (%)	A.Void		Dynamic Modulus Test				
					Gyr. (%)	Core (%)	Tem. (D.F)	Freq (Hz)	Stress (psi)	|E*| (psi)	PhAng (Deg)
233	MCA	12.5	PG67-22	6	9.1	6.5	40	25	150	1,912,860	14.59
							40	10	150	2,109,943	12.76
							40	5	150	1,787,049	11.31
							40	1	150	1,469,063	14.91
							40	0.5	150	1,327,586	11.93
							40	0.1	150	1,009,009	14.35
							70	25	75	1,309,122	18.33
							70	10	75	1,181,805	16.85
							70	5	75	1,074,831	17.49
							70	1	75	762,124	19.89
							70	0.5	75	660,560	20.36
							70	0.1	75	462,008	21.48
							100	25	40	799,068	31.42
							100	10	40	634,618	29.44
							100	5	40	507,648	27.23
							100	1	40	336,965	23.46
							100	0.5	40	277,624	22.10
							100	0.1	40	189,283	18.94
234	MCA	12.5	PG67-22	6	9.1	6.5	40	25	150	2,174,545	15.00
							40	10	150	2,019,122	13.14
							40	5	150	1,903,563	13.17
							40	1	150	1,587,741	14.82
							40	0.5	150	1,443,896	15.57
							40	0.1	150	1,088,121	18.11
							70	25	75	1,894,590	18.45
							70	10	75	1,519,430	18.60
							70	5	75	1,276,428	17.43
							70	1	75	935,299	18.60
							70	0.5	75	782,126	19.53
							70	0.1	75	496,728	22.89
							100	25	40	760,022	28.20
							100	10	40	610,866	26.46
							100	5	40	510,334	26.41
							100	1	40	331,734	24.59
							100	0.5	40	269,014	23.97
							100	0.1	40	181,383	21.16

DYNAMIC MODULUS TEST RESULTS (CON'T)
Sample Size: H150*D100

Spec. ID	Agg. Source	Nom. Size (mm)	Binder Grade	Binder Cont. (%)	A.Void Gyr. (%)	A.Void Core (%)	Dynamic Modulus Test Tem. (D.F)	Freq (Hz)	Stress (psi)	|E*| (psi)	PhAng (Deg)
241	MCA	12.5	PG67-22	6.5	5.9	4.1	40	25	150	2,116,868	14.40
							40	10	150	1,914,778	16.44
							40	5	150	1,732,216	16.75
							40	1	150	1,322,033	17.32
							40	0.5	150	1,152,880	17.69
							40	0.1	150	846,988	19.73
							70	25	75	1,498,272	20.15
							70	10	75	1,277,172	18.66
							70	5	75	1,115,106	19.38
							70	1	75	758,193	22.72
							70	0.5	75	612,904	24.43
							70	0.1	75	392,580	24.75
							100	25	40	852,151	34.30
							100	10	40	663,378	34.87
							100	5	40	486,024	33.76
							100	1	40	274,872	30.19
							100	0.5	40	220,256	28.24
							100	0.1	40	146,844	22.98
242	MCA	12.5	PG67-22	6.5	6.5	4.4	40	25	150	2,316,779	15.64
							40	10	150	2,018,598	15.84
							40	5	150	1,749,123	14.65
							40	1	150	1,266,050	15.64
							40	0.5	150	1,099,883	16.54
							40	0.1	150	776,792	23.42
							70	25	75	1,673,117	20.53
							70	10	75	1,379,137	19.86
							70	5	75	1,175,769	19.76
							70	1	75	816,764	21.45
							70	0.5	75	681,687	21.88
							70	0.1	75	444,248	22.74
							100	25	40	659,000	31.08
							100	10	40	513,581	29.62
							100	5	40	395,859	28.80
							100	1	40	242,316	26.34
							100	0.5	40	200,692	24.03
							100	0.1	40	135,464	18.63

DYNAMIC MODULUS TEST RESULTS (CON'T)
Sample Size: H150*D100

Spec. ID	Agg. Source	Nom. Size (mm)	Binder Grade	Binder Cont. (%)	A.Void Gyr. (%)	A.Void Core (%)	Dynamic Modulus Test Tem. (D.F)	Freq (Hz)	Stress (psi)	|E*| (psi)	PhAng (Deg)
243	MCA	12.5	PG67-22	6.5	6.3	4.3	40	25	150	2,608,399	14.66
							40	10	150	2,207,872	13.08
							40	5	150	1,992,255	13.15
							40	1	150	1,546,380	15.02
							40	0.5	150	1,348,926	15.84
							40	0.1	150	970,080	17.35
							70	25	75	1,456,852	17.00
							70	10	75	1,243,487	16.70
							70	5	75	1,130,735	16.14
							70	1	75	829,444	17.14
							70	0.5	75	710,444	17.95
							70	0.1	75	484,785	19.42
							100	25	40	612,504	28.53
							100	10	40	477,454	27.09
							100	5	40	391,111	26.47
							100	1	40	256,262	24.01
							100	0.5	40	213,906	23.03
							100	0.1	40	148,017	18.78
244	MCA	12.5	PG67-22	6.5	6	4.2	40	25	150	1,859,669	13.44
							40	10	150	1,563,350	14.56
							40	5	150	1,428,154	11.92
							40	1	150	1,162,812	14.22
							40	0.5	150	1,027,485	15.31
							40	0.1	150	741,496	18.02
							70	25	75	1,528,147	21.45
							70	10	75	1,290,102	20.10
							70	5	75	1,127,575	20.29
							70	1	75	782,183	22.45
							70	0.5	75	654,871	23.18
							70	0.1	75	409,073	23.79
							100	25	40	717,486	34.04
							100	10	40	533,425	33.07
							100	5	40	418,165	32.70
							100	1	40	233,801	29.02
							100	0.5	40	190,471	26.55
							100	0.1	40	127,772	21.29

DYNAMIC MODULUS TEST RESULTS (CON'T)
Sample Size: H150*D100

Spec. ID	Agg. Source	Nom. Size (mm)	Binder Grade	Binder Cont. (%)	A.Void Gyr. (%)	A.Void Core (%)	Dynamic Modulus Test Tem. (D.F)	Freq (Hz)	Stress (psi)	|E*| (psi)	PhAng (Deg)
251	MCA	12.5	PG67-22	6.5	9.3	6.6	40	25	150	2,438,412	18.54
							40	10	150	1,901,366	18.64
							40	5	150	1,646,211	17.64
							40	1	150	1,174,904	16.58
							40	0.5	150	1,102,150	17.54
							40	0.1	150	706,979	19.54
							70	25	75	1,792,251	21.00
							70	10	75	1,358,191	23.96
							70	5	75	1,254,805	23.67
							70	1	75	875,233	28.95
							70	0.5	75	548,154	28.47
							70	0.1	75	466,382	27.98
							100	25	40	563,461	31.80
							100	10	40	458,715	28.61
							100	5	40	354,815	30.90
							100	1	40	225,181	26.95
							100	0.5	40	182,005	24.83
							100	0.1	40	115,481	19.27
252	MCA	12.5	PG67-22	6.5	9.2	6.7	40	25	150	1,996,920	18.36
							40	10	150	1,684,628	15.75
							40	5	150	1,499,067	15.57
							40	1	150	1,165,701	16.65
							40	0.5	150	1,031,238	17.33
							40	0.1	150	755,418	19.58
							70	25	75	1,518,434	22.21
							70	10	75	1,278,475	28.25
							70	5	75	1,049,622	18.52
							70	1	75	726,364	27.23
							70	0.5	75	611,362	27.22
							70	0.1	75	405,935	26.72
							100	25	40	763,820	34.17
							100	10	40	584,254	30.48
							100	5	40	473,436	29.75
							100	1	40	290,437	27.99
							100	0.5	40	242,997	27.91
							100	0.1	40	158,602	22.92

DYNAMIC MODULUS TEST RESULTS (CON'T)
Sample Size: H150*D100

Spec. ID	Agg. Source	Nom. Size (mm)	Binder Grade	Binder Cont. (%)	A.Void Gyr. (%)	A.Void Core (%)	Dynamic Modulus Test Tem. (D.F)	Freq (Hz)	Stress (psi)	|E*| (psi)	PhAng (Deg)
253	MCA	12.5	PG67-22	6.5	8.8	6.6	40	25	150	2,247,411	13.70
							40	10	150	2,107,600	14.64
							40	5	150	1,974,521	14.62
							40	1	150	1,535,129	15.46
							40	0.5	150	1,450,524	13.53
							40	0.1	150	891,540	15.46
							70	25	75	1,521,510	22.67
							70	10	75	1,115,420	21.45
							70	5	75	980,210	21.36
							70	1	75	678,905	23.05
							70	0.5	75	681,545	23.34
							70	0.1	75	325,185	22.47
							100	25	40	800,843	27.69
							100	10	40	581,386	27.75
							100	5	40	473,545	27.73
							100	1	40	289,652	26.76
							100	0.5	40	230,105	25.30
							100	0.1	40	150,206	21.62
254	MCA	12.5	PG67-22	6.5	9.8	7	40	25	150	1,954,265	17.56
							40	10	150	1,775,725	15.61
							40	5	150	1,701,785	15.64
							40	1	150	1,449,739	15.45
							40	0.5	150	1,314,517	13.54
							40	0.1	150	998,847	14.65
							70	25	75	1,289,980	21.95
							70	10	75	1,069,208	20.47
							70	5	75	926,606	20.15
							70	1	75	613,580	23.27
							70	0.5	75	501,916	24.08
							70	0.1	75	385,691	24.55
							100	25	40	651,338	30.70
							100	10	40	502,017	29.49
							100	5	40	393,645	30.77
							100	1	40	228,961	27.35
							100	0.5	40	188,966	25.31
							100	0.1	40	129,992	20.07

DYNAMIC MODULUS TEST RESULTS (CON'T)
Sample Size: H150*D100

Spec. ID	Agg. Source	Nom. Size (mm)	Binder Grade	Binder Cont. (%)	A.Void		Dynamic Modulus Test				
					Gyr. (%)	Core (%)	Tem. (D.F)	Freq (Hz)	Stress (psi)	|E*| (psi)	PhAng (Deg)
261	MCA	25	PG67-22	5.2	6.5	4.2	40	25	150	3,237,709	15.61
							40	10	150	2,858,973	14.46
							40	5	150	2,439,328	15.46
							40	1	150	1,823,150	18.51
							40	0.5	150	1,608,685	19.05
							40	0.1	150	1,219,396	18.64
							70	25	75	2,520,826	21.16
							70	10	75	2,012,432	20.98
							70	5	75	1,628,110	22.94
							70	1	75	1,045,651	23.86
							70	0.5	75	866,373	23.97
							70	0.1	75	568,868	24.92
							100	25	40	1,535,204	32.10
							100	10	40	921,500	28.95
							100	5	40	854,625	29.40
							100	1	40	458,251	27.45
							100	0.5	40	385,614	24.84
							100	0.1	40	254,813	22.47
262	MCA	25	PG67-22	5.2	6.4	4	40	25	150	2,842,134	13.54
							40	10	150	2,563,530	12.04
							40	5	150	2,380,015	12.51
							40	1	150	2,012,208	18.64
							40	0.5	150	1,780,098	18.54
							40	0.1	150	1,287,641	14.56
							70	25	75	2,621,874	20.65
							70	10	75	2,018,880	17.88
							70	5	75	1,749,067	19.10
							70	1	75	1,220,044	19.69
							70	0.5	75	925,145	19.88
							70	0.1	75	672,050	22.34
							100	25	40	1,150,512	30.99
							100	10	40	749,645	28.38
							100	5	40	624,674	27.95
							100	1	40	388,747	26.99
							100	0.5	40	313,480	27.30
							100	0.1	40	202,151	24.19

DYNAMIC MODULUS TEST RESULTS (CON'T)
Sample Size: H150*D100

Spec. ID	Agg. Source	Nom. Size (mm)	Binder Grade	Binder Cont. (%)	A.Void		Dynamic Modulus Test				
					Gyr. (%)	Core (%)	Tem. (D.F)	Freq (Hz)	Stress (psi)	|E*| (psi)	PhAng (Deg)
263	MCA	25	PG67-22	5.2	6.3	4.1	40	25	150	2,548,164	14.10
							40	10	150	2,365,481	11.62
							40	5	150	1,967,180	11.15
							40	1	150	1,580,676	19.81
							40	0.5	150	1,651,581	16.00
							40	0.1	150	1,172,748	15.97
							70	25	75	2,113,373	16.30
							70	10	75	1,425,413	18.76
							70	5	75	1,211,883	18.83
							70	1	75	835,872	21.36
							70	0.5	75	696,695	22.46
							70	0.1	75	531,581	24.60
							100	25	40	1,125,887	26.80
							100	10	40	914,559	29.55
							100	5	40	727,378	29.44
							100	1	40	401,917	30.33
							100	0.5	40	324,233	28.60
							100	0.1	40	203,678	24.93
264	MCA	25	PG67-22	5.2	6.9	4.3	40	25	150	3,358,184	13.75
							40	10	150	3,351,812	11.93
							40	5	150	2,852,115	13.19
							40	1	150	2,254,810	14.55
							40	0.5	150	2,150,518	15.30
							40	0.1	150	1,580,215	18.14
							70	25	75	2,035,226	21.97
							70	10	75	1,700,496	18.91
							70	5	75	1,448,320	21.56
							70	1	75	975,789	22.64
							70	0.5	75	819,229	24.29
							70	0.1	75	543,900	24.94
							100	25	40	1,218,747	37.74
							100	10	40	952,228	38.28
							100	5	40	716,436	37.33
							100	1	40	415,163	30.02
							100	0.5	40	338,395	28.13
							100	0.1	40	208,019	23.07

DYNAMIC MODULUS TEST RESULTS (CON'T)
Sample Size: H150*D100

Spec. ID	Agg. Source	Nom. Size (mm)	Binder Grade	Binder Cont. (%)	A.Void Gyr. (%)	A.Void Core (%)	Dynamic Modulus Test Tem. (D.F)	Freq (Hz)	Stress (psi)	|E*| (psi)	PhAng (Deg)
271	MCA	25	PG67-22	5.2	10.8	7.3	40	25	150	2,205,917	14.80
							40	10	150	1,990,235	15.42
							40	5	150	1,750,948	16.52
							40	1	150	1,305,434	18.16
							40	0.5	150	1,139,560	17.64
							40	0.1	150	853,285	19.89
							70	25	75	1,351,545	21.10
							70	10	75	1,154,234	21.83
							70	5	75	1,010,472	21.95
							70	1	75	682,036	23.42
							70	0.5	75	578,722	24.08
							70	0.1	75	382,226	23.74
							100	25	40	561,755	34.00
							100	10	40	482,571	31.45
							100	5	40	325,164	30.32
							100	1	40	206,269	25.22
							100	0.5	40	176,522	22.15
							100	0.1	40	128,317	16.71
272	MCA	25	PG67-22	5.2	10.3	7.5	40	25	125	2,225,825	16.60
							40	10	125	1,943,634	13.97
							40	5	125	1,761,919	13.79
							40	1	125	1,389,742	15.37
							40	0.5	125	1,249,034	16.54
							40	0.1	125	968,149	17.89
							70	25	62	1,796,993	18.20
							70	10	62	1,503,938	21.98
							70	5	62	1,311,724	22.10
							70	1	62	850,766	25.86
							70	0.5	62	681,990	26.61
							70	0.1	62	462,871	25.63
							100	25	40	704,958	35.40
							100	10	40	555,974	35.08
							100	5	40	439,846	33.17
							100	1	40	266,465	26.15
							100	0.5	40	222,215	25.13
							100	0.1	40	150,193	20.28

DYNAMIC MODULUS TEST RESULTS (CON'T)
Sample Size: H150*D100

Spec. ID	Agg. Source	Nom. Size (mm)	Binder Grade	Binder Cont. (%)	A.Void Gyr. (%)	A.Void Core (%)	Dynamic Modulus Test Tem. (D.F)	Freq (Hz)	Stress (psi)	|E*| (psi)	PhAng (Deg)
273	MCA	25	PG67-22	5.2	9.9	7.3	40	25	150	2,164,361	12.82
							40	10	150	1,964,942	13.94
							40	5	150	1,780,705	12.92
							40	1	150	1,398,522	14.83
							40	0.5	150	1,238,355	15.62
							40	0.1	150	901,383	18.15
							70	25	75	1,559,315	19.53
							70	10	75	1,328,485	18.81
							70	5	75	1,139,048	19.88
							70	1	75	794,137	20.80
							70	0.5	75	657,356	21.50
							70	0.1	75	439,664	22.46
							100	25	40	808,231	34.43
							100	10	40	607,102	34.15
							100	5	40	454,263	32.02
							100	1	40	286,168	28.06
							100	0.5	40	241,325	25.45
							100	0.1	40	172,683	20.12
274	MCA	25	PG67-22	5.2	10.4	7.5	40	25	150	1,940,226	11.60
							40	10	150	1,792,729	11.22
							40	5	150	1,672,899	14.64
							40	1	150	1,381,694	14.51
							40	0.5	150	1,233,584	13.41
							40	0.1	150	907,610	16.50
							70	25	75	1,362,628	18.55
							70	10	75	1,196,432	16.36
							70	5	75	1,061,051	16.10
							70	1	75	796,871	25.61
							70	0.5	75	682,132	18.54
							70	0.1	75	443,739	20.08
							100	25	40	768,508	31.70
							100	10	40	590,700	32.06
							100	5	40	460,169	29.89
							100	1	40	279,891	27.62
							100	0.5	40	227,121	25.53
							100	0.1	40	163,571	20.46

APPENDIX B

STATISTICAL DESCRIPTIONS OF DYNAMIC MODULUS

STATISTICAL DESCRIPTIONS OF DYNAMIC MODULUS
Sample Size: H150*D100

Spec. ID	Nom. Size (mm)	Bind. Cont. (%)	Air Void (%)	Temp (D.F)	Freq (Hz)	|E*| Test (psi)	Mean (psi)	Std Dev (psi)	Std Err (psi)	C Var (%)
201	12.5	5.5	4.5	40	25	3,199,716	3,024,259	148,061	74,031	4.9
202	12.5	5.5	4.5	40	25	2,979,511				
203	12.5	5.5	4.5	40	25	2,848,369				
204	12.5	5.5	4.5	40	25	3,069,441				
201	12.5	5.5	4.5	40	10	2,981,345	2,658,157	218,288	109,144	8.2
202	12.5	5.5	4.5	40	10	2,520,074				
203	12.5	5.5	4.5	40	10	2,531,700				
204	12.5	5.5	4.5	40	10	2,599,508				
201	12.5	5.5	4.5	40	5	2,760,132	2,396,230	244,682	122,341	10.2
202	12.5	5.5	4.5	40	5	2,241,950				
203	12.5	5.5	4.5	40	5	2,317,979				
204	12.5	5.5	4.5	40	5	2,264,860				
201	12.5	5.5	4.5	40	1	2,304,990	1,947,691	241,042	120,521	12.4
202	12.5	5.5	4.5	40	1	1,825,738				
203	12.5	5.5	4.5	40	1	1,875,158				
204	12.5	5.5	4.5	40	1	1,784,878				
201	12.5	5.5	4.5	40	0.5	1,854,251	1,635,931	177,862	88,931	10.9
202	12.5	5.5	4.5	40	0.5	1,432,607				
203	12.5	5.5	4.5	40	0.5	1,682,230				
204	12.5	5.5	4.5	40	0.5	1,574,637				
201	12.5	5.5	4.5	40	0.1	1,531,404	1,263,955	185,551	92,776	14.7
202	12.5	5.5	4.5	40	0.1	1,141,575				
203	12.5	5.5	4.5	40	0.1	1,247,364				
204	12.5	5.5	4.5	40	0.1	1,135,476				
201	12.5	5.5	4.5	70	25	2,030,906	1,917,366	116,456	58,228	6.1
202	12.5	5.5	4.5	70	25	1,951,044				
203	12.5	5.5	4.5	70	25	1,754,807				
204	12.5	5.5	4.5	70	25	1,932,707				
201	12.5	5.5	4.5	70	10	1,735,194	1,645,308	75,905	37,952	4.6
202	12.5	5.5	4.5	70	10	1,675,293				
203	12.5	5.5	4.5	70	10	1,561,692				
204	12.5	5.5	4.5	70	10	1,609,054				
201	12.5	5.5	4.5	70	5	1,478,252	1,436,995	41,774	20,887	2.9
202	12.5	5.5	4.5	70	5	1,467,477				
203	12.5	5.5	4.5	70	5	1,405,038				
204	12.5	5.5	4.5	70	5	1,397,212				

STATISTICAL DESCRIPTIONS OF DYNAMIC MODULUS (CON'T)
Sample Size: H150*D100

Spec. ID	Nom. Size (mm)	Binder Cont. (%)	Air Void (%)	Temp (D.F)	Freq (Hz)	|E*| Test (psi)	Mean (psi)	Std Dev (psi)	Std Err (psi)	C Var (%)
201	12.5	5.5	4.5	70	1	1,017,167	1,019,315	31,424	15,712	3.1
202	12.5	5.5	4.5	70	1	1,043,235				
203	12.5	5.5	4.5	70	1	1,041,207				
204	12.5	5.5	4.5	70	1	975,652				
201	12.5	5.5	4.5	70	0.5	854,929	868,916	38,224	19,112	4.4
202	12.5	5.5	4.5	70	0.5	887,163				
203	12.5	5.5	4.5	70	0.5	910,635				
204	12.5	5.5	4.5	70	0.5	822,937				
201	12.5	5.5	4.5	70	0.1	565,695	593,837	45,682	22,841	7.7
202	12.5	5.5	4.5	70	0.1	627,539				
203	12.5	5.5	4.5	70	0.1	637,518				
204	12.5	5.5	4.5	70	0.1	544,597				
201	12.5	5.5	4.5	100	25	1,035,685	1,002,099	133,714	66,857	13.3
202	12.5	5.5	4.5	100	25	967,201				
203	12.5	5.5	4.5	100	25	842,613				
204	12.5	5.5	4.5	100	25	1,162,898				
201	12.5	5.5	4.5	100	10	920,835	798,676	122,094	61,047	15.3
202	12.5	5.5	4.5	100	10	745,061				
203	12.5	5.5	4.5	100	10	653,557				
204	12.5	5.5	4.5	100	10	875,252				
201	12.5	5.5	4.5	100	5	750,863	626,489	88,410	44,205	14.1
202	12.5	5.5	4.5	100	5	583,473				
203	12.5	5.5	4.5	100	5	548,258				
204	12.5	5.5	4.5	100	5	623,362				
201	12.5	5.5	4.5	100	1	430,000	364,777	54,512	27,256	14.9
202	12.5	5.5	4.5	100	1	385,920				
203	12.5	5.5	4.5	100	1	337,152				
204	12.5	5.5	4.5	100	1	306,035				
201	12.5	5.5	4.5	100	0.5	298,058	280,684	40,069	20,034	14.3
202	12.5	5.5	4.5	100	0.5	326,485				
203	12.5	5.5	4.5	100	0.5	263,614				
204	12.5	5.5	4.5	100	0.5	234,580				
201	12.5	5.5	4.5	100	0.1	185,058	168,188	26,334	13,167	15.7
202	12.5	5.5	4.5	100	0.1	193,918				
203	12.5	5.5	4.5	100	0.1	157,527				
204	12.5	5.5	4.5	100	0.1	136,249				

STATISTICAL DESCRIPTIONS OF DYNAMIC MODULUS (CON'T)
Sample Size: H150*D100

Spec. ID	Nom. Size (mm)	Binder Cont. (%)	Air Void (%)	Temp (D.F)	Freq (Hz)	|E*| Test (psi)	Mean (psi)	Std Dev (psi)	Std Err (psi)	C Var (%)
211	12.5	5.5	7.0	40	25	2,690,758	2,916,285	461,771	230,886	15.8
212	12.5	5.5	7.0	40	25	3,211,148				
213	12.5	5.5	7.0	40	25	3,381,360				
214	12.5	5.5	7.0	40	25	2,381,872				
211	12.5	5.5	7.0	40	10	2,457,337	2,618,891	402,618	201,309	15.4
212	12.5	5.5	7.0	40	10	3,058,520				
213	12.5	5.5	7.0	40	10	2,817,689				
214	12.5	5.5	7.0	40	10	2,142,016				
211	12.5	5.5	7.0	40	5	2,424,586	2,372,228	239,071	119,536	10.1
212	12.5	5.5	7.0	40	5	2,565,954				
213	12.5	5.5	7.0	40	5	2,473,813				
214	12.5	5.5	7.0	40	5	2,024,558				
211	12.5	5.5	7.0	40	1	1,758,993	1,868,694	272,514	136,257	14.6
212	12.5	5.5	7.0	40	1	2,251,651				
213	12.5	5.5	7.0	40	1	1,847,751				
214	12.5	5.5	7.0	40	1	1,616,379				
211	12.5	5.5	7.0	40	0.5	1,530,931	1,656,429	252,283	126,141	15.2
212	12.5	5.5	7.0	40	0.5	2,021,543				
213	12.5	5.5	7.0	40	0.5	1,617,779				
214	12.5	5.5	7.0	40	0.5	1,455,461				
211	12.5	5.5	7.0	40	0.1	1,098,147	1,189,303	146,065	73,032	12.3
212	12.5	5.5	7.0	40	0.1	1,405,369				
213	12.5	5.5	7.0	40	0.1	1,151,441				
214	12.5	5.5	7.0	40	0.1	1,102,256				
211	12.5	5.5	7.0	70	25	1,741,646	1,619,024	251,809	125,905	15.6
212	12.5	5.5	7.0	70	25	1,902,151				
213	12.5	5.5	7.0	70	25	1,336,429				
214	12.5	5.5	7.0	70	25	1,495,870				
211	12.5	5.5	7.0	70	10	1,607,403	1,419,204	198,708	99,354	14.0
212	12.5	5.5	7.0	70	10	1,545,615				
213	12.5	5.5	7.0	70	10	1,168,182				
214	12.5	5.5	7.0	70	10	1,355,616				
211	12.5	5.5	7.0	70	5	1,360,660	1,283,133	197,429	98,714	15.4
212	12.5	5.5	7.0	70	5	1,512,051				
213	12.5	5.5	7.0	70	5	1,053,864				
214	12.5	5.5	7.0	70	5	1,205,956				

STATISTICAL DESCRIPTIONS OF DYNAMIC MODULUS (CON'T)
Sample Size: H150*D100

Spec. ID	Nom. Size (mm)	Binder Cont. (%)	Air Void (%)	Temp (D.F)	Freq (Hz)	|E*| Test (psi)	|E*| Mean (psi)	|E*| Std Dev (psi)	|E*| Std Err (psi)	|E*| C Var (%)
211	12.5	5.5	7.0	70	1	965,774	909,873	128,868	64,434	14.2
212	12.5	5.5	7.0	70	1	1,050,054				
213	12.5	5.5	7.0	70	1	749,297				
214	12.5	5.5	7.0	70	1	874,365				
211	12.5	5.5	7.0	70	0.5	792,365	744,721	74,974	37,487	10.1
212	12.5	5.5	7.0	70	0.5	802,158				
213	12.5	5.5	7.0	70	0.5	638,452				
214	12.5	5.5	7.0	70	0.5	745,907				
211	12.5	5.5	7.0	70	0.1	493,536	530,382	81,026	40,513	15.3
212	12.5	5.5	7.0	70	0.1	640,402				
213	12.5	5.5	7.0	70	0.1	451,626				
214	12.5	5.5	7.0	70	0.1	535,964				
211	12.5	5.5	7.0	100	25	997,102	831,747	120,109	60,054	14.4
212	12.5	5.5	7.0	100	25	757,847				
213	12.5	5.5	7.0	100	25	729,927				
214	12.5	5.5	7.0	100	25	842,110				
211	12.5	5.5	7.0	100	10	724,100	614,259	73,972	36,986	12.0
212	12.5	5.5	7.0	100	10	592,084				
213	12.5	5.5	7.0	100	10	567,572				
214	12.5	5.5	7.0	100	10	573,281				
211	12.5	5.5	7.0	100	5	584,512	497,655	61,712	30,856	12.4
212	12.5	5.5	7.0	100	5	495,566				
213	12.5	5.5	7.0	100	5	443,355				
214	12.5	5.5	7.0	100	5	467,187				
211	12.5	5.5	7.0	100	1	352,485	303,487	42,789	21,394	14.1
212	12.5	5.5	7.0	100	1	316,026				
213	12.5	5.5	7.0	100	1	249,901				
214	12.5	5.5	7.0	100	1	295,537				
211	12.5	5.5	7.0	100	0.5	289,452	248,426	35,893	17,946	14.4
212	12.5	5.5	7.0	100	0.5	261,896				
213	12.5	5.5	7.0	100	0.5	205,125				
214	12.5	5.5	7.0	100	0.5	237,232				
211	12.5	5.5	7.0	100	0.1	185,021	163,699	25,015	12,508	15.3
212	12.5	5.5	7.0	100	0.1	180,624				
213	12.5	5.5	7.0	100	0.1	130,349				
214	12.5	5.5	7.0	100	0.1	158,803				

STATISTICAL DESCRIPTIONS OF DYNAMIC MODULUS (CON'T)
Sample Size: H150*D100

Spec. ID	Nom. Size (mm)	Binder Cont. (%)	Air Void (%)	Temp (D.F)	Freq (Hz)	|E*| Test (psi)	Mean (psi)	Std Dev (psi)	Std Err (psi)	C Var (%)
221	12.5	6	4.5	40	25	1,896,988	2,121,308	304,605	152,302	14.4
222	12.5	6	4.5	40	25	1,887,117				
223	12.5	6	4.5	40	25	2,166,075				
224	12.5	6	4.5	40	25	2,535,051				
221	12.5	6	4.5	40	10	1,798,556	1,923,996	199,369	99,684	10.4
222	12.5	6	4.5	40	10	1,767,598				
223	12.5	6	4.5	40	10	1,924,679				
224	12.5	6	4.5	40	10	2,205,150				
221	12.5	6	4.5	40	5	1,614,805	1,782,812	255,989	127,995	14.4
222	12.5	6	4.5	40	5	1,625,431				
223	12.5	6	4.5	40	5	1,732,600				
224	12.5	6	4.5	40	5	2,158,412				
221	12.5	6	4.5	40	1	1,280,157	1,394,519	194,135	97,068	13.9
222	12.5	6	4.5	40	1	1,297,612				
223	12.5	6	4.5	40	1	1,315,386				
224	12.5	6	4.5	40	1	1,684,922				
221	12.5	6	4.5	40	0.5	1,143,183	1,230,067	147,145	73,572	12.0
222	12.5	6	4.5	40	0.5	1,167,825				
223	12.5	6	4.5	40	0.5	1,159,006				
224	12.5	6	4.5	40	0.5	1,450,254				
221	12.5	6	4.5	40	0.1	844,363	888,092	66,888	33,444	7.5
222	12.5	6	4.5	40	0.1	868,751				
223	12.5	6	4.5	40	0.1	851,999				
224	12.5	6	4.5	40	0.1	987,254				
221	12.5	6	4.5	70	25	1,518,234	1,666,733	102,939	51,470	6.2
222	12.5	6	4.5	70	25	1,715,203				
223	12.5	6	4.5	70	25	1,682,212				
224	12.5	6	4.5	70	25	1,751,283				
221	12.5	6	4.5	70	10	1,255,990	1,416,250	128,461	64,230	9.1
222	12.5	6	4.5	70	10	1,556,025				
223	12.5	6	4.5	70	10	1,381,347				
224	12.5	6	4.5	70	10	1,471,639				
221	12.5	6	4.5	70	5	1,062,831	1,189,828	102,913	51,457	8.6
222	12.5	6	4.5	70	5	1,286,054				
223	12.5	6	4.5	70	5	1,150,843				
224	12.5	6	4.5	70	5	1,259,583				

STATISTICAL DESCRIPTIONS OF DYNAMIC MODULUS (CON'T)
Sample Size: H150*D100

Spec. ID	Nom. Size (mm)	Binder Cont. (%)	Air Void (%)	Temp (D.F)	Freq (Hz)	|E*| Test (psi)	Mean (psi)	Std Dev (psi)	Std Err (psi)	C Var (%)
221	12.5	6	4.5	70	1	691,503	787,379	71,034	35,517	9.0
222	12.5	6	4.5	70	1	815,566				
223	12.5	6	4.5	70	1	783,406				
224	12.5	6	4.5	70	1	859,039				
221	12.5	6	4.5	70	0.5	570,189	642,601	48,779	24,390	7.6
222	12.5	6	4.5	70	0.5	669,188				
223	12.5	6	4.5	70	0.5	657,209				
224	12.5	6	4.5	70	0.5	673,817				
221	12.5	6	4.5	70	0.1	354,775	403,861	40,476	20,238	10.0
222	12.5	6	4.5	70	0.1	432,001				
223	12.5	6	4.5	70	0.1	386,999				
224	12.5	6	4.5	70	0.1	441,667				
221	12.5	6	4.5	100	25	763,291	744,788	65,479	32,740	8.8
222	12.5	6	4.5	100	25	801,373				
223	12.5	6	4.5	100	25	650,238				
224	12.5	6	4.5	100	25	764,249				
221	12.5	6	4.5	100	10	520,907	540,434	60,730	30,365	11.2
222	12.5	6	4.5	100	10	608,927				
223	12.5	6	4.5	100	10	466,998				
224	12.5	6	4.5	100	10	564,905				
221	12.5	6	4.5	100	5	384,524	417,666	53,101	26,550	12.7
222	12.5	6	4.5	100	5	479,094				
223	12.5	6	4.5	100	5	363,602				
224	12.5	6	4.5	100	5	443,442				
221	12.5	6	4.5	100	1	223,995	240,748	21,305	10,653	8.8
222	12.5	6	4.5	100	1	264,567				
223	12.5	6	4.5	100	1	221,582				
224	12.5	6	4.5	100	1	252,848				
221	12.5	6	4.5	100	0.5	170,739	191,772	19,394	9,697	10.1
222	12.5	6	4.5	100	0.5	211,108				
223	12.5	6	4.5	100	0.5	180,158				
224	12.5	6	4.5	100	0.5	205,084				
221	12.5	6	4.5	100	0.1	114,874	128,177	10,772	5,386	8.4
222	12.5	6	4.5	100	0.1	135,060				
223	12.5	6	4.5	100	0.1	124,205				
224	12.5	6	4.5	100	0.1	138,570				

STATISTICAL DESCRIPTIONS OF DYNAMIC MODULUS (CON'T)
Sample Size: H150*D100

Spec. ID	Nom. Size (mm)	Binder Cont. (%)	Air Void (%)	Temp (D.F)	Freq (Hz)	|E*| Test (psi)	|E*| Mean (psi)	|E*| Std Dev (psi)	|E*| Std Err (psi)	|E*| C Var (%)
231	12.5	6	7.0	40	25	1,994,560	2,030,770	109,533	54,766	5.4
232	12.5	6	7.0	40	25	2,041,113				
233	12.5	6	7.0	40	25	1,912,860				
234	12.5	6	7.0	40	25	2,174,545				
231	12.5	6	7.0	40	10	1,818,508	1,956,102	132,733	66,366	6.8
232	12.5	6	7.0	40	10	1,876,836				
233	12.5	6	7.0	40	10	2,109,943				
234	12.5	6	7.0	40	10	2,019,122				
231	12.5	6	7.0	40	5	1,698,569	1,781,247	89,247	44,624	5.0
232	12.5	6	7.0	40	5	1,735,808				
233	12.5	6	7.0	40	5	1,787,049				
234	12.5	6	7.0	40	5	1,903,563				
231	12.5	6	7.0	40	1	1,447,651	1,467,671	91,488	45,744	6.2
232	12.5	6	7.0	40	1	1,366,229				
233	12.5	6	7.0	40	1	1,469,063				
234	12.5	6	7.0	40	1	1,587,741				
231	12.5	6	7.0	40	0.5	1,342,462	1,334,624	89,754	44,877	6.7
232	12.5	6	7.0	40	0.5	1,224,551				
233	12.5	6	7.0	40	0.5	1,327,586				
234	12.5	6	7.0	40	0.5	1,443,896				
231	12.5	6	7.0	40	0.1	1,063,650	1,021,557	72,105	36,052	7.1
232	12.5	6	7.0	40	0.1	925,446				
233	12.5	6	7.0	40	0.1	1,009,009				
234	12.5	6	7.0	40	0.1	1,088,121				
231	12.5	6	7.0	70	25	1,486,469	1,493,463	210,937	105,469	14.1
232	12.5	6	7.0	70	25	1,387,699				
233	12.5	6	7.0	70	25	1,309,122				
234	12.5	6	7.0	70	25	1,790,561				
231	12.5	6	7.0	70	10	1,290,460	1,298,104	154,976	77,488	11.9
232	12.5	6	7.0	70	10	1,200,722				
233	12.5	6	7.0	70	10	1,181,805				
234	12.5	6	7.0	70	10	1,519,430				
231	12.5	6	7.0	70	5	1,112,131	1,129,392	100,915	50,457	8.9
232	12.5	6	7.0	70	5	1,054,179				
233	12.5	6	7.0	70	5	1,074,831				
234	12.5	6	7.0	70	5	1,276,428				

STATISTICAL DESCRIPTIONS OF DYNAMIC MODULUS (CON'T)
Sample Size: H150*D100

Spec. ID	Nom. Size (mm)	Binder Cont. (%)	Air Void (%)	Temp (D.F)	Freq (Hz)	|E*| Test (psi)	Mean (psi)	Std Dev (psi)	Std Err (psi)	C Var (%)
231	12.5	6	7.0	70	1	747,098	801,534	89,449	44,724	11.2
232	12.5	6	7.0	70	1	761,614				
233	12.5	6	7.0	70	1	762,124				
234	12.5	6	7.0	70	1	935,299				
231	12.5	6	7.0	70	0.5	626,827	680,096	69,483	34,741	10.2
232	12.5	6	7.0	70	0.5	650,871				
233	12.5	6	7.0	70	0.5	660,560				
234	12.5	6	7.0	70	0.5	782,126				
231	12.5	6	7.0	70	0.1	408,148	452,761	36,891	18,446	8.1
232	12.5	6	7.0	70	0.1	444,160				
233	12.5	6	7.0	70	0.1	462,008				
234	12.5	6	7.0	70	0.1	496,728				
231	12.5	6	7.0	100	25	645,450	744,903	68,224	34,112	9.2
232	12.5	6	7.0	100	25	775,071				
233	12.5	6	7.0	100	25	799,068				
234	12.5	6	7.0	100	25	760,022				
231	12.5	6	7.0	100	10	512,852	593,692	54,839	27,420	9.2
232	12.5	6	7.0	100	10	616,432				
233	12.5	6	7.0	100	10	634,618				
234	12.5	6	7.0	100	10	610,866				
231	12.5	6	7.0	100	5	432,233	487,360	37,055	18,527	7.6
232	12.5	6	7.0	100	5	499,223				
233	12.5	6	7.0	100	5	507,648				
234	12.5	6	7.0	100	5	510,334				
231	12.5	6	7.0	100	1	267,657	311,317	31,552	15,776	10.1
232	12.5	6	7.0	100	1	308,911				
233	12.5	6	7.0	100	1	336,965				
234	12.5	6	7.0	100	1	331,734				
231	12.5	6	7.0	100	0.5	221,303	255,670	24,779	12,390	9.7
232	12.5	6	7.0	100	0.5	254,738				
233	12.5	6	7.0	100	0.5	277,624				
234	12.5	6	7.0	100	0.5	269,014				
231	12.5	6	7.0	100	0.1	148,704	170,524	18,319	9,159	10.7
232	12.5	6	7.0	100	0.1	162,726				
233	12.5	6	7.0	100	0.1	189,283				
234	12.5	6	7.0	100	0.1	181,383				

STATISTICAL DESCRIPTIONS OF DYNAMIC MODULUS (CON'T)
Sample Size: H150*D100

Spec. ID	Nom. Size (mm)	Binder Cont. (%)	Air Void (%)	Temp (D.F)	Freq (Hz)	|E*| Test (psi)	Mean (psi)	Std Dev (psi)	Std Err (psi)	C Var (%)
241	12.5	6.5	4.5	40	25	2,116,868	2,225,429	316,532	158,266	14.2
242	12.5	6.5	4.5	40	25	2,316,779				
243	12.5	6.5	4.5	40	25	2,608,399				
244	12.5	6.5	4.5	40	25	1,859,669				
241	12.5	6.5	4.5	40	10	1,914,778	1,926,150	270,596	135,298	14.0
242	12.5	6.5	4.5	40	10	2,018,598				
243	12.5	6.5	4.5	40	10	2,207,872				
244	12.5	6.5	4.5	40	10	1,563,350				
241	12.5	6.5	4.5	40	5	1,732,216	1,725,437	231,067	115,534	13.4
242	12.5	6.5	4.5	40	5	1,749,123				
243	12.5	6.5	4.5	40	5	1,992,255				
244	12.5	6.5	4.5	40	5	1,428,154				
241	12.5	6.5	4.5	40	1	1,322,033	1,324,319	162,066	81,033	12.2
242	12.5	6.5	4.5	40	1	1,266,050				
243	12.5	6.5	4.5	40	1	1,546,380				
244	12.5	6.5	4.5	40	1	1,162,812				
241	12.5	6.5	4.5	40	0.5	1,152,880	1,157,294	137,706	68,853	11.9
242	12.5	6.5	4.5	40	0.5	1,099,883				
243	12.5	6.5	4.5	40	0.5	1,348,926				
244	12.5	6.5	4.5	40	0.5	1,027,485				
241	12.5	6.5	4.5	40	0.1	846,988	833,839	100,856	50,428	12.1
242	12.5	6.5	4.5	40	0.1	776,792				
243	12.5	6.5	4.5	40	0.1	970,080				
244	12.5	6.5	4.5	40	0.1	741,496				
241	12.5	6.5	4.5	70	25	1,498,272	1,539,097	94,007	47,004	6.1
242	12.5	6.5	4.5	70	25	1,673,117				
243	12.5	6.5	4.5	70	25	1,456,852				
244	12.5	6.5	4.5	70	25	1,528,147				
241	12.5	6.5	4.5	70	10	1,277,172	1,297,475	57,879	28,940	4.5
242	12.5	6.5	4.5	70	10	1,379,137				
243	12.5	6.5	4.5	70	10	1,243,487				
244	12.5	6.5	4.5	70	10	1,290,102				
241	12.5	6.5	4.5	70	5	1,115,106	1,137,296	26,521	13,261	2.3
242	12.5	6.5	4.5	70	5	1,175,769				
243	12.5	6.5	4.5	70	5	1,130,735				
244	12.5	6.5	4.5	70	5	1,127,575				

STATISTICAL DESCRIPTIONS OF DYNAMIC MODULUS (CON'T)
Sample Size: H150*D100

Spec. ID	Nom. Size (mm)	Binder Cont. (%)	Air Void (%)	Temp (D.F)	Freq (Hz)	|E*| Test (psi)	|E*| Mean (psi)	|E*| Std Dev (psi)	|E*| Std Err (psi)	|E*| C Var (%)
241	12.5	6.5	4.5	70	1	758,193	796,646	32,497	16,249	4.1
242	12.5	6.5	4.5	70	1	816,764				
243	12.5	6.5	4.5	70	1	829,444				
244	12.5	6.5	4.5	70	1	782,183				
241	12.5	6.5	4.5	70	0.5	612,904	664,977	41,474	20,737	6.2
242	12.5	6.5	4.5	70	0.5	681,687				
243	12.5	6.5	4.5	70	0.5	710,444				
244	12.5	6.5	4.5	70	0.5	654,871				
241	12.5	6.5	4.5	70	0.1	392,580	432,672	40,882	20,441	9.4
242	12.5	6.5	4.5	70	0.1	444,248				
243	12.5	6.5	4.5	70	0.1	484,785				
244	12.5	6.5	4.5	70	0.1	409,073				
241	12.5	6.5	4.5	100	25	852,151	710,285	103,873	51,937	14.6
242	12.5	6.5	4.5	100	25	659,000				
243	12.5	6.5	4.5	100	25	612,504				
244	12.5	6.5	4.5	100	25	717,486				
241	12.5	6.5	4.5	100	10	663,378	546,960	80,997	40,499	14.8
242	12.5	6.5	4.5	100	10	513,581				
243	12.5	6.5	4.5	100	10	477,454				
244	12.5	6.5	4.5	100	10	533,425				
241	12.5	6.5	4.5	100	5	486,024	422,790	43,775	21,888	10.4
242	12.5	6.5	4.5	100	5	395,859				
243	12.5	6.5	4.5	100	5	391,111				
244	12.5	6.5	4.5	100	5	418,165				
241	12.5	6.5	4.5	100	1	274,872	251,813	17,946	8,973	7.1
242	12.5	6.5	4.5	100	1	242,316				
243	12.5	6.5	4.5	100	1	256,262				
244	12.5	6.5	4.5	100	1	233,801				
241	12.5	6.5	4.5	100	0.5	220,256	206,331	13,349	6,675	6.5
242	12.5	6.5	4.5	100	0.5	200,692				
243	12.5	6.5	4.5	100	0.5	213,906				
244	12.5	6.5	4.5	100	0.5	190,471				
241	12.5	6.5	4.5	100	0.1	146,844	139,524	9,666	4,833	6.9
242	12.5	6.5	4.5	100	0.1	135,464				
243	12.5	6.5	4.5	100	0.1	148,017				
244	12.5	6.5	4.5	100	0.1	127,772				

STATISTICAL DESCRIPTIONS OF DYNAMIC MODULUS (CON'T)
Sample Size: H150*D100

Spec. ID	Nom. Size (mm)	Binder Cont. (%)	Air Void (%)	Temp (D.F)	Freq (Hz)	|E*| Test (psi)	Mean (psi)	Std Dev (psi)	Std Err (psi)	C Var (%)
251	12.5	6.5	7.0	40	25	2,438,412	2,159,252	226,623	113,311	10.5
252	12.5	6.5	7.0	40	25	1,996,920				
253	12.5	6.5	7.0	40	25	2,247,411				
254	12.5	6.5	7.0	40	25	1,954,265				
251	12.5	6.5	7.0	40	10	1,901,366	1,867,330	183,175	91,588	9.8
252	12.5	6.5	7.0	40	10	1,684,628				
253	12.5	6.5	7.0	40	10	2,107,600				
254	12.5	6.5	7.0	40	10	1,775,725				
251	12.5	6.5	7.0	40	5	1,646,211	1,705,396	198,759	99,380	11.7
252	12.5	6.5	7.0	40	5	1,499,067				
253	12.5	6.5	7.0	40	5	1,974,521				
254	12.5	6.5	7.0	40	5	1,701,785				
251	12.5	6.5	7.0	40	1	1,174,904	1,331,368	189,259	94,629	14.2
252	12.5	6.5	7.0	40	1	1,165,701				
253	12.5	6.5	7.0	40	1	1,535,129				
254	12.5	6.5	7.0	40	1	1,449,739				
251	12.5	6.5	7.0	40	0.5	1,102,150	1,224,607	192,795	96,397	15.7
252	12.5	6.5	7.0	40	0.5	1,031,238				
253	12.5	6.5	7.0	40	0.5	1,450,524				
254	12.5	6.5	7.0	40	0.5	1,314,517				
251	12.5	6.5	7.0	40	0.1	706,979	838,196	132,570	66,285	15.8
252	12.5	6.5	7.0	40	0.1	755,418				
253	12.5	6.5	7.0	40	0.1	891,540				
254	12.5	6.5	7.0	40	0.1	998,847				
251	12.5	6.5	7.0	70	25	1,792,251	1,530,544	205,418	102,709	13.4
252	12.5	6.5	7.0	70	25	1,518,434				
253	12.5	6.5	7.0	70	25	1,521,510				
254	12.5	6.5	7.0	70	25	1,289,980				
251	12.5	6.5	7.0	70	10	1,358,191	1,205,324	135,806	67,903	11.3
252	12.5	6.5	7.0	70	10	1,278,475				
253	12.5	6.5	7.0	70	10	1,115,420				
254	12.5	6.5	7.0	70	10	1,069,208				
251	12.5	6.5	7.0	70	5	1,254,805	1,052,811	143,771	71,886	13.7
252	12.5	6.5	7.0	70	5	1,049,622				
253	12.5	6.5	7.0	70	5	980,210				
254	12.5	6.5	7.0	70	5	926,606				

STATISTICAL DESCRIPTIONS OF DYNAMIC MODULUS (CON'T)
Sample Size: H150*D100

Spec. ID	Nom. Size (mm)	Binder Cont. (%)	Air Void (%)	Temp (D.F)	Freq (Hz)	|E*| Test (psi)	Mean (psi)	Std Dev (psi)	Std Err (psi)	C Var (%)
251	12.5	6.5	7.0	70	1	875,233	723,521	111,209	55,604	15.4
252	12.5	6.5	7.0	70	1	726,364				
253	12.5	6.5	7.0	70	1	678,905				
254	12.5	6.5	7.0	70	1	613,580				
251	12.5	6.5	7.0	70	0.5	548,154	585,744	78,048	39,024	13.3
252	12.5	6.5	7.0	70	0.5	611,362				
253	12.5	6.5	7.0	70	0.5	681,545				
254	12.5	6.5	7.0	70	0.5	501,916				
251	12.5	6.5	7.0	70	0.1	466,382	395,798	58,233	29,116	14.7
252	12.5	6.5	7.0	70	0.1	405,935				
253	12.5	6.5	7.0	70	0.1	325,185				
254	12.5	6.5	7.0	70	0.1	385,691				
251	12.5	6.5	7.0	100	25	563,461	694,866	108,240	54,120	15.6
252	12.5	6.5	7.0	100	25	763,820				
253	12.5	6.5	7.0	100	25	800,843				
254	12.5	6.5	7.0	100	25	651,338				
251	12.5	6.5	7.0	100	10	458,715	531,593	61,748	30,874	11.6
252	12.5	6.5	7.0	100	10	584,254				
253	12.5	6.5	7.0	100	10	581,386				
254	12.5	6.5	7.0	100	10	502,017				
251	12.5	6.5	7.0	100	5	354,815	423,860	59,460	29,730	14.0
252	12.5	6.5	7.0	100	5	473,436				
253	12.5	6.5	7.0	100	5	473,545				
254	12.5	6.5	7.0	100	5	393,645				
251	12.5	6.5	7.0	100	1	225,181	258,558	36,392	18,196	14.1
252	12.5	6.5	7.0	100	1	290,437				
253	12.5	6.5	7.0	100	1	289,652				
254	12.5	6.5	7.0	100	1	228,961				
251	12.5	6.5	7.0	100	0.5	182,005	211,018	30,083	15,042	14.3
252	12.5	6.5	7.0	100	0.5	242,997				
253	12.5	6.5	7.0	100	0.5	230,105				
254	12.5	6.5	7.0	100	0.5	188,966				
251	12.5	6.5	7.0	100	0.1	115,481	138,570	19,522	9,761	14.1
252	12.5	6.5	7.0	100	0.1	158,602				
253	12.5	6.5	7.0	100	0.1	150,206				
254	12.5	6.5	7.0	100	0.1	129,992				

STATISTICAL DESCRIPTIONS OF DYNAMIC MODULUS (CON'T)
Sample Size: H150*D100

Spec. ID	Nom. Size (mm)	Binder Cont. (%)	Air Void (%)	Temp (D.F)	Freq (Hz)	|E*| Test (psi)	Mean (psi)	Std Dev (psi)	Std Err (psi)	C Var (%)
261	25	5.2	4.5	40	25	3,237,709	2,996,548	371,408	185,704	12.4
262	25	5.2	4.5	40	25	2,842,134				
263	25	5.2	4.5	40	25	2,548,164				
264	25	5.2	4.5	40	25	3,358,184				
261	25	5.2	4.5	40	10	2,858,973	2,784,949	428,872	214,436	15.4
262	25	5.2	4.5	40	10	2,563,530				
263	25	5.2	4.5	40	10	2,365,481				
264	25	5.2	4.5	40	10	3,351,812				
261	25	5.2	4.5	40	5	2,439,328	2,409,660	362,084	181,042	15.0
262	25	5.2	4.5	40	5	2,380,015				
263	25	5.2	4.5	40	5	1,967,180				
264	25	5.2	4.5	40	5	2,852,115				
261	25	5.2	4.5	40	1	1,823,150	1,917,711	285,832	142,916	14.9
262	25	5.2	4.5	40	1	2,012,208				
263	25	5.2	4.5	40	1	1,580,676				
264	25	5.2	4.5	40	1	2,254,810				
261	25	5.2	4.5	40	0.5	1,608,685	1,797,721	246,217	123,108	13.7
262	25	5.2	4.5	40	0.5	1,780,098				
263	25	5.2	4.5	40	0.5	1,651,581				
264	25	5.2	4.5	40	0.5	2,150,518				
261	25	5.2	4.5	40	0.1	1,219,396	1,315,000	182,997	91,498	13.9
262	25	5.2	4.5	40	0.1	1,287,641				
263	25	5.2	4.5	40	0.1	1,172,748				
264	25	5.2	4.5	40	0.1	1,580,215				
261	25	5.2	4.5	70	25	2,520,826	2,322,825	291,672	145,836	12.6
262	25	5.2	4.5	70	25	2,621,874				
263	25	5.2	4.5	70	25	2,113,373				
264	25	5.2	4.5	70	25	2,035,226				
261	25	5.2	4.5	70	10	2,012,432	1,789,305	284,485	142,242	15.9
262	25	5.2	4.5	70	10	2,018,880				
263	25	5.2	4.5	70	10	1,425,413				
264	25	5.2	4.5	70	10	1,700,496				
261	25	5.2	4.5	70	5	1,628,110	1,509,345	233,652	116,826	15.5
262	25	5.2	4.5	70	5	1,749,067				
263	25	5.2	4.5	70	5	1,211,883				
264	25	5.2	4.5	70	5	1,448,320				

STATISTICAL DESCRIPTIONS OF DYNAMIC MODULUS (CON'T)
Sample Size: H150*D100

Spec. ID	Nom. Size (mm)	Binder Cont. (%)	Air Void (%)	Temp (D.F)	Freq (Hz)	|E*| Test (psi)	Mean (psi)	Std Dev (psi)	Std Err (psi)	C Var (%)
261	25	5.2	4.5	70	1	1,045,651	1,019,339	159,720	79,860	15.7
262	25	5.2	4.5	70	1	1,220,044				
263	25	5.2	4.5	70	1	835,872				
264	25	5.2	4.5	70	1	975,789				
261	25	5.2	4.5	70	0.5	866,373	826,861	96,992	48,496	11.7
262	25	5.2	4.5	70	0.5	925,145				
263	25	5.2	4.5	70	0.5	696,695				
264	25	5.2	4.5	70	0.5	819,229				
261	25	5.2	4.5	70	0.1	568,868	579,100	63,879	31,939	11.0
262	25	5.2	4.5	70	0.1	672,050				
263	25	5.2	4.5	70	0.1	531,581				
264	25	5.2	4.5	70	0.1	543,900				
261	25	5.2	4.5	100	25	1,535,204	1,257,588	189,200	94,600	15.0
262	25	5.2	4.5	100	25	1,150,512				
263	25	5.2	4.5	100	25	1,125,887				
264	25	5.2	4.5	100	25	1,218,747				
261	25	5.2	4.5	100	10	921,500	884,483	91,370	45,685	10.3
262	25	5.2	4.5	100	10	749,645				
263	25	5.2	4.5	100	10	914,559				
264	25	5.2	4.5	100	10	952,228				
261	25	5.2	4.5	100	5	854,625	730,778	94,540	47,270	12.9
262	25	5.2	4.5	100	5	624,674				
263	25	5.2	4.5	100	5	727,378				
264	25	5.2	4.5	100	5	716,436				
261	25	5.2	4.5	100	1	458,251	416,020	30,149	15,075	7.2
262	25	5.2	4.5	100	1	388,747				
263	25	5.2	4.5	100	1	401,917				
264	25	5.2	4.5	100	1	415,163				
261	25	5.2	4.5	100	0.5	385,614	340,431	31,803	15,902	9.3
262	25	5.2	4.5	100	0.5	313,480				
263	25	5.2	4.5	100	0.5	324,233				
264	25	5.2	4.5	100	0.5	338,395				
261	25	5.2	4.5	100	0.1	254,813	217,165	25,221	12,611	11.6
262	25	5.2	4.5	100	0.1	202,151				
263	25	5.2	4.5	100	0.1	203,678				
264	25	5.2	4.5	100	0.1	208,019				

STATISTICAL DESCRIPTIONS OF DYNAMIC MODULUS (CON'T)
Sample Size: H150*D100

Spec. ID	Nom. Size (mm)	Binder Cont. (%)	Air Void (%)	Temp (D.F)	Freq (Hz)	|E*| Test (psi)	|E*| Mean (psi)	|E*| Std Dev (psi)	|E*| Std Err (psi)	|E*| C Var (%)
271	25	5.2	7.0	40	25	2,205,917	2,134,082	131,750	65,875	6.2
272	25	5.2	7.0	40	25	2,225,825				
273	25	5.2	7.0	40	25	2,164,361				
274	25	5.2	7.0	40	25	1,940,226				
271	25	5.2	7.0	40	10	1,990,235	1,922,885	88,837	44,418	4.6
272	25	5.2	7.0	40	10	1,943,634				
273	25	5.2	7.0	40	10	1,964,942				
274	25	5.2	7.0	40	10	1,792,729				
271	25	5.2	7.0	40	5	1,750,948	1,741,618	47,432	23,716	2.7
272	25	5.2	7.0	40	5	1,761,919				
273	25	5.2	7.0	40	5	1,780,705				
274	25	5.2	7.0	40	5	1,672,899				
271	25	5.2	7.0	40	1	1,305,434	1,368,848	42,831	21,415	3.1
272	25	5.2	7.0	40	1	1,389,742				
273	25	5.2	7.0	40	1	1,398,522				
274	25	5.2	7.0	40	1	1,381,694				
271	25	5.2	7.0	40	0.5	1,139,560	1,215,133	50,795	25,397	4.2
272	25	5.2	7.0	40	0.5	1,249,034				
273	25	5.2	7.0	40	0.5	1,238,355				
274	25	5.2	7.0	40	0.5	1,233,584				
271	25	5.2	7.0	40	0.1	853,285	907,607	47,099	23,550	5.2
272	25	5.2	7.0	40	0.1	968,149				
273	25	5.2	7.0	40	0.1	901,383				
274	25	5.2	7.0	40	0.1	907,610				
271	25	5.2	7.0	70	25	1,351,545	1,517,620	209,277	104,639	13.8
272	25	5.2	7.0	70	25	1,796,993				
273	25	5.2	7.0	70	25	1,559,315				
274	25	5.2	7.0	70	25	1,362,628				
271	25	5.2	7.0	70	10	1,154,234	1,295,772	157,379	78,690	12.1
272	25	5.2	7.0	70	10	1,503,938				
273	25	5.2	7.0	70	10	1,328,485				
274	25	5.2	7.0	70	10	1,196,432				
271	25	5.2	7.0	70	5	1,010,472	1,130,574	131,840	65,920	11.7
272	25	5.2	7.0	70	5	1,311,724				
273	25	5.2	7.0	70	5	1,139,048				
274	25	5.2	7.0	70	5	1,061,051				

STATISTICAL DESCRIPTIONS OF DYNAMIC MODULUS (CON'T)
Sample Size: H150*D100

Spec. ID	Nom. Size (mm)	Binder Cont. (%)	Air Void (%)	Temp (D.F)	Freq (Hz)	|E*| Test (psi)	|E*| Mean (psi)	|E*| Std Dev (psi)	|E*| Std Err (psi)	|E*| C Var (%)
271	25	5.2	7.0	70	1	682,036	780,953	70,912	35,456	9.1
272	25	5.2	7.0	70	1	850,766				
273	25	5.2	7.0	70	1	794,137				
274	25	5.2	7.0	70	1	796,871				
271	25	5.2	7.0	70	0.5	578,722	650,050	48,957	24,479	7.5
272	25	5.2	7.0	70	0.5	681,990				
273	25	5.2	7.0	70	0.5	657,356				
274	25	5.2	7.0	70	0.5	682,132				
271	25	5.2	7.0	70	0.1	382,226	432,125	34,770	17,385	8.0
272	25	5.2	7.0	70	0.1	462,871				
273	25	5.2	7.0	70	0.1	439,664				
274	25	5.2	7.0	70	0.1	443,739				
271	25	5.2	7.0	100	25	561,755	710,863	108,123	54,061	15.2
272	25	5.2	7.0	100	25	704,958				
273	25	5.2	7.0	100	25	808,231				
274	25	5.2	7.0	100	25	768,508				
271	25	5.2	7.0	100	10	482,571	559,087	55,285	27,642	9.9
272	25	5.2	7.0	100	10	555,974				
273	25	5.2	7.0	100	10	607,102				
274	25	5.2	7.0	100	10	590,700				
271	25	5.2	7.0	100	5	325,164	419,861	63,705	31,853	15.2
272	25	5.2	7.0	100	5	439,846				
273	25	5.2	7.0	100	5	454,263				
274	25	5.2	7.0	100	5	460,169				
271	25	5.2	7.0	100	1	206,269	259,698	36,555	18,278	14.1
272	25	5.2	7.0	100	1	266,465				
273	25	5.2	7.0	100	1	286,168				
274	25	5.2	7.0	100	1	279,891				
271	25	5.2	7.0	100	0.5	176,522	216,796	28,045	14,023	12.9
272	25	5.2	7.0	100	0.5	222,215				
273	25	5.2	7.0	100	0.5	241,325				
274	25	5.2	7.0	100	0.5	227,121				
271	25	5.2	7.0	100	0.1	128,317	153,691	19,273	9,637	12.5
272	25	5.2	7.0	100	0.1	150,193				
273	25	5.2	7.0	100	0.1	172,683				
274	25	5.2	7.0	100	0.1	163,571				

APPENDIX C

STATISTICAL DESCRIPTIONS OF PHASE ANGLE

STATISTICAL DESCRIPTIONS OF PHASE ANGLE
Sample Size: H150*D100

Spec. ID	Nom. Size (mm)	Bind. Cont. (%)	Air Void (%)	Temp (D.F)	Freq (Hz)	Phase Angle				
						Test (Deg)	Mean (Deg)	Std Dev (Deg)	Std Err (Deg)	C Var (%)
201	12.5	5.5	4.5	40	25	13.05	14.21	1.93	0.96	13.6
202	12.5	5.5	4.5	40	25	15.05				
203	12.5	5.5	4.5	40	25	12.25				
204	12.5	5.5	4.5	40	25	16.50				
201	12.5	5.5	4.5	40	10	11.10	11.69	1.22	0.61	10.4
202	12.5	5.5	4.5	40	10	11.30				
203	12.5	5.5	4.5	40	10	10.86				
204	12.5	5.5	4.5	40	10	13.50				
201	12.5	5.5	4.5	40	5	12.76	13.02	1.87	0.93	14.3
202	12.5	5.5	4.5	40	5	11.54				
203	12.5	5.5	4.5	40	5	12.06				
204	12.5	5.5	4.5	40	5	15.72				
201	12.5	5.5	4.5	40	1	13.40	14.03	1.74	0.87	12.4
202	12.5	5.5	4.5	40	1	12.78				
203	12.5	5.5	4.5	40	1	13.33				
204	12.5	5.5	4.5	40	1	16.61				
201	12.5	5.5	4.5	40	0.5	14.28	15.07	1.62	0.81	10.7
202	12.5	5.5	4.5	40	0.5	14.05				
203	12.5	5.5	4.5	40	0.5	14.46				
204	12.5	5.5	4.5	40	0.5	17.48				
201	12.5	5.5	4.5	40	0.1	16.26	17.33	1.84	0.92	10.6
202	12.5	5.5	4.5	40	0.1	15.81				
203	12.5	5.5	4.5	40	0.1	17.32				
204	12.5	5.5	4.5	40	0.1	19.92				
201	12.5	5.5	4.5	70	25	25.26	21.49	2.92	1.46	13.6
202	12.5	5.5	4.5	70	25	22.13				
203	12.5	5.5	4.5	70	25	20.07				
204	12.5	5.5	4.5	70	25	18.50				
201	12.5	5.5	4.5	70	10	22.97	19.13	2.59	1.29	13.5
202	12.5	5.5	4.5	70	10	17.88				
203	12.5	5.5	4.5	70	10	17.37				
204	12.5	5.5	4.5	70	10	18.30				
201	12.5	5.5	4.5	70	5	23.44	19.99	2.44	1.22	12.2
202	12.5	5.5	4.5	70	5	18.27				
203	12.5	5.5	4.5	70	5	18.24				
204	12.5	5.5	4.5	70	5	20.00				

STATISTICAL DESCRIPTIONS OF PHASE ANGLE (CON'T)
Sample Size: H150*D100

Spec. ID	Nom. Size (mm)	Binder Cont. (%)	Air Void (%)	Temp (D.F)	Freq (Hz)	Phase Angle Test (Deg)	Mean (Deg)	Std Dev (Deg)	Std Err (Deg)	C Var (%)
201	12.5	5.5	4.5	70	1	24.01	21.10	2.06	1.03	9.8
202	12.5	5.5	4.5	70	1	20.31				
203	12.5	5.5	4.5	70	1	19.19				
204	12.5	5.5	4.5	70	1	20.89				
201	12.5	5.5	4.5	70	0.5	24.63	21.74	2.18	1.09	10.0
202	12.5	5.5	4.5	70	0.5	21.23				
203	12.5	5.5	4.5	70	0.5	19.37				
204	12.5	5.5	4.5	70	0.5	21.71				
201	12.5	5.5	4.5	70	0.1	25.46	23.06	1.96	0.98	8.5
202	12.5	5.5	4.5	70	0.1	22.82				
203	12.5	5.5	4.5	70	0.1	20.69				
204	12.5	5.5	4.5	70	0.1	23.27				
201	12.5	5.5	4.5	100	25	34.31	32.76	2.87	1.43	8.8
202	12.5	5.5	4.5	100	25	29.74				
203	12.5	5.5	4.5	100	25	31.04				
204	12.5	5.5	4.5	100	25	35.95				
201	12.5	5.5	4.5	100	10	33.09	31.49	3.00	1.50	9.5
202	12.5	5.5	4.5	100	10	28.38				
203	12.5	5.5	4.5	100	10	29.64				
204	12.5	5.5	4.5	100	10	34.86				
201	12.5	5.5	4.5	100	5	33.75	32.34	4.24	2.12	13.1
202	12.5	5.5	4.5	100	5	28.90				
203	12.5	5.5	4.5	100	5	28.99				
204	12.5	5.5	4.5	100	5	37.71				
201	12.5	5.5	4.5	100	1	32.86	29.39	4.17	2.08	14.2
202	12.5	5.5	4.5	100	1	24.00				
203	12.5	5.5	4.5	100	1	28.21				
204	12.5	5.5	4.5	100	1	32.50				
201	12.5	5.5	4.5	100	0.5	31.93	29.05	4.63	2.31	15.9
202	12.5	5.5	4.5	100	0.5	23.18				
203	12.5	5.5	4.5	100	0.5	27.61				
204	12.5	5.5	4.5	100	0.5	33.46				
201	12.5	5.5	4.5	100	0.1	26.15	24.63	3.49	1.74	14.2
202	12.5	5.5	4.5	100	0.1	19.72				
203	12.5	5.5	4.5	100	0.1	24.85				
204	12.5	5.5	4.5	100	0.1	27.80				

STATISTICAL DESCRIPTIONS OF PHASE ANGLE (CON'T)
Sample Size: H150*D100

Spec. ID	Nom. Size (mm)	Binder Cont. (%)	Air Void (%)	Temp (D.F)	Freq (Hz)	Phase Angle Test (Deg)	Mean (Deg)	Std Dev (Deg)	Std Err (Deg)	C Var (%)
211	12.5	5.5	7.0	40	25	12.30	14.01	1.90	0.95	13.5
212	12.5	5.5	7.0	40	25	12.80				
213	12.5	5.5	7.0	40	25	16.50				
214	12.5	5.5	7.0	40	25	14.45				
211	12.5	5.5	7.0	40	10	10.92	12.16	1.53	0.76	12.6
212	12.5	5.5	7.0	40	10	10.80				
213	12.5	5.5	7.0	40	10	13.83				
214	12.5	5.5	7.0	40	10	13.08				
211	12.5	5.5	7.0	40	5	10.55	11.80	1.52	0.76	12.9
212	12.5	5.5	7.0	40	5	10.56				
213	12.5	5.5	7.0	40	5	13.65				
214	12.5	5.5	7.0	40	5	12.44				
211	12.5	5.5	7.0	40	1	13.57	13.97	1.90	0.95	13.6
212	12.5	5.5	7.0	40	1	12.03				
213	12.5	5.5	7.0	40	1	16.59				
214	12.5	5.5	7.0	40	1	13.67				
211	12.5	5.5	7.0	40	0.5	14.57	15.85	2.24	1.12	14.2
212	12.5	5.5	7.0	40	0.5	15.54				
213	12.5	5.5	7.0	40	0.5	19.10				
214	12.5	5.5	7.0	40	0.5	14.17				
211	12.5	5.5	7.0	40	0.1	16.68	17.52	1.88	0.94	10.7
212	12.5	5.5	7.0	40	0.1	16.53				
213	12.5	5.5	7.0	40	0.1	20.34				
214	12.5	5.5	7.0	40	0.1	16.53				
211	12.5	5.5	7.0	70	25	20.10	18.78	1.89	0.94	10.0
212	12.5	5.5	7.0	70	25	16.08				
213	12.5	5.5	7.0	70	25	20.05				
214	12.5	5.5	7.0	70	25	18.90				
211	12.5	5.5	7.0	70	10	17.21	16.20	1.39	0.70	8.6
212	12.5	5.5	7.0	70	10	14.81				
213	12.5	5.5	7.0	70	10	15.20				
214	12.5	5.5	7.0	70	10	17.57				
211	12.5	5.5	7.0	70	5	18.37	17.86	1.37	0.68	7.7
212	12.5	5.5	7.0	70	5	15.84				
213	12.5	5.5	7.0	70	5	18.89				
214	12.5	5.5	7.0	70	5	18.32				

STATISTICAL DESCRIPTIONS OF PHASE ANGLE (CON'T)
Sample Size: H150*D100

Spec. ID	Nom. Size (mm)	Binder Cont. (%)	Air Void (%)	Temp (D.F)	Freq (Hz)	Phase Angle Test (Deg)	Mean (Deg)	Std Dev (Deg)	Std Err (Deg)	C Var (%)
211	12.5	5.5	7.0	70	1	21.33	21.41	1.17	0.58	5.5
212	12.5	5.5	7.0	70	1	22.59				
213	12.5	5.5	7.0	70	1	21.88				
214	12.5	5.5	7.0	70	1	19.84				
211	12.5	5.5	7.0	70	0.5	22.69	21.55	1.10	0.55	5.1
212	12.5	5.5	7.0	70	0.5	20.32				
213	12.5	5.5	7.0	70	0.5	22.23				
214	12.5	5.5	7.0	70	0.5	20.95				
211	12.5	5.5	7.0	70	0.1	25.22	23.73	1.37	0.68	5.8
212	12.5	5.5	7.0	70	0.1	24.47				
213	12.5	5.5	7.0	70	0.1	23.01				
214	12.5	5.5	7.0	70	0.1	22.20				
211	12.5	5.5	7.0	100	25	35.40	31.52	3.58	1.79	11.4
212	12.5	5.5	7.0	100	25	28.83				
213	12.5	5.5	7.0	100	25	33.70				
214	12.5	5.5	7.0	100	25	28.14				
211	12.5	5.5	7.0	100	10	27.29	28.65	2.37	1.18	8.3
212	12.5	5.5	7.0	100	10	27.48				
213	12.5	5.5	7.0	100	10	32.19				
214	12.5	5.5	7.0	100	10	27.62				
211	12.5	5.5	7.0	100	5	30.80	29.45	3.12	1.56	10.6
212	12.5	5.5	7.0	100	5	26.72				
213	12.5	5.5	7.0	100	5	33.22				
214	12.5	5.5	7.0	100	5	27.04				
211	12.5	5.5	7.0	100	1	21.33	25.11	2.82	1.41	11.2
212	12.5	5.5	7.0	100	1	25.60				
213	12.5	5.5	7.0	100	1	28.15				
214	12.5	5.5	7.0	100	1	25.34				
211	12.5	5.5	7.0	100	0.5	27.98	26.24	2.35	1.17	9.0
212	12.5	5.5	7.0	100	0.5	24.37				
213	12.5	5.5	7.0	100	0.5	28.54				
214	12.5	5.5	7.0	100	0.5	24.06				
211	12.5	5.5	7.0	100	0.1	23.70	22.00	1.88	0.94	8.5
212	12.5	5.5	7.0	100	0.1	20.89				
213	12.5	5.5	7.0	100	0.1	23.48				
214	12.5	5.5	7.0	100	0.1	19.94				

STATISTICAL DESCRIPTIONS OF PHASE ANGLE (CON'T)
Sample Size: H150*D100

Spec. ID	Nom. Size (mm)	Binder Cont. (%)	Air Void (%)	Temp (D.F)	Freq (Hz)	Phase Angle Test (Deg)	Mean (Deg)	Std Dev (Deg)	Std Err (Deg)	C Var (%)
221	12.5	6	4.5	40	25	23.85	21.04	2.53	1.27	12.0
222	12.5	6	4.5	40	25	19.54				
223	12.5	6	4.5	40	25	22.40				
224	12.5	6	4.5	40	25	18.35				
221	12.5	6	4.5	40	10	14.53	13.99	0.73	0.36	5.2
222	12.5	6	4.5	40	10	13.28				
223	12.5	6	4.5	40	10	14.70				
224	12.5	6	4.5	40	10	13.46				
221	12.5	6	4.5	40	5	14.29	14.43	1.17	0.59	8.1
222	12.5	6	4.5	40	5	12.82				
223	12.5	6	4.5	40	5	15.34				
224	12.5	6	4.5	40	5	15.25				
221	12.5	6	4.5	40	1	15.83	16.45	2.09	1.05	12.7
222	12.5	6	4.5	40	1	13.91				
223	12.5	6	4.5	40	1	17.22				
224	12.5	6	4.5	40	1	18.84				
221	12.5	6	4.5	40	0.5	16.74	16.18	1.55	0.78	9.6
222	12.5	6	4.5	40	0.5	14.47				
223	12.5	6	4.5	40	0.5	18.04				
224	12.5	6	4.5	40	0.5	15.46				
221	12.5	6	4.5	40	0.1	19.86	18.81	1.49	0.74	7.9
222	12.5	6	4.5	40	0.1	16.92				
223	12.5	6	4.5	40	0.1	20.13				
224	12.5	6	4.5	40	0.1	18.32				
221	12.5	6	4.5	70	25	24.14	22.97	2.29	1.15	10.0
222	12.5	6	4.5	70	25	21.75				
223	12.5	6	4.5	70	25	25.54				
224	12.5	6	4.5	70	25	20.46				
221	12.5	6	4.5	70	10	22.64	19.95	2.85	1.43	14.3
222	12.5	6	4.5	70	10	17.52				
223	12.5	6	4.5	70	10	22.19				
224	12.5	6	4.5	70	10	17.45				
221	12.5	6	4.5	70	5	23.03	22.28	1.57	0.78	7.0
222	12.5	6	4.5	70	5	23.33				
223	12.5	6	4.5	70	5	22.82				
224	12.5	6	4.5	70	5	19.95				

STATISTICAL DESCRIPTIONS OF PHASE ANGLE (CON'T)
Sample Size: H150*D100

Spec. ID	Nom. Size (mm)	Binder Cont. (%)	Air Void (%)	Temp (D.F)	Freq (Hz)	Phase Angle				
						Test (Deg)	Mean (Deg)	Std Dev (Deg)	Std Err (Deg)	C Var (%)
221	12.5	6	4.5	70	1	25.47	24.52	1.78	0.89	7.3
222	12.5	6	4.5	70	1	26.48				
223	12.5	6	4.5	70	1	23.54				
224	12.5	6	4.5	70	1	22.57				
221	12.5	6	4.5	70	0.5	25.20	25.00	1.78	0.89	7.1
222	12.5	6	4.5	70	0.5	27.44				
223	12.5	6	4.5	70	0.5	23.79				
224	12.5	6	4.5	70	0.5	23.56				
221	12.5	6	4.5	70	0.1	23.84	25.11	1.90	0.95	7.6
222	12.5	6	4.5	70	0.1	27.88				
223	12.5	6	4.5	70	0.1	23.88				
224	12.5	6	4.5	70	0.1	24.85				
221	12.5	6	4.5	100	25	39.78	34.52	4.60	2.30	13.3
222	12.5	6	4.5	100	25	28.79				
223	12.5	6	4.5	100	25	35.95				
224	12.5	6	4.5	100	25	33.55				
221	12.5	6	4.5	100	10	38.11	34.32	2.72	1.36	7.9
222	12.5	6	4.5	100	10	32.04				
223	12.5	6	4.5	100	10	34.43				
224	12.5	6	4.5	100	10	32.71				
221	12.5	6	4.5	100	5	36.00	33.56	1.63	0.81	4.8
222	12.5	6	4.5	100	5	32.69				
223	12.5	6	4.5	100	5	32.71				
224	12.5	6	4.5	100	5	32.85				
221	12.5	6	4.5	100	1	30.65	29.52	1.57	0.78	5.3
222	12.5	6	4.5	100	1	30.07				
223	12.5	6	4.5	100	1	27.20				
224	12.5	6	4.5	100	1	30.17				
221	12.5	6	4.5	100	0.5	27.00	26.79	1.64	0.82	6.1
222	12.5	6	4.5	100	0.5	27.99				
223	12.5	6	4.5	100	0.5	24.42				
224	12.5	6	4.5	100	0.5	27.75				
221	12.5	6	4.5	100	0.1	21.55	21.27	1.45	0.73	6.8
222	12.5	6	4.5	100	0.1	22.32				
223	12.5	6	4.5	100	0.1	19.14				
224	12.5	6	4.5	100	0.1	22.06				

STATISTICAL DESCRIPTIONS OF PHASE ANGLE (CON'T)
Sample Size: H150*D100

Spec. ID	Nom. Size (mm)	Binder Cont. (%)	Air Void (%)	Temp (D.F)	Freq (Hz)	Phase Angle Test (Deg)	Mean (Deg)	Std Dev (Deg)	Std Err (Deg)	C Var (%)
231	12.5	6	7.0	40	25	11.99	14.26	1.55	0.77	10.9
232	12.5	6	7.0	40	25	15.44				
233	12.5	6	7.0	40	25	14.59				
234	12.5	6	7.0	40	25	15.00				
231	12.5	6	7.0	40	10	12.94	13.60	1.31	0.65	9.6
232	12.5	6	7.0	40	10	15.54				
233	12.5	6	7.0	40	10	12.76				
234	12.5	6	7.0	40	10	13.14				
231	12.5	6	7.0	40	5	12.54	12.81	1.21	0.60	9.4
232	12.5	6	7.0	40	5	14.20				
233	12.5	6	7.0	40	5	11.31				
234	12.5	6	7.0	40	5	13.17				
231	12.5	6	7.0	40	1	12.54	14.50	1.37	0.69	9.5
232	12.5	6	7.0	40	1	15.74				
233	12.5	6	7.0	40	1	14.91				
234	12.5	6	7.0	40	1	14.82				
231	12.5	6	7.0	40	0.5	11.92	13.50	1.86	0.93	13.8
232	12.5	6	7.0	40	0.5	14.56				
233	12.5	6	7.0	40	0.5	11.93				
234	12.5	6	7.0	40	0.5	15.57				
231	12.5	6	7.0	40	0.1	16.59	17.00	2.02	1.01	11.9
232	12.5	6	7.0	40	0.1	18.94				
233	12.5	6	7.0	40	0.1	14.35				
234	12.5	6	7.0	40	0.1	18.11				
231	12.5	6	7.0	70	25	16.40	18.07	1.17	0.58	6.5
232	12.5	6	7.0	70	25	19.11				
233	12.5	6	7.0	70	25	18.33				
234	12.5	6	7.0	70	25	18.45				
231	12.5	6	7.0	70	10	20.48	18.39	1.57	0.78	8.5
232	12.5	6	7.0	70	10	17.61				
233	12.5	6	7.0	70	10	16.85				
234	12.5	6	7.0	70	10	18.60				
231	12.5	6	7.0	70	5	21.11	18.34	1.85	0.93	10.1
232	12.5	6	7.0	70	5	17.31				
233	12.5	6	7.0	70	5	17.49				
234	12.5	6	7.0	70	5	17.43				

STATISTICAL DESCRIPTIONS OF PHASE ANGLE (CON'T)
Sample Size: H150*D100

Spec. ID	Nom. Size (mm)	Binder Cont. (%)	Air Void (%)	Temp (D.F)	Freq (Hz)	Phase Angle Test (Deg)	Mean (Deg)	Std Dev (Deg)	Std Err (Deg)	C Var (%)
231	12.5	6	7.0	70	1	23.53	20.51	2.11	1.06	10.3
232	12.5	6	7.0	70	1	20.00				
233	12.5	6	7.0	70	1	19.89				
234	12.5	6	7.0	70	1	18.60				
231	12.5	6	7.0	70	0.5	24.09	21.24	1.99	1.00	9.4
232	12.5	6	7.0	70	0.5	20.96				
233	12.5	6	7.0	70	0.5	20.36				
234	12.5	6	7.0	70	0.5	19.53				
231	12.5	6	7.0	70	0.1	25.25	23.21	1.56	0.78	6.7
232	12.5	6	7.0	70	0.1	23.20				
233	12.5	6	7.0	70	0.1	21.48				
234	12.5	6	7.0	70	0.1	22.89				
231	12.5	6	7.0	100	25	29.02	29.61	1.37	0.69	4.6
232	12.5	6	7.0	100	25	29.80				
233	12.5	6	7.0	100	25	31.42				
234	12.5	6	7.0	100	25	28.20				
231	12.5	6	7.0	100	10	27.63	28.09	1.32	0.66	4.7
232	12.5	6	7.0	100	10	28.84				
233	12.5	6	7.0	100	10	29.44				
234	12.5	6	7.0	100	10	26.46				
231	12.5	6	7.0	100	5	27.78	27.73	1.30	0.65	4.7
232	12.5	6	7.0	100	5	29.49				
233	12.5	6	7.0	100	5	27.23				
234	12.5	6	7.0	100	5	26.41				
231	12.5	6	7.0	100	1	26.85	25.63	1.93	0.97	7.5
232	12.5	6	7.0	100	1	27.61				
233	12.5	6	7.0	100	1	23.46				
234	12.5	6	7.0	100	1	24.59				
231	12.5	6	7.0	100	0.5	25.75	24.54	1.91	0.96	7.8
232	12.5	6	7.0	100	0.5	26.34				
233	12.5	6	7.0	100	0.5	22.10				
234	12.5	6	7.0	100	0.5	23.97				
231	12.5	6	7.0	100	0.1	22.54	21.49	1.91	0.96	8.9
232	12.5	6	7.0	100	0.1	23.30				
233	12.5	6	7.0	100	0.1	18.94				
234	12.5	6	7.0	100	0.1	21.16				

STATISTICAL DESCRIPTIONS OF PHASE ANGLE (CON'T)
Sample Size: H150*D100

Spec. ID	Nom. Size (mm)	Binder Cont. (%)	Air Void (%)	Temp (D.F)	Freq (Hz)	Phase Angle Test (Deg)	Mean (Deg)	Std Dev (Deg)	Std Err (Deg)	C Var (%)
241	12.5	6.5	4.5	40	25	14.40	14.54	0.90	0.45	6.2
242	12.5	6.5	4.5	40	25	15.64				
243	12.5	6.5	4.5	40	25	14.66				
244	12.5	6.5	4.5	40	25	13.44				
241	12.5	6.5	4.5	40	10	16.44	14.98	1.49	0.74	9.9
242	12.5	6.5	4.5	40	10	15.84				
243	12.5	6.5	4.5	40	10	13.08				
244	12.5	6.5	4.5	40	10	14.56				
241	12.5	6.5	4.5	40	5	16.75	14.12	2.08	1.04	14.7
242	12.5	6.5	4.5	40	5	14.65				
243	12.5	6.5	4.5	40	5	13.15				
244	12.5	6.5	4.5	40	5	11.92				
241	12.5	6.5	4.5	40	1	17.32	15.55	1.32	0.66	8.5
242	12.5	6.5	4.5	40	1	15.64				
243	12.5	6.5	4.5	40	1	15.02				
244	12.5	6.5	4.5	40	1	14.22				
241	12.5	6.5	4.5	40	0.5	17.69	16.35	1.03	0.51	6.3
242	12.5	6.5	4.5	40	0.5	16.54				
243	12.5	6.5	4.5	40	0.5	15.84				
244	12.5	6.5	4.5	40	0.5	15.31				
241	12.5	6.5	4.5	40	0.1	19.73	19.63	2.72	1.36	13.8
242	12.5	6.5	4.5	40	0.1	23.42				
243	12.5	6.5	4.5	40	0.1	17.35				
244	12.5	6.5	4.5	40	0.1	18.02				
241	12.5	6.5	4.5	70	25	20.15	19.78	1.93	0.97	9.8
242	12.5	6.5	4.5	70	25	20.53				
243	12.5	6.5	4.5	70	25	17.00				
244	12.5	6.5	4.5	70	25	21.45				
241	12.5	6.5	4.5	70	10	18.66	18.83	1.55	0.78	8.2
242	12.5	6.5	4.5	70	10	19.86				
243	12.5	6.5	4.5	70	10	16.70				
244	12.5	6.5	4.5	70	10	20.10				
241	12.5	6.5	4.5	70	5	19.38	18.89	1.87	0.94	9.9
242	12.5	6.5	4.5	70	5	19.76				
243	12.5	6.5	4.5	70	5	16.14				
244	12.5	6.5	4.5	70	5	20.29				

STATISTICAL DESCRIPTIONS OF PHASE ANGLE (CON'T)
Sample Size: H150*D100

Spec. ID	Nom. Size (mm)	Binder Cont. (%)	Air Void (%)	Temp (D.F)	Freq (Hz)	Phase Angle				
						Test (Deg)	Mean (Deg)	Std Dev (Deg)	Std Err (Deg)	C Var (%)
241	12.5	6.5	4.5	70	1	22.72	20.94	2.59	1.30	12.4
242	12.5	6.5	4.5	70	1	21.45				
243	12.5	6.5	4.5	70	1	17.14				
244	12.5	6.5	4.5	70	1	22.45				
241	12.5	6.5	4.5	70	0.5	24.43	21.86	2.81	1.40	12.8
242	12.5	6.5	4.5	70	0.5	21.88				
243	12.5	6.5	4.5	70	0.5	17.95				
244	12.5	6.5	4.5	70	0.5	23.18				
241	12.5	6.5	4.5	70	0.1	24.75	22.68	2.32	1.16	10.2
242	12.5	6.5	4.5	70	0.1	22.74				
243	12.5	6.5	4.5	70	0.1	19.42				
244	12.5	6.5	4.5	70	0.1	23.79				
241	12.5	6.5	4.5	100	25	34.30	31.99	2.73	1.36	8.5
242	12.5	6.5	4.5	100	25	31.08				
243	12.5	6.5	4.5	100	25	28.53				
244	12.5	6.5	4.5	100	25	34.04				
241	12.5	6.5	4.5	100	10	34.87	31.16	3.48	1.74	11.2
242	12.5	6.5	4.5	100	10	29.62				
243	12.5	6.5	4.5	100	10	27.09				
244	12.5	6.5	4.5	100	10	33.07				
241	12.5	6.5	4.5	100	5	33.76	30.43	3.40	1.70	11.2
242	12.5	6.5	4.5	100	5	28.80				
243	12.5	6.5	4.5	100	5	26.47				
244	12.5	6.5	4.5	100	5	32.70				
241	12.5	6.5	4.5	100	1	30.19	27.39	2.77	1.39	10.1
242	12.5	6.5	4.5	100	1	26.34				
243	12.5	6.5	4.5	100	1	24.01				
244	12.5	6.5	4.5	100	1	29.02				
241	12.5	6.5	4.5	100	0.5	28.24	25.46	2.37	1.19	9.3
242	12.5	6.5	4.5	100	0.5	24.03				
243	12.5	6.5	4.5	100	0.5	23.03				
244	12.5	6.5	4.5	100	0.5	26.55				
241	12.5	6.5	4.5	100	0.1	22.98	20.42	2.10	1.05	10.3
242	12.5	6.5	4.5	100	0.1	18.63				
243	12.5	6.5	4.5	100	0.1	18.78				
244	12.5	6.5	4.5	100	0.1	21.29				

STATISTICAL DESCRIPTIONS OF PHASE ANGLE (CON'T)
Sample Size: H150*D100

Spec. ID	Nom. Size (mm)	Binder Cont. (%)	Air Void (%)	Temp (D.F)	Freq (Hz)	Phase Angle Test (Deg)	Mean (Deg)	Std Dev (Deg)	Std Err (Deg)	C Var (%)
251	12.5	6.5	7.0	40	25	18.54	17.04	2.27	1.13	13.3
252	12.5	6.5	7.0	40	25	18.36				
253	12.5	6.5	7.0	40	25	13.70				
254	12.5	6.5	7.0	40	25	17.56				
251	12.5	6.5	7.0	40	10	18.64	16.16	1.73	0.86	10.7
252	12.5	6.5	7.0	40	10	15.75				
253	12.5	6.5	7.0	40	10	14.64				
254	12.5	6.5	7.0	40	10	15.61				
251	12.5	6.5	7.0	40	5	17.64	15.87	1.27	0.63	8.0
252	12.5	6.5	7.0	40	5	15.57				
253	12.5	6.5	7.0	40	5	14.62				
254	12.5	6.5	7.0	40	5	15.64				
251	12.5	6.5	7.0	40	1	16.58	16.04	0.67	0.34	4.2
252	12.5	6.5	7.0	40	1	16.65				
253	12.5	6.5	7.0	40	1	15.46				
254	12.5	6.5	7.0	40	1	15.45				
251	12.5	6.5	7.0	40	0.5	17.54	15.49	2.25	1.13	14.6
252	12.5	6.5	7.0	40	0.5	17.33				
253	12.5	6.5	7.0	40	0.5	13.53				
254	12.5	6.5	7.0	40	0.5	13.54				
251	12.5	6.5	7.0	40	0.1	19.54	17.31	2.62	1.31	15.1
252	12.5	6.5	7.0	40	0.1	19.58				
253	12.5	6.5	7.0	40	0.1	15.46				
254	12.5	6.5	7.0	40	0.1	14.65				
251	12.5	6.5	7.0	70	25	21.00	21.96	0.70	0.35	3.2
252	12.5	6.5	7.0	70	25	22.21				
253	12.5	6.5	7.0	70	25	22.67				
254	12.5	6.5	7.0	70	25	21.95				
251	12.5	6.5	7.0	70	10	23.96	23.53	3.47	1.74	14.8
252	12.5	6.5	7.0	70	10	28.25				
253	12.5	6.5	7.0	70	10	21.45				
254	12.5	6.5	7.0	70	10	20.47				
251	12.5	6.5	7.0	70	5	23.67	20.93	2.17	1.08	10.4
252	12.5	6.5	7.0	70	5	18.52				
253	12.5	6.5	7.0	70	5	21.36				
254	12.5	6.5	7.0	70	5	20.15				

STATISTICAL DESCRIPTIONS OF PHASE ANGLE (CON'T)
Sample Size: H150*D100

Spec. ID	Nom. Size (mm)	Binder Cont. (%)	Air Void (%)	Temp (D.F)	Freq (Hz)	Phase Angle Test (Deg)	Mean (Deg)	Std Dev (Deg)	Std Err (Deg)	C Var (%)
251	12.5	6.5	7.0	70	1	28.95	25.63	2.93	1.47	11.4
252	12.5	6.5	7.0	70	1	27.23				
253	12.5	6.5	7.0	70	1	23.05				
254	12.5	6.5	7.0	70	1	23.27				
251	12.5	6.5	7.0	70	0.5	28.47	25.78	2.46	1.23	9.5
252	12.5	6.5	7.0	70	0.5	27.22				
253	12.5	6.5	7.0	70	0.5	23.34				
254	12.5	6.5	7.0	70	0.5	24.08				
251	12.5	6.5	7.0	70	0.1	27.98	25.43	2.43	1.21	9.6
252	12.5	6.5	7.0	70	0.1	26.72				
253	12.5	6.5	7.0	70	0.1	22.47				
254	12.5	6.5	7.0	70	0.1	24.55				
251	12.5	6.5	7.0	100	25	31.80	31.09	2.69	1.34	8.7
252	12.5	6.5	7.0	100	25	34.17				
253	12.5	6.5	7.0	100	25	27.69				
254	12.5	6.5	7.0	100	25	30.70				
251	12.5	6.5	7.0	100	10	28.61	29.08	1.17	0.59	4.0
252	12.5	6.5	7.0	100	10	30.48				
253	12.5	6.5	7.0	100	10	27.75				
254	12.5	6.5	7.0	100	10	29.49				
251	12.5	6.5	7.0	100	5	30.90	29.79	1.46	0.73	4.9
252	12.5	6.5	7.0	100	5	29.75				
253	12.5	6.5	7.0	100	5	27.73				
254	12.5	6.5	7.0	100	5	30.77				
251	12.5	6.5	7.0	100	1	26.95	27.26	0.54	0.27	2.0
252	12.5	6.5	7.0	100	1	27.99				
253	12.5	6.5	7.0	100	1	26.76				
254	12.5	6.5	7.0	100	1	27.35				
251	12.5	6.5	7.0	100	0.5	24.83	25.84	1.40	0.70	5.4
252	12.5	6.5	7.0	100	0.5	27.91				
253	12.5	6.5	7.0	100	0.5	25.30				
254	12.5	6.5	7.0	100	0.5	25.31				
251	12.5	6.5	7.0	100	0.1	19.27	20.97	1.63	0.81	7.8
252	12.5	6.5	7.0	100	0.1	22.92				
253	12.5	6.5	7.0	100	0.1	21.62				
254	12.5	6.5	7.0	100	0.1	20.07				

STATISTICAL DESCRIPTIONS OF PHASE ANGLE (CON'T)
Sample Size: H150*D100

Spec. ID	Nom. Size (mm)	Binder Cont. (%)	Air Void (%)	Temp (D.F)	Freq (Hz)	Phase Angle Test (Deg)	Mean (Deg)	Std Dev (Deg)	Std Err (Deg)	C Var (%)
261	25	5.2	4.5	40	25	15.61	14.25	0.94	0.47	6.6
262	25	5.2	4.5	40	25	13.54				
263	25	5.2	4.5	40	25	14.10				
264	25	5.2	4.5	40	25	13.75				
261	25	5.2	4.5	40	10	14.46	12.51	1.31	0.66	10.5
262	25	5.2	4.5	40	10	12.04				
263	25	5.2	4.5	40	10	11.62				
264	25	5.2	4.5	40	10	11.93				
261	25	5.2	4.5	40	5	15.46	13.08	1.80	0.90	13.8
262	25	5.2	4.5	40	5	12.51				
263	25	5.2	4.5	40	5	11.15				
264	25	5.2	4.5	40	5	13.19				
261	25	5.2	4.5	40	1	18.51	17.88	2.29	1.15	12.8
262	25	5.2	4.5	40	1	18.64				
263	25	5.2	4.5	40	1	19.81				
264	25	5.2	4.5	40	1	14.55				
261	25	5.2	4.5	40	0.5	19.05	17.22	1.85	0.93	10.7
262	25	5.2	4.5	40	0.5	18.54				
263	25	5.2	4.5	40	0.5	16.00				
264	25	5.2	4.5	40	0.5	15.30				
261	25	5.2	4.5	40	0.1	18.64	16.83	1.90	0.95	11.3
262	25	5.2	4.5	40	0.1	14.56				
263	25	5.2	4.5	40	0.1	15.97				
264	25	5.2	4.5	40	0.1	18.14				
261	25	5.2	4.5	70	25	21.16	20.02	2.54	1.27	12.7
262	25	5.2	4.5	70	25	20.65				
263	25	5.2	4.5	70	25	16.30				
264	25	5.2	4.5	70	25	21.97				
261	25	5.2	4.5	70	10	20.98	19.13	1.31	0.66	6.9
262	25	5.2	4.5	70	10	17.88				
263	25	5.2	4.5	70	10	18.76				
264	25	5.2	4.5	70	10	18.91				
261	25	5.2	4.5	70	5	22.94	20.61	1.98	0.99	9.6
262	25	5.2	4.5	70	5	19.10				
263	25	5.2	4.5	70	5	18.83				
264	25	5.2	4.5	70	5	21.56				

STATISTICAL DESCRIPTIONS OF PHASE ANGLE (CON'T)
Sample Size: H150*D100

Spec. ID	Nom. Size (mm)	Binder Cont. (%)	Air Void (%)	Temp (D.F)	Freq (Hz)	Phase Angle				
						Test (Deg)	Mean (Deg)	Std Dev (Deg)	Std Err (Deg)	C Var (%)
261	25	5.2	4.5	70	1	23.86	21.89	1.79	0.89	8.2
262	25	5.2	4.5	70	1	19.69				
263	25	5.2	4.5	70	1	21.36				
264	25	5.2	4.5	70	1	22.64				
261	25	5.2	4.5	70	0.5	23.97	22.65	2.01	1.01	8.9
262	25	5.2	4.5	70	0.5	19.88				
263	25	5.2	4.5	70	0.5	22.46				
264	25	5.2	4.5	70	0.5	24.29				
261	25	5.2	4.5	70	0.1	24.92	24.20	1.25	0.62	5.2
262	25	5.2	4.5	70	0.1	22.34				
263	25	5.2	4.5	70	0.1	24.60				
264	25	5.2	4.5	70	0.1	24.94				
261	25	5.2	4.5	100	25	32.10	31.91	4.51	2.25	14.1
262	25	5.2	4.5	100	25	30.99				
263	25	5.2	4.5	100	25	26.80				
264	25	5.2	4.5	100	25	37.74				
261	25	5.2	4.5	100	10	28.95	31.29	4.68	2.34	15.0
262	25	5.2	4.5	100	10	28.38				
263	25	5.2	4.5	100	10	29.55				
264	25	5.2	4.5	100	10	38.28				
261	25	5.2	4.5	100	5	29.40	31.03	4.26	2.13	13.7
262	25	5.2	4.5	100	5	27.95				
263	25	5.2	4.5	100	5	29.44				
264	25	5.2	4.5	100	5	37.33				
261	25	5.2	4.5	100	1	27.45	28.70	1.72	0.86	6.0
262	25	5.2	4.5	100	1	26.99				
263	25	5.2	4.5	100	1	30.33				
264	25	5.2	4.5	100	1	30.02				
261	25	5.2	4.5	100	0.5	24.84	27.22	1.67	0.84	6.1
262	25	5.2	4.5	100	0.5	27.30				
263	25	5.2	4.5	100	0.5	28.60				
264	25	5.2	4.5	100	0.5	28.13				
261	25	5.2	4.5	100	0.1	22.47	23.67	1.10	0.55	4.7
262	25	5.2	4.5	100	0.1	24.19				
263	25	5.2	4.5	100	0.1	24.93				
264	25	5.2	4.5	100	0.1	23.07				

STATISTICAL DESCRIPTIONS OF PHASE ANGLE (CON'T)
Sample Size: H150*D100

Spec. ID	Nom. Size (mm)	Binder Cont. (%)	Air Void (%)	Temp (D.F)	Freq (Hz)	Phase Angle Test (Deg)	Mean (Deg)	Std Dev (Deg)	Std Err (Deg)	C Var (%)
271	25	5.2	7.0	40	25	14.80	13.96	2.20	1.10	15.8
272	25	5.2	7.0	40	25	16.60				
273	25	5.2	7.0	40	25	12.82				
274	25	5.2	7.0	40	25	11.60				
271	25	5.2	7.0	40	10	15.42	13.64	1.75	0.88	12.9
272	25	5.2	7.0	40	10	13.97				
273	25	5.2	7.0	40	10	13.94				
274	25	5.2	7.0	40	10	11.22				
271	25	5.2	7.0	40	5	16.52	14.47	1.54	0.77	10.6
272	25	5.2	7.0	40	5	13.79				
273	25	5.2	7.0	40	5	12.92				
274	25	5.2	7.0	40	5	14.64				
271	25	5.2	7.0	40	1	18.16	15.72	1.67	0.83	10.6
272	25	5.2	7.0	40	1	15.37				
273	25	5.2	7.0	40	1	14.83				
274	25	5.2	7.0	40	1	14.51				
271	25	5.2	7.0	40	0.5	17.64	15.80	1.80	0.90	11.4
272	25	5.2	7.0	40	0.5	16.54				
273	25	5.2	7.0	40	0.5	15.62				
274	25	5.2	7.0	40	0.5	13.41				
271	25	5.2	7.0	40	0.1	19.89	18.11	1.39	0.70	7.7
272	25	5.2	7.0	40	0.1	17.89				
273	25	5.2	7.0	40	0.1	18.15				
274	25	5.2	7.0	40	0.1	16.50				
271	25	5.2	7.0	70	25	21.10	19.35	1.30	0.65	6.7
272	25	5.2	7.0	70	25	18.20				
273	25	5.2	7.0	70	25	19.53				
274	25	5.2	7.0	70	25	18.55				
271	25	5.2	7.0	70	10	21.83	19.75	2.69	1.34	13.6
272	25	5.2	7.0	70	10	21.98				
273	25	5.2	7.0	70	10	18.81				
274	25	5.2	7.0	70	10	16.36				
271	25	5.2	7.0	70	5	21.95	20.01	2.80	1.40	14.0
272	25	5.2	7.0	70	5	22.10				
273	25	5.2	7.0	70	5	19.88				
274	25	5.2	7.0	70	5	16.10				

STATISTICAL DESCRIPTIONS OF PHASE ANGLE (CON'T)
Sample Size: H150*D100

Spec. ID	Nom. Size (mm)	Binder Cont. (%)	Air Void (%)	Temp (D.F)	Freq (Hz)	Phase Angle Test (Deg)	Mean (Deg)	Std Dev (Deg)	Std Err (Deg)	C Var (%)
271	25	5.2	7.0	70	1	23.42	23.92	2.35	1.18	9.8
272	25	5.2	7.0	70	1	25.86				
273	25	5.2	7.0	70	1	20.80				
274	25	5.2	7.0	70	1	25.61				
271	25	5.2	7.0	70	0.5	24.08	22.68	3.46	1.73	15.3
272	25	5.2	7.0	70	0.5	26.61				
273	25	5.2	7.0	70	0.5	21.50				
274	25	5.2	7.0	70	0.5	18.54				
271	25	5.2	7.0	70	0.1	23.74	22.98	2.33	1.16	10.1
272	25	5.2	7.0	70	0.1	25.63				
273	25	5.2	7.0	70	0.1	22.46				
274	25	5.2	7.0	70	0.1	20.08				
271	25	5.2	7.0	100	25	34.00	33.88	1.57	0.78	4.6
272	25	5.2	7.0	100	25	35.40				
273	25	5.2	7.0	100	25	34.43				
274	25	5.2	7.0	100	25	31.70				
271	25	5.2	7.0	100	10	31.45	33.19	1.71	0.86	5.2
272	25	5.2	7.0	100	10	35.08				
273	25	5.2	7.0	100	10	34.15				
274	25	5.2	7.0	100	10	32.06				
271	25	5.2	7.0	100	5	30.32	31.35	1.52	0.76	4.9
272	25	5.2	7.0	100	5	33.17				
273	25	5.2	7.0	100	5	32.02				
274	25	5.2	7.0	100	5	29.89				
271	25	5.2	7.0	100	1	25.22	26.76	1.31	0.66	4.9
272	25	5.2	7.0	100	1	26.15				
273	25	5.2	7.0	100	1	28.06				
274	25	5.2	7.0	100	1	27.62				
271	25	5.2	7.0	100	0.5	22.15	24.57	1.62	0.81	6.6
272	25	5.2	7.0	100	0.5	25.13				
273	25	5.2	7.0	100	0.5	25.45				
274	25	5.2	7.0	100	0.5	25.53				
271	25	5.2	7.0	100	0.1	16.71	19.39	1.79	0.90	9.2
272	25	5.2	7.0	100	0.1	20.28				
273	25	5.2	7.0	100	0.1	20.12				
274	25	5.2	7.0	100	0.1	20.46				

APPENDIX D

SAS PROGRAM FOR TEST 1

```
/* TEST 1: MULTIPLE FACTORIAL DESIGN*/
/* DYNMOD   = Dynamic Modulus (Response)*/
/* AGGSZ    = aggregate size varied at two levels (12.5 and 25.0 mm)*/
/* AVOID    = air voids varied at two levels (4.5 and 7.0%)*/
/* TEMP           = temperature varied at three levels (40, 70, and
100oF)*/
/* FREQ           = frequency varied at six levels (25, 10, 5, 1, 0.5,
and 0.1Hz)*/

OPTIONS NOCENTER LINESIZE=85;

DATA EXPDATA;
   INPUT AGGSZ AVOID TEMP FREQ DYNMOD;
   DATALINES;
12.5  4.5   40    25    1896988
12.5  4.5   40    10    1798556
……………………………………………………………………………
25    7.0   100   0.5   227121
25    7.0   100   0.1   163571
   ;

PROC PRINT DATA=EXPDATA;
   TITLE1 'ANALYSIS OF DYNAMIC MODULUS BASED ON AGGREGATE SIZE, AIR
VOIDS, TEMPERATURE AND FREQUENCY';
   TITLE2 'TEST 1: MULTIPLE FACTORIAL DESIGN';

PROC RANK DATA=EXPDATA OUT=REXPDATA;
   RANKS RDYNMOD;
   VAR DYNMOD;

PROC PRINT DATA=REXPDATA;
   TITLE2 'DATA SET CREATED CONTAINING THE RANKED RESPONSE';

PROC GLM DATA=REXPDATA;
   CLASS AGGSZ AVOID TEMP FREQ;
   MODEL RDYNMOD = AGGSZ|AVOID|TEMP|FREQ;
   MEANS AGGSZ AVOID TEMP FREQ / DUNCAN;
   OUTPUT OUT = SUMMARY P=YHAT R=RESIDUAL;
   TITLE2 'THE ANALYSIS';

PROC PRINT DATA=SUMMARY;
   TITLE2 'DATA SET CREATED CONTAINING THE PREDICTED AND RESIDUAL
VALUES';

PROC UNIVARIATE DATA=SUMMARY NORMAL PLOT;
   VAR RESIDUAL;
   TITLE2 'MODEL ADEQUACY CHECKS';

PROC PLOT DATA=SUMMARY;
   PLOT RESIDUAL*YHAT='*';
   TITLE2 'PLOT OF THE RESIDUALS VS PREDICTED VALUES';
   PLOT RESIDUAL*AGGSZ='*';
   TITLE2 'PLOT OF THE RESIDUALS VS AGGREGATE SIZE';
   PLOT RESIDUAL*AVOID='*';
   TITLE2 'PLOT OF THE RESIDUALS VS AIR VOIDS';
   PLOT RESIDUAL*TEMP='*';
   TITLE2 'PLOT OF THE RESIDUALS VS TEMPERATURE';
```

```
   PLOT RESIDUAL*FREQ='*';
   TITLE2 'PLOT OF THE RESIDUALS VS FREQUENCY';
RUN;

PROC SUMMARY;
   CLASS AGGSZ AVOID TEMP FREQ;
   VAR RDYNMOD;
   OUTPUT OUT=INTERACT MEAN=MEAN;

PROC PRINT DATA=INTERACT;
   TITLE2 'DATA SET CREATED BY PROC SUMMARY CONTAINING MEANS';

DATA TWAY;
   SET INTERACT;
   IF _TYPE_=7 THEN OUTPUT TWAY;
PROC SORT DATA=TWAY;
   BY AVOID;
PROC PRINT DATA=TWAY;
   TITLE2 'DATASET FOR THE INTERACTION PLOT OF AVOID, TEMP AND FREQ';
PROC PLOT DATA=TWAY;
   PLOT MEAN*FREQ=TEMP;
      BY AVOID;
   TITLE2 'INTERACTION PLOT OF AVOID AND TEMP';

DATA TEMPXFREQ;
   SET INTERACT;
   IF _TYPE_=3 THEN OUTPUT TEMPXFREQ;
PROC PRINT DATA=TEMPXFREQ;
   TITLE2 'DATASET FOR THE INTERACTION PLOT OF TEMP AND FREQ';
PROC PLOT DATA=TEMPXFREQ;
   PLOT MEAN*FREQ=TEMP;
   TITLE2 'INTERACTION PLOT OF TEMP AND FREQ';

DATA AVOIDXFREQ;
   SET INTERACT;
   IF _TYPE_=5 THEN OUTPUT AVOIDXFREQ;
PROC PRINT DATA=AVOIDXFREQ;
   TITLE2 'DATASET FOR THE INTERACTION PLOT OF AVOID AND FREQ';
PROC PLOT DATA=AVOIDXFREQ;
   PLOT MEAN*FREQ=AVOID;
   TITLE2 'INTERACTION PLOT OF AVOID AND FREQ';

DATA AGGSZXAVOID;
   SET INTERACT;
   IF _TYPE_=12 THEN OUTPUT AGGSZXAVOID;
PROC PRINT DATA=AGGSZXAVOID;
   TITLE2 'DATASET FOR THE INTERACTION PLOT OF AGGSZ AND AVOID';
PROC PLOT DATA=AGGSZXAVOID;
   PLOT MEAN*AGGSZ=AVOID;
   TITLE2 'INTERACTION PLOT OF AGGSZ AND AVOID';

DATA AGGSZ;
   SET INTERACT;
   IF _TYPE_=8 THEN OUTPUT AGGSZ;
PROC PRINT DATA=AGGSZ;
   TITLE2 'DATASET FOR THE PLOT OF AGGSZ';
PROC PLOT DATA=AGGSZ;
```

```
   PLOT MEAN*AGGSZ='*';
   TITLE2 'PLOT FOR AGGSZ';

DATA AVOID;
   SET INTERACT;
   IF _TYPE_=4 THEN OUTPUT AVOID;
PROC PRINT DATA=AVOID;
   TITLE2 'DATASET FOR THE PLOT OF AVOID';
PROC PLOT DATA=AVOID;
   PLOT MEAN*AVOID='*';
   TITLE2 'PLOT FOR AVOID';

DATA TEMP;
   SET INTERACT;
   IF _TYPE_=2 THEN OUTPUT TEMP;
PROC PRINT DATA=TEMP;
   TITLE2 'DATASET FOR THE PLOT OF TEMP';
PROC PLOT DATA=TEMP;
   PLOT MEAN*TEMP='*';
   TITLE2 'PLOT FOR TEMP';

DATA FREQ;
   SET INTERACT;
   IF _TYPE_=1 THEN OUTPUT FREQ;
PROC PRINT DATA=FREQ;
   TITLE2 'DATASET FOR THE PLOT OF FREQ';
PROC PLOT DATA=FREQ;
   PLOT MEAN*FREQ='*';
   TITLE2 'PLOT FOR FREQ';

QUIT;
```

APPENDIX E

SAS PROGRAM FOR TEST 2

```
/* TEST 2: MULTIPLE FACTORIAL DESIGN*/
/* DYNMOD       = Dynamic Modulus (Response)*/
/* BINDC        = Binder Content varied at three levels (-0.5%, opt,
and +0.5%)*/
/* AVOID        = air voids varied at two levels (4.5 and 7.0%)*/
/* TEMP         = temperature varied at three levels (40, 70, and
100oF)*/
/* FREQ         = frequency varied at six levels (25, 10, 5, 1, 0.5,
and 0.1Hz)*/

OPTIONS NOCENTER LINESIZE=85;

DATA EXPDATA;
   INPUT BINDC$ AVOID TEMP FREQ DYNMOD;
   DATALINES;
-0.5  4.5   40    25    3199716
-0.5  4.5   40    10    2981345
……………………………………………………………………………………………
+0.5  7.0   100   0.5   188966
+0.5  7.0   100   0.1   129992
   ;

PROC PRINT DATA=EXPDATA;
   TITLE1 'ANALYSIS OF DYNAMIC MODULUS BASED ON BINDER CONTENT, AIR
VOIDS, TEMPERATURE AND FREQUENCY';
   TITLE2 'TEST 2: MULTIPLE FACTORIAL DESIGN';

PROC RANK DATA=EXPDATA OUT=REXPDATA;
   RANKS RDYNMOD;
   VAR DYNMOD;

PROC PRINT DATA=REXPDATA;
   TITLE2 'DATA SET CREATED CONTAINING THE RANKED RESPONSE';

PROC GLM DATA=REXPDATA;
   CLASS BINDC AVOID TEMP FREQ;
   MODEL  RDYNMOD = BINDC|AVOID|TEMP|FREQ;
   MEANS  BINDC AVOID TEMP FREQ / DUNCAN;
   OUTPUT OUT = SUMMARY P=YHAT R=RESIDUAL;
   TITLE2 'THE ANALYSIS';

PROC PRINT DATA=SUMMARY;
   TITLE2 'DATA SET CREATED CONTAINING THE PREDICTED AND RESIDUAL
VALUES';

PROC UNIVARIATE DATA=SUMMARY NORMAL PLOT;
   VAR RESIDUAL;
   TITLE2 'MODEL ADEQUACY CHECKS';

PROC PLOT DATA=SUMMARY;
   PLOT RESIDUAL*YHAT='*';
   TITLE2 'PLOT OF THE RESIDUALS VS PREDICTED VALUES';
   PLOT RESIDUAL*BINDC='*';
   TITLE2 'PLOT OF THE RESIDUALS VS BINDER CONTENT';
   PLOT RESIDUAL*AVOID='*';
   TITLE2 'PLOT OF THE RESIDUALS VS AIR VOIDS';
   PLOT RESIDUAL*TEMP='*';
```

```
   TITLE2 'PLOT OF THE RESIDUALS VS TEMPERATURE';
   PLOT RESIDUAL*FREQ='*';
   TITLE2 'PLOT OF THE RESIDUALS VS FREQUENCY';
RUN;

PROC SUMMARY;
   CLASS BINDC AVOID TEMP FREQ;
   VAR RDYNMOD;
   OUTPUT OUT=INTERACT MEAN=MEAN;

PROC PRINT DATA=INTERACT;
   TITLE2 'DATA SET CREATED BY PROC SUMMARY CONTAINING MEANS';

DATA TWAY;
   SET INTERACT;
   IF _TYPE_=11 THEN OUTPUT TWAY;
PROC SORT DATA=TWAY;
   BY BINDC;
PROC PRINT DATA=TWAY;
   TITLE2 'DATASET FOR THE INTERACTION PLOT OF BINDC, TEMP AND FREQ';
PROC PLOT DATA=TWAY;
   PLOT MEAN*FREQ=TEMP;
      BY BINDC;
   TITLE2 'INTERACTION PLOT OF TEMP AND FREQ';

DATA BINXTEMP;
   SET INTERACT;
   IF _TYPE_=10 THEN OUTPUT BINXTEMP;
PROC PRINT DATA=BINXTEMP;
   TITLE2 'DATASET FOR THE INTERACTION PLOT OF BINDC AND TEMP';
PROC PLOT DATA=BINXTEMP;
   PLOT MEAN*BINDC=TEMP;
   TITLE2 'INTERACTION PLOT OF BINDC AND TEMP';

DATA TEMPXFREQ;
   SET INTERACT;
   IF _TYPE_=3 THEN OUTPUT TEMPXFREQ;
PROC PRINT DATA=TEMPXFREQ;
   TITLE2 'DATASET FOR THE INTERACTION PLOT OF TEMP AND FREQ';
PROC PLOT DATA=TEMPXFREQ;
   PLOT MEAN*FREQ=TEMP;
   TITLE2 'INTERACTION PLOT OF TEMP AND FREQ';

DATA VOIDXTEMP;
   SET INTERACT;
   IF _TYPE_=6 THEN OUTPUT VOIDXTEMP;
PROC PRINT DATA=VOIDXTEMP;
   TITLE2 'DATASET FOR THE INTERACTION PLOT OF AVOID AND TEMP';
PROC PLOT DATA=VOIDXTEMP;
   PLOT MEAN*TEMP=AVOID;
   TITLE2 'INTERACTION PLOT OF AVOID AND TEMP';

DATA VOIDXBIND;
   SET INTERACT;
   IF _TYPE_=12 THEN OUTPUT VOIDXBIND;
PROC PRINT DATA=VOIDXBIND;
   TITLE2 'DATASET FOR THE INTERACTION PLOT OF AVOID AND BINDC';
```

```
PROC PLOT DATA=VOIDXBIND;
   PLOT MEAN*BINDC=AVOID;
   TITLE2 'INTERACTION PLOT OF BINDC AND AVOID';

DATA BINDC;
   SET INTERACT;
   IF _TYPE_=8 THEN OUTPUT BINDC;
PROC PRINT DATA=BINDC;
   TITLE2 'DATASET FOR THE PLOT OF BINDC';
PROC PLOT DATA=BINDC;
   PLOT MEAN*BINDC='*';
   TITLE2 'PLOT FOR BINDC';

DATA AVOID;
   SET INTERACT;
   IF _TYPE_=4 THEN OUTPUT AVOID;
PROC PRINT DATA=AVOID;
   TITLE2 'DATASET FOR THE PLOT OF AVOID';
PROC PLOT DATA=AVOID;
   PLOT MEAN*AVOID='*';
   TITLE2 'PLOT FOR AVOID';

DATA TEMP;
   SET INTERACT;
   IF _TYPE_=2 THEN OUTPUT TEMP;
PROC PRINT DATA=TEMP;
   TITLE2 'DATASET FOR THE PLOT OF TEMP';
PROC PLOT DATA=TEMP;
   PLOT MEAN*TEMP='*';
   TITLE2 'PLOT FOR TEMP';

DATA FREQ;
   SET INTERACT;
   IF _TYPE_=1 THEN OUTPUT FREQ;
PROC PRINT DATA=FREQ;
   TITLE2 'DATASET FOR THE PLOT OF FREQ';
PROC PLOT DATA=FREQ;
   PLOT MEAN*FREQ='*';
   TITLE2 'PLOT FOR FREQ';

QUIT;
```

APPENDIX F

SAS PROGRAM FOR TEST 3

```
/* TEST 3: MULTIPLE FACTORIAL DESIGN*/
/* DYNMOD   = Dynamic Modulus (Response)*/
/* MIX            = (Block) mix types varied at four levels (12.5-0.5,
12.5OPT, 12.5+0.5, 25OPT)*/
/* AVOID    = air voids varied at two levels (4.5 and 7.0%)*/
/* TEMP           = temperature varied at three levels (40, 70, and
100oF)*/
/* FREQ           = frequency varied at six levels (25, 10, 5, 1, 0.5,
and 0.1Hz)*/

OPTIONS NOCENTER LINESIZE=85;

DATA EXPDATA;
   INPUT MIX$ AVOID TEMP FREQ DYNMOD;
   DATALINES;
12.5-0.5    4.5    40     25     3199716
12.5-0.5    4.5    40     10     2981345
.......................................................................
25OPT 7.0    100    0.5    227121
25OPT 7.0    100    0.1    163571
   ;

PROC PRINT DATA=EXPDATA;
   TITLE1 'ANALYSIS OF DYNAMIC MODULUS BASED ON AIR VOIDS, TEMPERATURE
AND FREQUENCY BLOCK ON MIX TYPE';
   TITLE2 'TEST 3: MULTIPLE FACTORIAL DESIGN';

PROC RANK DATA=EXPDATA OUT=REXPDATA;
   RANKS RDYNMOD;
   VAR DYNMOD;

PROC PRINT DATA=REXPDATA;
   TITLE2 'DATA SET CREATED CONTAINING THE RANKED RESPONSE';

PROC GLM DATA=REXPDATA;
   CLASS MIX AVOID TEMP FREQ;
   MODEL  RDYNMOD = AVOID|TEMP|FREQ MIX;
   MEANS  AVOID TEMP FREQ MIX / DUNCAN;
   OUTPUT OUT = SUMMARY P=YHAT R=RESIDUAL;
   TITLE2 'THE ANALYSIS';

PROC PRINT DATA=SUMMARY;
   TITLE2 'DATA SET CREATED CONTAINING THE PREDICTED AND RESIDUAL
VALUES';

PROC UNIVARIATE DATA=SUMMARY NORMAL PLOT;
   VAR RESIDUAL;
   TITLE2 'MODEL ADEQUACY CHECKS';

PROC PLOT DATA=SUMMARY;
   PLOT RESIDUAL*YHAT='*';
   TITLE2 'PLOT OF THE RESIDUALS VS PREDICTED VALUES';
   PLOT RESIDUAL*MIX='*';
   TITLE2 'PLOT OF THE RESIDUALS VS MIX TYPE';
   PLOT RESIDUAL*AVOID='*';
   TITLE2 'PLOT OF THE RESIDUALS VS AIR VOIDS';
   PLOT RESIDUAL*TEMP='*';
```

```
   TITLE2 'PLOT OF THE RESIDUALS VS TEMPERATURE';
   PLOT RESIDUAL*FREQ='*';
   TITLE2 'PLOT OF THE RESIDUALS VS FREQUENCY';
RUN;

PROC SUMMARY;
   CLASS MIX AVOID TEMP FREQ;
   VAR RDYNMOD;
   OUTPUT OUT=INTERACT MEAN=MEAN;

PROC PRINT DATA=INTERACT;
   TITLE2 'DATA SET CREATED BY PROC SUMMARY CONTAINING MEANS';

DATA TEMPXFRE;
   SET INTERACT;
   IF _TYPE_=3 THEN OUTPUT TEMPXFRE;
PROC PRINT DATA=TEMPXFRE;
   TITLE2 'DATASET FOR THE INTERACTION PLOT OF TEMP AND FREQ';
PROC PLOT DATA=TEMPXFRE;
   PLOT MEAN*FREQ=TEMP;
   TITLE2 'INTERACTION PLOT OF TEMP AND FREQ';

DATA AVOIDXTEMP;
   SET INTERACT;
   IF _TYPE_=6 THEN OUTPUT AVOIDXTEMP;
PROC PRINT DATA=AVOIDXTEMP;
   TITLE2 'DATASET FOR THE INTERACTION PLOT OF AVOID AND TEMP';
PROC PLOT DATA=AVOIDXTEMP;
   PLOT MEAN*TEMP=AVOID;
   TITLE2 'INTERACTION PLOT OF AVOID AND TEMP';

DATA AVOID;
   SET INTERACT;
   IF _TYPE_=4 THEN OUTPUT AVOID;
PROC PRINT DATA=AVOID;
   TITLE2 'DATASET FOR THE PLOT OF AVOID';
PROC PLOT DATA=AVOID;
   PLOT MEAN*AVOID='*';
   TITLE2 'PLOT FOR AVOID';

DATA TEMP;
   SET INTERACT;
   IF _TYPE_=2 THEN OUTPUT TEMP;
PROC PRINT DATA=TEMP;
   TITLE2 'DATASET FOR THE PLOT OF TEMP';
PROC PLOT DATA=TEMP;
   PLOT MEAN*TEMP='*';
   TITLE2 'PLOT FOR TEMP';

DATA FREQ;
   SET INTERACT;
   IF _TYPE_=1 THEN OUTPUT FREQ;
PROC PRINT DATA=FREQ;
   TITLE2 'DATASET FOR THE PLOT OF FREQ';
PROC PLOT DATA=FREQ;
   PLOT MEAN*FREQ='*';
   TITLE2 'PLOT FOR FREQ';
```

```
DATA MAX;
   SET INTERACT;
   IF _TYPE_=8 THEN OUTPUT MIX;
PROC PRINT DATA=MIX;
   TITLE2 'DATASET FOR THE PLOT OF MIX';
PROC PLOT DATA=MIX;
   PLOT MEAN*MIX='*';
   TITLE2 'PLOT FOR MIX';

QUIT;
```